REVIEWS OF
MODERN PHYSICS

VOLUME 10 JANUARY, 1938 NUMBER 1

Order-Disorder Transformations in Alloys

FOSTER C. NIX AND WILLIAM SHOCKLEY
Bell Telephone Laboratories, New York, N. Y.

TABLE OF CONTENTS

Introduction 2

Part I. Theories of the Order-Disorder Phenomenon

Division A. Equilibrium Theories for Alloys of Simple Unvaried Compositions
Section 1. The Theory of Bragg and Williams 6
Section 2. The Theory of Bethe 17
Section 3. The Energy *Versus* Entropy Representation 24
Section 4. The Method of Kirkwood 27

Division B. Equilibrium Theories for Alloys of Arbitrary Composition
Section 5. The Energy of Formation of Alloys 31
Section 6. The Dependence of Critical Temperature upon Composition 32
Section 7. Phase Diagrams for the Order-Disorder Phenomenon 33
Section 8. Treatments not Using the Nearest Neighbor Assumption 35
Section 9. The Thermodynamic Potentials of Ordered Phases 36

Division C. Theories for Alloys Which Are Not in Thermal Equilibrium
Section 10. The Time of Relaxation 37
Section 11. The Theory of Temperature Hysteresis. 39

Division D. Adaptation of the Idealized Theory to Actuality
Section 12. The Origin of the Ordering Energy 40
Section 13. The Effect of Lattice Vibrations 41

Part II. Experimental Studies of Superstructures

Section 14. Energy Content Measurements 43
Section 15. Curie Point of Long Distance Order as a Function of Composition 46
Section 16. Ordered Structures 47
Section 17. Phenomena Which May Indicate the Degree of Order 50
Section 18. Behavior of Alloys not in Thermal Equilibrium 51
Section 19. Influence of Order and Composition on the Electrical Resistivity 54
Section 20. Effect of Order on Mechanical Properties 56
Section 21. Effect of Plastic Deformation on Order 57
Section 22. Effect of Order on Magnetic Properties 59
Section 23. Criteria for Establishing the Presence of Ordered Structures 61

Appendices 63

Bibliography 68

INTRODUCTION

Ordered substitutional alloys

AMONG the many types of alloys there is one which is known as a "substitutional solid solution." Sometimes this is made by the addition of various quantities of metal B to metal A. It is found that the crystals of the alloy are very like those of the pure metal save that upon some of the lattice sites B atoms have been substituted for A atoms. For many years it was thought that this substitution was a purely random affair and that there was no order in the way in which the atoms are arranged on the lattice sites. Recently,[23A, 25A] however, it has been determined by that final arbiter of crystal structure, x-ray diffraction, that in a large number of cases the atoms are arranged in as definite a way as are the two different elements in an ionic salt.

The earliest prediction of ordered structures was based not on x-ray evidence but on some chemical experiments of Tammann.[19A, 21A] He found that suitably conditioned Cu-Au alloys containing more than 50 atomic percent Cu were attacked by nitric acid which dissolved the Cu but none of the Au. Samples containing 50 atomic percent Cu or less were not affected. On the basis of this evidence he concluded that a 50 atomic percent Cu-Au alloy contained an ordered arrangement of atoms and any extra Cu atoms did not fit in and were easily removed.

At present, however, the conclusive evidence of ordered arrangements, or superstructures, or superlattices as they are also called, is furnished by the presence of "superstructure lines" on x-ray diffraction patterns. Fig. 1 shows schematically a superstructure and an x-ray beam. Here we see A and B atoms arranged in a regular array. It is quite obvious in this case that some sites, called α-sites, are appropriate to A atoms and some, called β-sites, to B atoms. An A atom is called "right" when in an α-site and "wrong" when in a β-site; and similar definitions apply to B atoms. In the perfectly ordered state of Fig. 1, all atoms are right. Now imagine that an x-ray beam falls on the crystal and is reflected in such a way that its path length difference between two planes of α-sites is one wave-length and between adjacent α- and β-planes, one-half wave-length. Then the waves in the outgoing beam scattered by the A atoms will all be exactly in phase with each other and exactly out of phase with those scattered by the B atoms. If the scattering factors of the two kinds of atoms are different, the opposing waves will not cancel and a line will result on the x-ray plate. Consider now what occurs if the atoms are disordered so that equal numbers of A and B atoms are upon the α-sites and upon the β-sites. Then the α-sites give rise to scattered waves whose amplitude is the average for A and B atoms and the same is true of the β-sites. The α and β scattered waves now being equal in amplitude cancel each other completely, and no line appears on the plate.

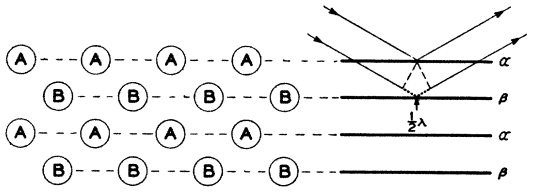

FIG. 1. Superstructure and origin of superstructure line.

Such lines, the occurrence of which is contingent upon the presence of a superstructure, are appropriately known as "superstructure lines." Their presence upon an x-ray picture is proof positive of the existence of a superstructure, and to some extent their intensity is a measure of its approach to perfection. Fig. 2 represents an x-ray pattern from Cu_3Au in a disordered state (right), a well-ordered state (left) and a state of intermediate order (middle). The superstructure lines are identified on the left.

The earliest superstructure lines were observed by Bain[23A] for Cu_3Au and Phragmén[25B] for Fe_3Si and the first analysis of an ordered structure from its x-ray pattern was made by Johansson and Linde[25A] for the alloy CuAu. For these cases the large difference in scattering factors greatly facilitated the experimentation. In some cases the atoms have nearly the same scattering power and the superstructure lines are so weak that they can hardly be detected. Recently improved techniques have made possible the analysis of such alloys, an outstanding example being the

work of Jones and Sykes[37I] upon β-brass, for which the two elements Cu and Zn are adjacent in the periodic table. A review of the ordered structures now determined by x-rays is given in Part II, Section 16.

All superstructures so far analyzed are characterized by a common feature: in them atoms of one species tend to surround themselves by atoms of the other species. We use the word "tend" advisedly because although in some cases the atoms surround themselves as completely as possible with unlike neighbors, in others they stop definitely short of this limit. However, the above statement is adequate for our purposes here and we shall postpone a more exact statement of the situation until Sections 5 and 16.

The order-disorder transformation

Interesting investigations of superstructures can be made by studying the effects of heating. Let us follow the course of this process starting at a low temperature with a perfectly ordered superlattice like that indicated in Fig. 1.

As the temperature is increased, the first effect is only a greater amplitude of thermal vibration of the atoms about their equilibrium positions. When this effect becomes large enough, occasional pairs or small groups of atoms acquire sufficient energy to break away from their places in the lattice and interchange positions with each other. This interchanging results in a certain number of atoms becoming "wrong"—an A atom on a β-site or a B-atom on an α-site is called wrong.

Thus disorder enters the arrangement of the atoms in two closely associated aspects: from a local point of view, the neighbors of some atoms are of the same species, whereas according to the tendency to have unlike neighbors, they should be different; from a long distance point of view, some β-positions are occupied by A atoms. Definitions of order have been made to describe these two aspects: "short range" or "short distance" or "local" order, denoted by σ and defined quantitatively in Section 2, is a measure of how well on the average each atom is surrounded by unlike neighbors; $\sigma=1$ represents the best ordered arrangement and $\sigma=0$ the worst. "Long range" or "long distance" order,

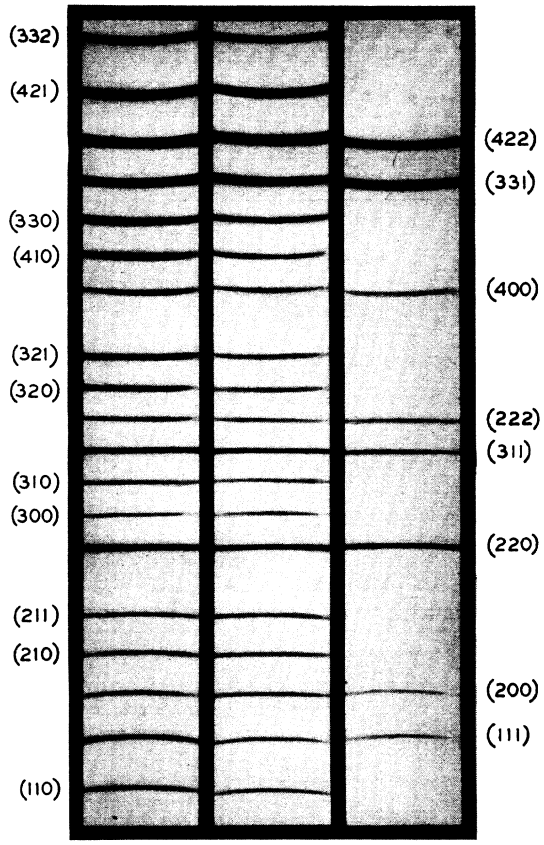

FIG. 2. X-ray diffraction pattern showing superstructure lines (retouched).

denoted by S and defined quantitatively in Section 1, is a measure of how completely the α-sites are occupied by A atoms and the β-sites by B atoms; $S=1$ represents perfect order and $S=0$ disorder.

The tendency of atoms to surround themselves by unlike neighbors results in the formation of the perfect superlattice at very low temperatures. At higher temperatures, where thermal agitation leads to atoms becoming wrong, this tendency acts to restore wrong atoms to right positions. At every temperature less than a certain critical temperature, described below, there is a certain equilibrium condition with a definite number of wrong atoms; at this condition, the rate at which right atoms go wrong owing to thermal agitation is equal to the rate at which wrong atoms go right owing to thermal agitation aided by the ordering influence of the

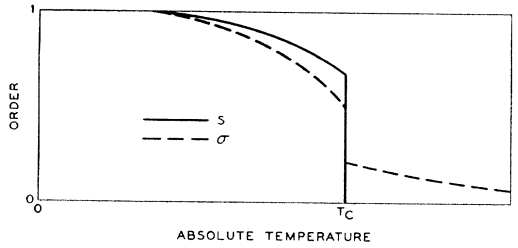

FIG. 3. Long range and short range order *versus* temperature.

right neighbors of wrong atoms. As the number of wrong atoms increases with increasing temperature, some of the neighbors of a wrong atom will also be wrong and will tend to keep it as it is rather than to make it right. Hence with increasing temperature there is not only increasing disorder but also increasing ease of disordering. This process mounts at a more and more rapid rate until a certain critical temperature, T_c, is reached and there the long range order S vanishes abruptly. By analogy with the theory of ferromagnetism, this temperature is known as the "Curie point of order." In Fig. 3, we show one possible form for this process; there is another form described in Section 1 for which there is no discontinuity in the value of S but instead a continuous decrease to zero.

Even above T_c, however, there is still a degree of local order resulting from the tendency of the atoms to have unlike neighbors. Although this tendency is no longer strong enough to produce long distance order throughout the entire crystal, in opposition to the disruptive influence of thermal agitation, it still prevents the occurrence of a completely random state of affairs and maintains a considerable number of unlike pairs of neighbors. In order to overcome this effect the crystal must be heated to yet higher temperatures.

The development of detailed theories to explain and predict the various stages of the order-disorder transformation constitutes the primary object of the theoretical portion, Part I, of this paper. Such theories have been developed by numerous investigators, among the pioneers being Gorsky,[28B] Borelius, Johansson and Linde,[28A], Wagner and Schottky[31F] and Dehlinger and Graf.[30A] Later Borelius[34A] extended the work greatly and discussed in particular the question of temperature hysteresis. Bragg and Williams[34C] redeveloped the theory and extended and simplified it in many respects. More recent developments have been initiated primarily by the work of Bethe.[35B] In the theoretical discussion given here we have made no attempt at a historical presentation, and the material has been arranged as seemed best from the point of view of content and ease of explanation. Other topics taken up in this part have to do with the approach of a disturbed system toward its equilibrium state of order and with effects arising when the composition of the alloy is changed.

Energy considerations

Energy is required to produce disorder and move the atoms into wrong positions in opposition to the ordering force. This excess energy manifests itself as an "anomalous specific heat" —that is, a heat capacity in addition to what is predicted on the basis of the Dulong-Petit law for ordinary thermal motion. This energy and specific heat are associated with the arrangement or configuration of the atoms in the lattice and are frequently referred to as "configurational energy" and "configurational specific heat." The rate of disordering increases from zero to a maximum value just below T_c. This leads to a similar behavior shown in Fig. 4 for the con-

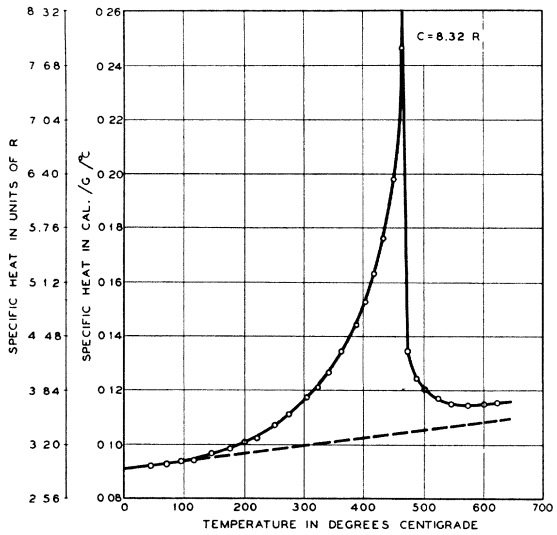

FIG. 4. Specific heat-*vs.*-temperature of a β-brass alloy, containing 48.9 atomic percent Zn. The dashed line is calculated from the specific heats of Cu and Zn, assuming a pure mixture.

figurational specific heat.[36F] The contribution above T_c comes from the local order σ, which continues to require energy for its decrease at higher temperatures.

Energy measurements which give rise to such curves as that of Fig. 4 furnish an important tool for investigating superstructures. Where x-rays do not yield an answer, the existence of such specific heat curves is indirect evidence of a superstructure (the question of confusion with specific heat due to ferromagnetism can easily be settled). We shall discuss such energy measurements in Part II, Section 14.

Other manifestations of order

There are other physical properties besides those of a thermal nature which are profoundly influenced by the state of order in an alloy. These are of interest for two reasons: first, they furnish a class of indirect evidence, like that given by the anomalous heat quantities, which is useful in studying order-disorder transformations and in predicting the presence of ordered structures; and second, they suggest the deliberate utilization of the state of order to obtain materials with new and desirable properties. One of the most striking of the indirect manifestations of order is the behavior shown in Fig. 5 of the specific resistivity.[36I] We see that superimposed upon the normal linear dependence on temperature there is a rapidly increasing rise terminated by a discontinuous jump at T_c; the reader will at once appreciate its close correspondence to the increase in long range disorder with increasing temperature, Fig. 3. Magnetic and mechanical properties are also order-dependent.

A general summary of the influence which the state of order has upon these and various other properties occupies several sections of Part II. A discussion is also given of how these variations lead to the predictions of ordered structures in cases not yet conclusively investigated by x-rays.

Cooperational phenomena

The phenomena of order in alloys are included in a general class known under the name of "cooperational phenomena." Physical systems

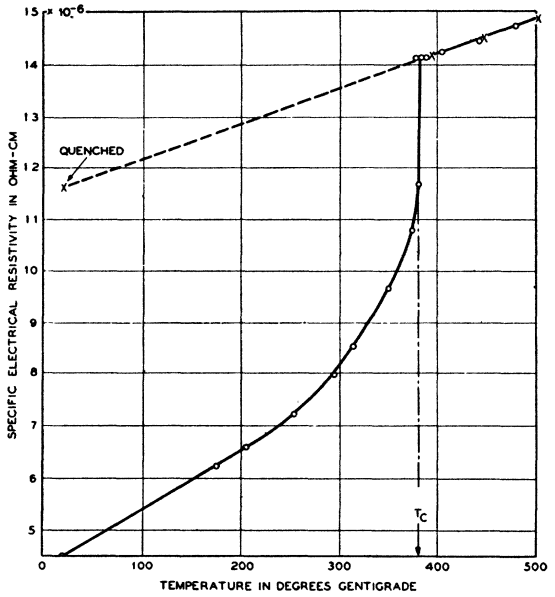

FIG. 5. Electrical resistivity-*vs.*-temperature for Cu_3Au. The alloy was in equilibrium at temperatures above 350°C.

exhibiting cooperational effects contain certain units which act jointly in producing a certain cooperational property, the amount of this property so produced being then a measure of the degree of cooperation: in our case, the atoms united in forming a superlattice. The process of cooperation is in general of the following character: the ability of the units to join forces in opposition to disruptive influences, like thermal agitation, is greatly enhanced by any increase in the existing degree of cooperation—so greatly enhanced, in fact, that when the disruptive influence is not too large, the units establish a cooperational state.

The three best known cooperational phenomena are ferromagnetism, the libration-rotation transition in solids, and the order-disorder transformation in alloys. Of these three, the youngest and apparently best equipped with a satisfactory statistical theory is the third. The recent developments in it have, we believe, furnished a new and enlightening viewpoint which will aid in the understanding of the entire field; and, in fact, the extension of some new methods of the order-disorder theory to other cooperational phenomena is now in progress.[37V]

PART I. THEORIES OF THE ORDER-DISORDER PHENOMENON

A. Equilibrium theories for simple unvaried compositions

In the following four sections we shall deal with alloys having certain fixed simple compositions. We shall further suppose that for all states of order—from perfect order to randomness—there is no significant change in the arrangement of the lattice sites; that is, the only effect which we consider is one of arrangement of the atoms upon an unalterable framework. Some of the theories are sufficiently general to apply to a wide variety of lattice types. For the others we shall deal specifically with simple cubic, body-centered cubic, and face-centered cubic arrangements of lattice sites. For these cases all sites are intrinsically equivalent, and it will be only the arrangement of the atoms in the lattice which makes any one site appropriate for one species of atom rather than for another.

In some actual cases, there are slight distortions of the lattice, usually associated with states of order; in others, there may actually be produced upon ordering an entire rearrangement of sites. We shall postpone a discussion of these effects until Part II, and in accord with our assumptions, we shall disregard their influence in our theory. We shall also disregard those vexing questions of terminology which arise for alloys, where in a strict sense the absence of a repeated unit cell makes the use of the word "lattice" incorrect.

We shall be concerned entirely with binary alloys (the two chemical elements shall be denoted by A and B) and with only two compositions of these: one having equal numbers of A and B atoms and described by the chemical formula AB, the other having three B atoms for each A atom and described by AB_3. Later, when we generalize our considerations, the composition will be specified by the atomic percent of A, the above cases corresponding to 50 and 25, respectively. For the present cases it is always possible to choose a regular set of α-sites—one for each A atom—which form a lattice by themselves. The remaining sites are β-sites and are just sufficient to accommodate the B atoms. Owing to the equivalence of all sites, it is always possible to choose the α-sites in several equivalent ways and it is immaterial which selection is made.

The energy, specific heat, and other properties of an alloy depend upon many factors besides those associated with atomic configurations or state of order. For example the energy of the alloy will depend not only upon this arrangement but also upon the state of thermal vibration. In the theories, unless otherwise stated, it will be assumed that the effects of changes of order and the effects due to thermal vibrations can be separated from each other and that this separation has been carried out. The energy, entropy, and specific heats calculated below will be those associated with the state of order. They are the so-called "anomalous" or "configurational" parts. The ordinary quantities, such as are associated with the Dulong-Petit law, will not be considered.

1. The theory of Bragg and Williams[34C, 35E, 35V]

The basic concept of the theory of Bragg and Williams is that of long range order. Our first task will be to give this a quantitative definition. We shall then see how it leads to a theory predicting a critical temperature, sometimes with and sometimes without a latent heat. The absence of short range order from this theory is a defect, which will be remedied in the treatment of Bethe's theory in the next section.

Let us now suppose that the α-sites have been chosen, and the A atoms placed upon them. The remaining β-sites are then occupied by B atoms. Let the total number of atoms, which is also the total number of sites, be N. Throughout this work we shall deal with one gram atom of material; hence $N=6.06\times10^{23}$ and $Nk=R$ $=1.986$ cal./°C g atom. Let F_A be the fraction of atoms which are A atoms and also the fraction of sites which are α-sites; then $1-F_A=F_B$ is the corresponding quantity for B and β.

When the perfectly ordered arrangement is disturbed, some of the A atoms will move to β-sites, displacing an equal number of B atoms which move to α-sites. We describe such situations by stating the fraction of α-sites still occupied by right atoms; let this fraction be r_α.

The fraction of α-sites wrongly occupied is $1-r_\alpha=w_\alpha$. Similarly r_β and w_β represent the correctly and incorrectly occupied β-sites. The number of A atoms on the β-sites is $w_\beta F_B N$ and is equal to the number of B atoms on α-sites, $w_\alpha F_A N$. From these considerations we can deduce the equations

$$1=F_A+F_B=r_\alpha+w_\alpha=r_\beta+w_\beta, \quad (1.1)$$

$$w_\alpha F_A=w_\beta F_B. \quad (1.2)$$

In the state of perfect order r_α and r_β are unity and w_α and w_β are zero. In the state of randomness the probability that any given site is occupied by an A atom is F_A; hence the fraction of the α-sites occupied by A atoms is also F_A and in terms of our notation we find $r_\alpha=w_\beta=F_A$ and $w_\alpha=r_\beta=F_B$. The Bragg-Williams order parameter, S, is to be so defined that it is unity for perfect order and zero for the random state.

	Perfect Order	Random State
r_α	1	F_A
w_α	0	F_B
r_β	1	F_B
w_β	0	F_A
S	1	0

The tabulation suggests several definitions for S in terms of the other parameters; as may be verified from Eqs. (1.1) and (1.2), these are equivalent, and we write

$$S=\frac{r_\alpha-F_A}{1-F_A}=1-\frac{w_\alpha}{F_B}=\frac{r_\beta-F_B}{1-F_B}=1-\frac{w_\beta}{F_A}. \quad (1.3)$$

Order as a function of ordering energy and temperature $S(V, T)$

We must next consider thermal equilibrium at a certain fixed temperature, T. First of all we suppose that at the equilibrium condition there is a definite ordering energy V which acts in such a way that interchanging an A atom upon an α-site with a B atom on a β-site, thus producing two wrong atoms, raises the energy of the crystal by V. This energy is assumed to be the same for all pairs of sites in the lattice and does not vary depending on fluctuations of local order. This assumption is not in keeping with the description of the order-disorder transformation given in the introduction, which was, as we shall see later, based on Bethe's theory of Section 2.

At the end of this section we shall give a rigorous derivation of the equilibrium condition using the free-energy principle of statistical mechanics. Before doing this, however, we shall follow the more simple procedure used first by Bragg and Williams to obtain their result. We need only consider the A atoms, since once their positions are fixed, the distribution of the B atoms is automatically determined. Let us next consider that all but one of the A atoms are immobile and inquire into the probability that this one is right or wrong. This atom will move about the lattice by exchanging positions with adjoining B atoms. It will spend a fraction f_α of the time on α positions and f_β on β-positions, and it is our problem to find the ratio f_α/f_β, that is, the relative probability of this atom being in a right position compared to its being in a wrong position. Fortunately we can disregard the dynamics of the process of interchange of positions and, knowing only that such a process exists, find our answer in the Boltzmann statistics. There are $w_\alpha F_A N$ available (i.e., not occupied by other A atoms) right positions for this atom and $r_\beta F_B N$ available wrong positions. These wrong positions are, however, weighted unfavorably by the Boltzmann factor $\exp(-V/kT)$ corresponding to the extra energy V of having an A atom in wrong position. Hence, for the A atom under consideration the ratio of the probability of being right to the probability of being wrong is

$$(w_\alpha F_A N)/[r_\beta F_B N \exp(-V/kT)]. \quad (1.4)$$

Now if the alloy is in equilibrium, the behavior of this A atom must be typical of all the A atoms and the distribution of A atoms between α- and β-sites must be given by the above proportion. The numbers of A atoms in α- and in β-sites are, respectively $r_\alpha F_A N$ and $w_\beta F_B N$; hence the condition for statistical equilibrium is

$$r_\alpha F_A N/w_\beta F_B N = (w_\alpha F_A N/r_\beta F_B N)\exp(V/kT) \quad (1.5)$$

or expressing our results in words

$$\frac{\text{number of } \alpha\text{-sites occupied by } A \text{ atoms}}{\text{number of } \beta\text{-sites occupied by } A \text{ atoms}}=\frac{\text{number of } \alpha\text{-sites not occupied by } A \text{ atoms}}{\text{number of } \beta\text{-sites not occupied by } A \text{ atoms}}\exp\frac{V}{kT}. \quad (1.6)$$

These expressions are readily simplified to

$$r_\alpha r_\beta / w_\alpha w_\beta = \exp\,(V/kT); \qquad (1.7)$$

and this may be expressed in terms of S as

$$\{[1/F_B(1-S)]-1\}\{[1/F_A(1-S)]-1\} = \exp\,(V/kT). \qquad (1.8)$$

It may be readily verified that the quantities in the braces are positive and that the value zero for S corresponds to zero for V/kT—that is to zero ordering energy or infinite temperature, while unity for S corresponds to infinity for V/kT. Intermediate values of V/kT will give values of S between that for perfect order and that for randomness.

It is of advantage to note that in Eq. (1.8) S appears as a function of a single variable (V/kT). We express the explicit form of the dependence to be obtained by solving (1.8) for S by the symbolism:

$$S = S(V/kT) = S(X), \qquad (1.9)$$

$$X = V/kT. \qquad (1.10)$$

Bragg and Williams consider the behavior of S specified by the above form for varying V while T is held fixed. Under these circumstances they refer to it as "S-of-V," i.e., $S(V)$; this emphasizes that the derivation was obtained by assuming a certain fixed value of V and then finding the equilibrium value of S from it. We shall deal with the form as a function of X; however, the physical picture is the same.

For the simple case denoted by AB (*viz.* $F_A = F_B = \frac{1}{2}$), Eq. (1.8) may easily be solved for S, yielding

$$S = \tanh\,(X/4). \qquad (1.11)$$

Dependence of ordering energy upon order, $V(S)$

We have just determined how the ordering energy V and the temperature T lead by Boltzmann statistics to a value S for the order. However, this is only half of the story for the ordering energy V is in itself determined directly by the state of order in the alloy. Let us for the moment postpone a further consideration of the $S(X)$ relationship and concentrate upon the way in which V depends upon the state of order.

When the alloy is perfectly ordered, the creation of a pair of wrong atoms requires a certain definite amount of energy which we shall denote by V_0. However, as the alloy becomes disordered, the amount of energy required to effect such an interchange becomes less. This can be seen most easily for the state of randomness. For this there is no physical way of telling which set of lattice sites are α and which are β; the difference between them being a purely mathematical one carried over by our memory of the situation which existed while we still were imagining a superlattice. For the case of randomness, then, there will be no energy involved in the interchange of atoms between the physically meaningless α- and β-sites and V will be zero. Hence V depends on the order in such a way as to have its maximum value, V_0, for $S=1$ and its minimum, zero, for $S=0$. The simplest assumption to make for the relationship between V and S satisfying these conditions and the one which we shall accept for the purpose of this section is the one made by Bragg and Williams:

$$V = V_0 S. \qquad (1.12)$$

This description of the ordering energy is, as Bragg and Williams point out, rather coarse grained. Actually the ordering energy between any pair of atoms depends on the arrangement of their immediate neighbors and only indirectly on the distribution of atoms upon the α- and β-sites over the entire lattice. This defect is largely removed in the theory of Bethe, discussed in Section 2, in which the entire energy of the superlattice arises from the interaction of nearest neighboring pairs of atoms.

The relationship $V = V_0 S$ is denoted by $V(S)$ and called the "V-of-S relationship" by Bragg and Williams; this serves to emphasize the ideas involved in its origin—that it specifies how the force tending to produce order in the lattice depends upon the state of order already prevailing there. One important respect in which $V(S)$ differs from $S(X)$ is its definiteness; no matter what the temperature is or whether the system is or is not in equilibrium, whenever the order has value S the ordering energy has value $V = V_0 S$; on the other hand when the system is not in equilibrium, then the other interrelation $S(X)$ between S, V, and T ceases to hold.

The Bragg-Williams assumption about the ordering energy leads to a simple expression for the energy of the alloy. In order to change the alloy from order S to order $S+dS$ we must move a certain number of A atoms from wrong to right positions. This number is readily found from the definition of order Eq. (1.3) to be

$$F_A N dr_\alpha = F_A N F_B dS.$$

For each one of these moves the energy decreases by $V = V_0 S$; hence the change in energy of the alloy is

$$dE = -VF_A N F_B dS$$
$$= -NV_0 F_A F_B S dS.$$

This can be readily integrated and choosing the state of perfect order as the zero of energy we find

$$E(S) = \tfrac{1}{2} N V_0 F_A F_B (1-S^2) = E_0(1-S^2), \quad (1.13)$$

$$E_0 = \tfrac{1}{2} N V_0 F_A F_B. \quad (1.14)$$

Here E_0 represents the entire energy of the order-disorder transformation of one gram atom of alloy. Throughout this section, no matter what theory we are treating, we shall always mean by E_0 the energy required to change the alloy from the state of best order to that of randomness. For the cases AB and AB_3 we find $E_0 = NV_0/8$ and $3NV_0/32$, respectively; these values are given in row one of Table I, p. 15.

Statistical equilibrium, case of AB

If the temperature is regarded as constant with value T_1, there are now two equations for the two unknowns V and S. The simultaneous solution of these equations leads to the condition of equilibrium. For clarity we write them once more in a slightly modified form

$$S = S(V/kT_1) = S(X), \quad (1.15)$$

$$S = \frac{V}{V_0} = \left(\frac{kT_1}{V_0}\right)\left(\frac{V}{kT_1}\right) = \frac{kT_1}{V_0} X. \quad (1.16)$$

We see now that the right sides of these equations can be regarded as two functions of $X(=V/kT_1)$. The equilibrium condition corresponds to a value of X for which they are equal, i.e. $(kT_1/V_0)X = S(X)$, the corresponding values of V and S then being the equilibrium values. In order to solve these equations, Bragg and Williams plot the right sides as functions of X. The crossing point of the two curves then specifies the desired condition.

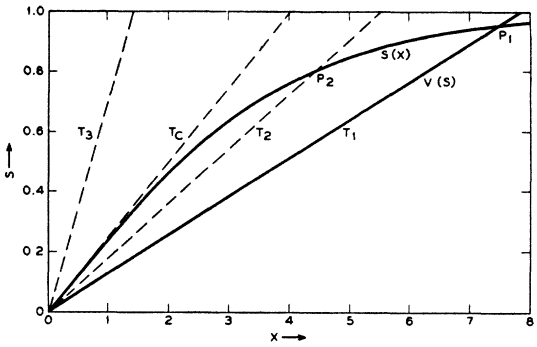

FIG. 6. $V(S)$ for several temperatures and $S(X)$, AB case.

Figure 6 is such a plot, drawn for the AB case. The $S(X)$ curve shows that for large values of X, i.e., high ordering energies or low temperatures S approaches unity—perfect order—while for small V or high T, S approaches zero. The $V(S)$ relationship is, of course, represented by a straight line through the origin with slope (kT_1/V_0). The intersection point P_1, gives the equilibrium values of S and V for the temperature T_1. For higher temperatures, T_2 say, the slope of the $V(S)$ line is steeper[1] and the $S(X)$ curve is, of course, the same. The intersection point moves to P_2, with a lower degree of order. As yet higher temperatures are attained, P moves lower and lower on the $S(X)$ curve until finally, at T_3 for example, the $V(S)$ line no longer intersects $S(X)$ except at the origin.

It is of interest to find the temperature at which P just reaches the origin; this is the critical temperature, and above it there is no long distance order. It occurs when the line $S = (kT/V_0)X$ is tangent to $S(X)$ at the origin, hence when (kT/V_0), the slope of $V(S)$, is equal to $dS(X)/dX$ at $X=0$. From Eq. (1.11) we easily find that for $X=0$

$$dS/dX = \tfrac{1}{4}.$$

Hence we obtain

$$kT/V_0 = \tfrac{1}{4} \text{ or using } E_0 = NV_0/8,$$

$$T_c = V_0/4k = 2E_0/R, \quad (1.17)$$

[1] This does not mean that the relationship $V(S)$ has changed but that the relationship between V and X has.

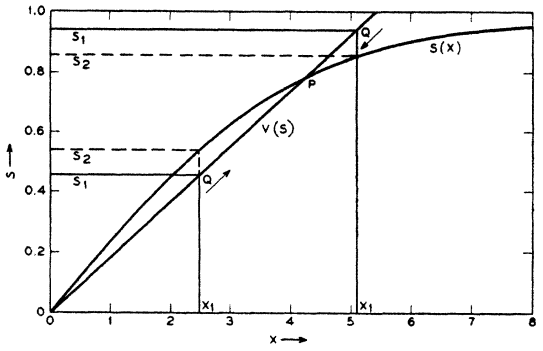

FIG. 7. Illustrating the approach of the system towards equilibrium.

where T_c denotes the critical temperature. This value will be found in the second row of Table I.

Nonequilibrium behavior

Under some circumstances the alloy will not be in the equilibrium state; its state of order will change with time. In a later section we shall discuss this matter quantitatively and for the present content ourselves with showing in which direction the system will tend.

Suppose that the alloy is at the temperature T which corresponds to the line $V(S)$ on Fig. 7. Since this line is the mathematical expression for $V=V_0S$, which—according to assumption—is always true, any possible state of the system is represented by a point on this line. Suppose initially the system has order S_1 indicated in the lower part of the figure. Then its state is represented by the point Q whose X coordinate is X_1. Now if the temperature and ordering energy were given unalterable values which lead to the value X_1 for X, then the equilibrium value of order would be $S_2=S(X_1)$. Hence when the system is in the state specified by X_1, it will strive towards the order S_2. For this case S_2 is greater than S_1; hence the order of the system will increase with time and the point Q will move toward P. A repetition of this argument shows that Q will move upwards whenever S_2 is above S_1 and downwards when S_2 is below S_1; that is upwards whenever $S(X)$ is above $V(S)$.

We see, therefore, that P is a point of stable equilibrium. This cannot be said for the origin, however, for although it represents a solution of the equations, we see that any fluctuation from it will lead to situations with $S(X)$ greater than $V(S)$ which will then tend to higher values of S until P is reached.

Statistical equilibrium, case of AB_3

Bragg and Williams have treated cases other than those corresponding to alloys represented by the formula AB. The type AB_3, which corresponds to several physically interesting cases such as Cu_3Au, is of considerable interest and its S *vs.* X plot is shown in Fig. 8. This figure is only schematic for it has been necessary to exaggerate greatly the reversal of curvature of the $S(X)$ curve in order to make it apparent on a plot of this size. We see that there is an important difference between this and the AB case because it now is possible to have three simultaneous solutions to the equations (1.15) and (1.16):

$$S=S(X),$$
$$S=(V/V_0)=(kT/V_0)X.$$

The $V(S)$ line which corresponds to temperature T_2 gives three intersections; the origin, P', and P. If we apply the nonequilibrium theory of the preceding paragraphs to this situation, we see that P' is unstable and that an initial state of order giving point Q will tend to P if it starts above P' and to the origin if it starts below P'.

From this reasoning we should conclude that at any temperature giving three intersections, there would be two stable states of the alloy, one being that of complete disorder. These two states, which will have different degrees of order and different energy contents, may be regarded as different phases of the substance and the idea that they can be in equilibrium over a common

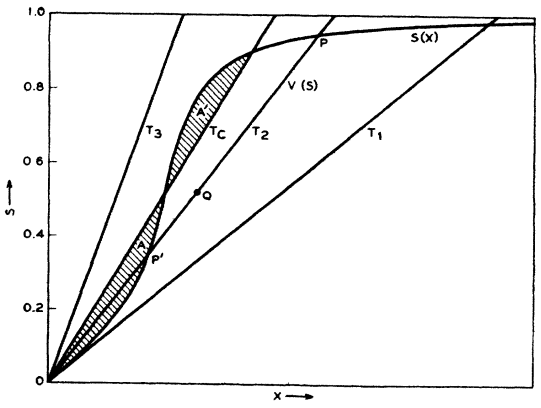

FIG. 8. $V(S)$ for several temperatures and $S(X)$, AB_3 case.

large temperature range can be shown to contradict the Gibbs phase rule. By arguments based on considerations of free energy given later in this section, it can be shown that for temperatures below a certain critical temperature T_c, P has a lower free energy than $S=0$ and hence gives the thermodynamical equilibrium state; above T_c, $S=0$ is the equilibrium state. The line corresponding to T_c is shown on the figure, for it the loops A and A' have equal areas, and as will be shown later, this condition implies the equality of the two free energies. At the critical temperature the conditions are found to be

$$S=0.467$$

and
$$T_c=0.205\,V_0/k=2.18E_0/R. \qquad (1.18)$$

Details of the predictions of the theory

Order.—When the computational work necessary to determine the dependence of order on temperature is carried out, the curves marked Bragg-Williams of Figs. 9 to 14 are obtained. The other curves refer to theories described later. In all cases the temperature scale is given in reduced units: RT divided by the entire configurational energy change from perfect order to randomness. We see that the order of the AB alloy decreases to zero at a certain critical temperature, taking on all values between unity and zero. For AB_3, however, there is a jump at T_c and the order falls from 0.467 directly to zero. The reader will easily verify that these results are entirely in harmony with the qualitative predictions based on Figs. 6 and 8.

Energy.—The dependence of order upon temperature can be inserted in Eq. (1.13), $E(S)=E_0(1-S^2)$ and the energy-*vs.*-temperature curves in Figs. 11 and 12 obtained.

For AB_3, there is a discontinuity in order and hence in energy at T_c. This change in energy manifests itself as a latent heat which must be given to the alloy in order to transform it from the state of order $S=0.467$ to the state of order $S=0$ at the critical temperature. The value of the latent heat Q, is easily calculated from the relationship $E(S)$:

$$Q=E(0)-E(.467)=(0.467)^2E_0$$
$$=0.218E_0=0.0205NV_0=0.100RT_c. \qquad (1.19)$$

It is in the Bragg-Williams theory, that as we have just been saying, the whole of the energy of transformation E_0 is required to get the alloy to the state of order $S=0$ at a temperature just above T_c. This is not true in the theories described later involving the notion of short distance order: according to these only a part, denoted by $E(T_c+)$, of E_0 is required. We shall denote by $E(T_c-)$ the energy required to get up to the critical temperature without making the transition. Hence $E(T_c+)-E(T_c-)=Q$ represents the latent heat. These quantities are given in Table I. The energy yet to be gained through destruction of local order above T_c is $(E_0-E(T_c+))=E_c(\sigma)$.

It is of interest to compare the critical temperature with the energy $E(T_c+)$ required to bring the alloy to the state of zero long range order, that is, to $S=0$. For this purpose $RT_c/E(T_c+)$ is tabulated. All theories give about the same value—approximately 2—for this quantity.

Specific heat.—The configurational specific heat is found by differentiating: $C=dE/dT$. This quantity has the interesting property, as is proved below, of being the same function of S or RT/E_0 for all values of V_0. As may be concluded from dimensional arguments, or from the details of the calculations given above, the equilibrium value of S must be a function of $RT/E_0=y$. Combining this with Eq. (1.13) we find

$$C=(d/dT)E_0(1-S^2)=-2E_0S(d/d\,)S(y)$$
$$=-2RS(d/dy)S(y). \qquad (1.20)$$

Thus neither E_0, V_0, nor T appear explicitly and C depends only upon the analytical form of S as a function of RT/E_0.

The algebraic work involved in calculating dS/dy is tedious and the reader is referred to reference 38C for details. The results for AB and AB_3 are shown in Figs. 13 and 14.

Entropy.—With the increase of energy and disorder as the temperature rises, there is associated an increase in entropy. This can be calculated in two ways; by thermodynamics, $d\Phi=dQ/T=dE/T$; or by the Boltzmann relation, $\Phi=k\ln W$ where W is the *a priori* probability. When we give the free energy treatment, we show that these are equivalent. For our present purposes it is much more convenient to use Boltzmann's relation.

For a given value of S, other than unity, there will be a large number of ways of arranging the

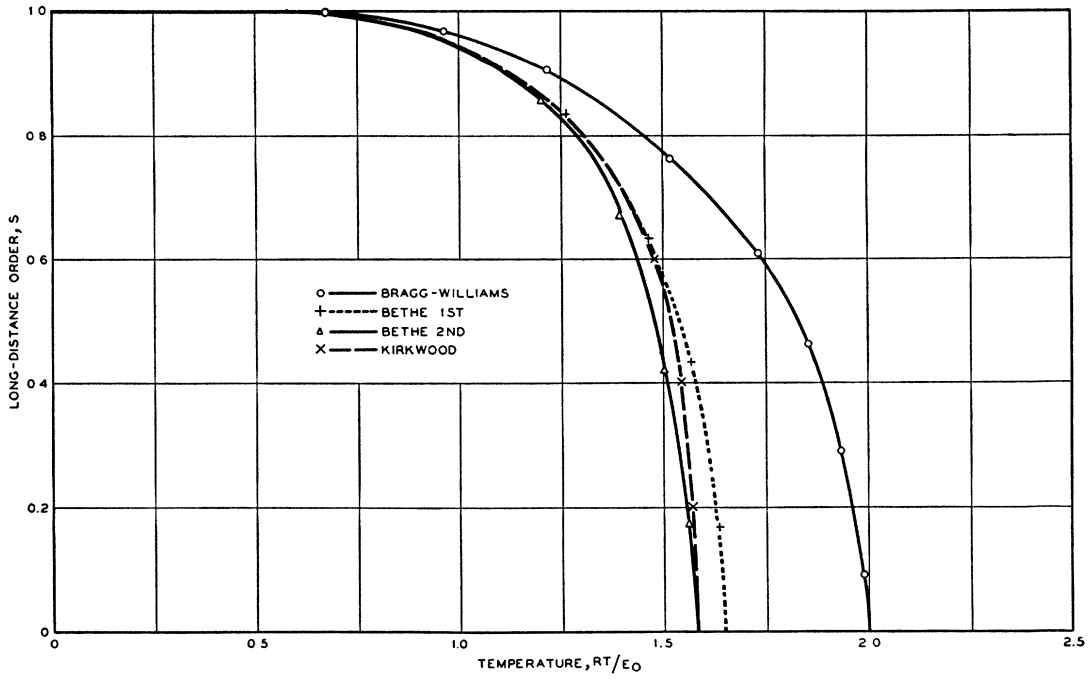

FIG. 9. Long range order *versus* temperature for the AB case. Simple cubic lattice for Bethe and Kirkwood curves.

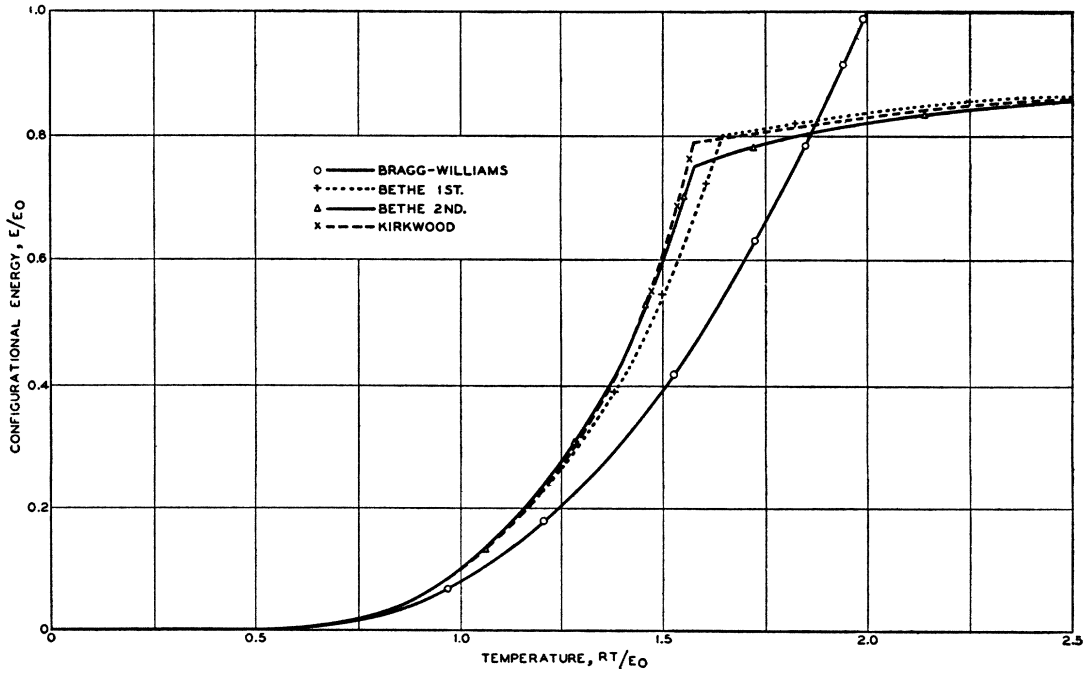

FIG. 11. Configurational energy *versus* temperature for the AB case. Simple cubic lattice for Bethe and Kirkwood curves.

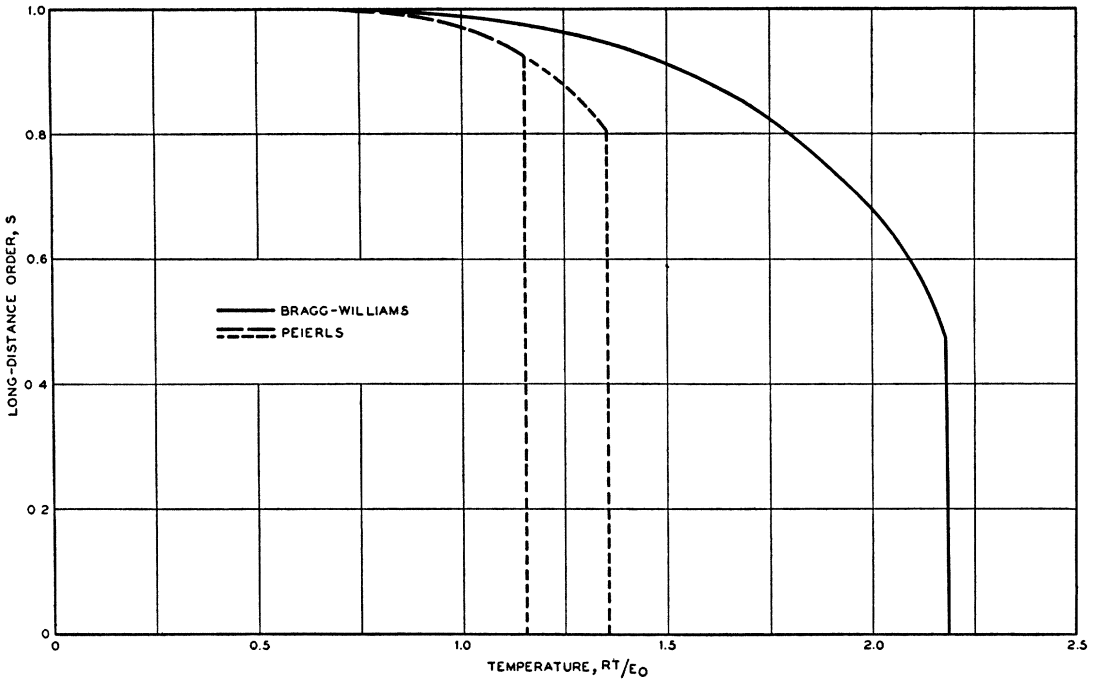

FIG. 10. Long range order *versus* temperature for the AB_3 case. Face-centered cubic lattice for Peierls curve.

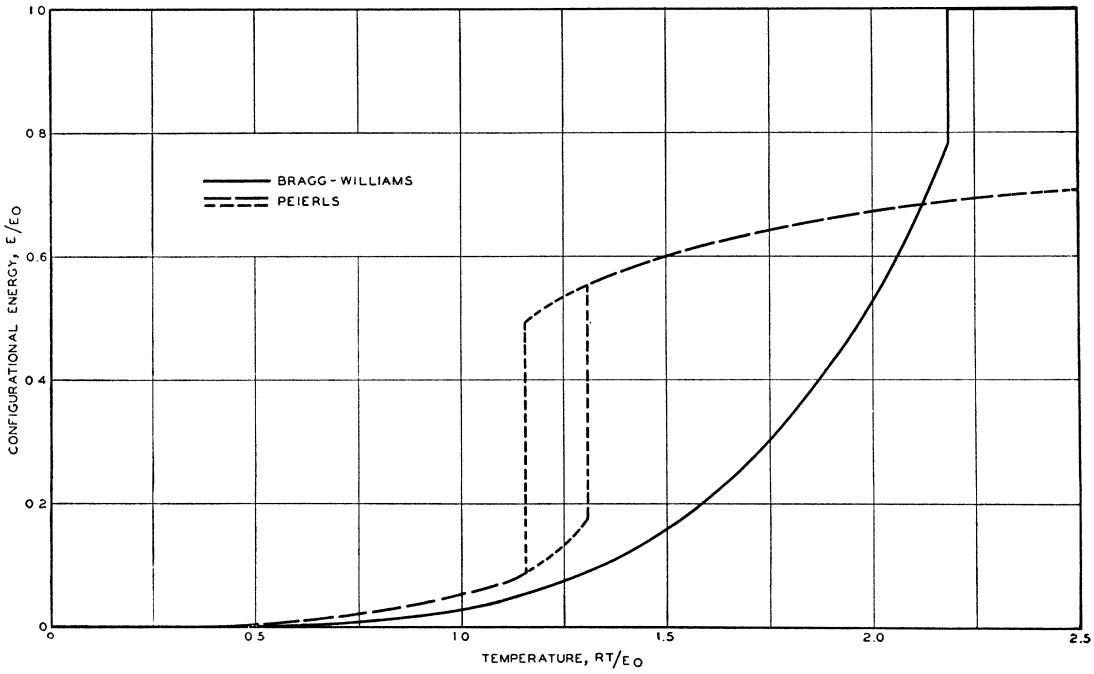

FIG. 12. Configurational energy *versus* temperature for the AB_3 case. Face-centered cubic lattice for Peierls curve.

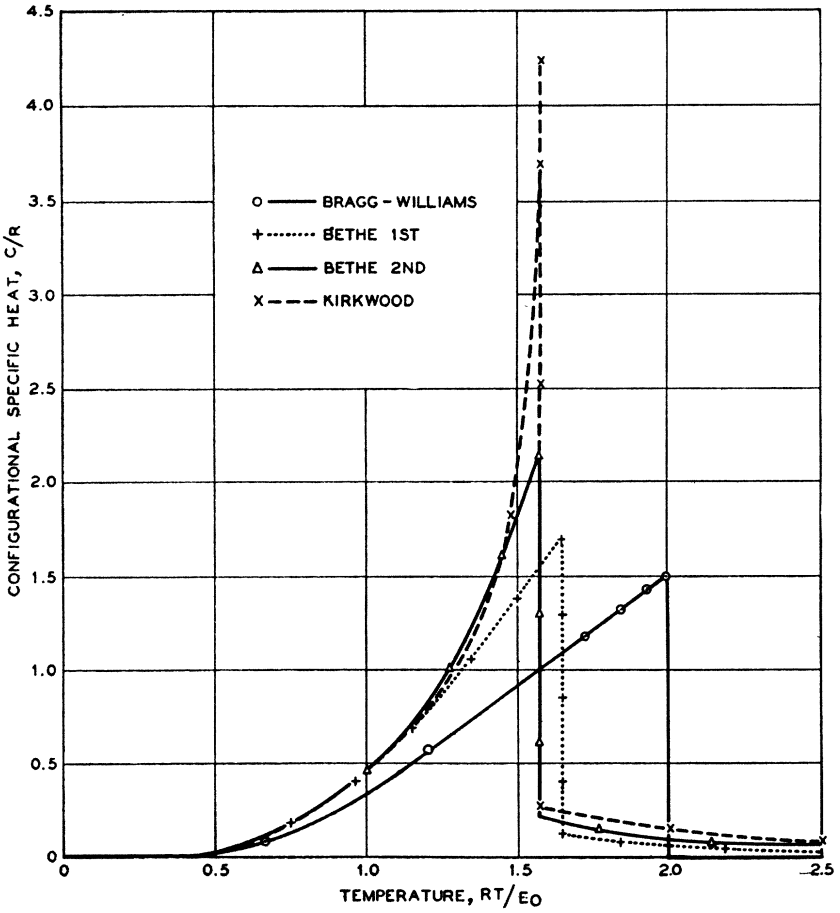

FIG. 13. Configurational specific heat *versus* temperature for the AB case. Simple cubic lattice for Bethe and Kirkwood curves.

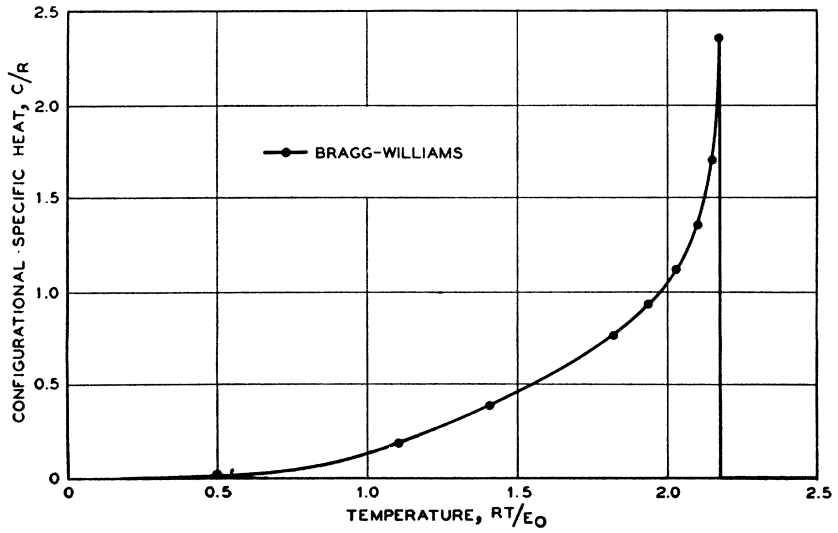

FIG. 14. Configurational specific heat *versus* temperature for the AB_3 *case.*

TABLE I. *Eo, Energy of transformation from perfect order to randomness; Tc, critical temperature; E(Tc−), configurational energy just below Tc; Q, latent heat at Tc; E(Tc+), configurational energy just above Tc, energy necessary to destroy superlattice; $E_c(\sigma)$, energy retained by short range order just above Tc; Φ(Tc−), entropy just below Tc; Φ(Q), entropy change due to latent heat; Φ(Tc+), entropy just above Tc; $\Phi_c(\sigma)$, entropy retained by short range order just above Tc; Φ(∞), total entropy change; C(Tc−), specific heat just below Tc; C(Tc+), specific heat just above Tc.*

ALL QUANTITIES REFER TO 1 GRAM ATOM	*AB* BRAGG-WILLIAMS	*AB* SIMPLE CUBIC *Z*=6 BETHE'S 1ST	*AB* SIMPLE CUBIC *Z*=6 BETHE'S 2ND	*AB* SIMPLE CUBIC *Z*=6 KIRKWOOD	*AB* BODY-CENTERED CUBIC *Z*=8 BETHE'S 1ST	*AB* BODY-CENTERED CUBIC *Z*=8 KIRKWOOD	AB_3 BRAGG-WILLIAMS	AB_3 FACE-CENTERED CUBIC *Z*=12 PEIERLS
Eo	*NVo*/8	3*Nv*/2	3*Nv*/2	3*Nv*/2	2*Nv*	2*Nv*	3*NVo*/32	3*Nv*/4
RTc/Eo	2	1.644	1.581	1.577	1.738	1.707	2.19	1.33
E(*Tc*−)/*Eo*	1	0.800	0.754	0.789	0.857	0.854	0.792	0.18
Q/*Eo*	0	0	0	0	0	0	0.218	0.36
E(*Tc*+)/*Eo*	1	0.800	0.754	0.789	0.857	0.854	1.00	0.54
Ec(σ)	0	0.200	0.246	0.211	0.143	0.146	0	0.46
RTc/*E*(*Tc*+)	2	2.055	2.097	2	2.028	2	2.19	2.38
Φ(*Tc*−)/*R*	0.693	0.633	0.628	0.626	0.652	0.650	0.462	0.19
Φ(*Q*)/*R*	0	0	0	0	0	0	0.100	0.27
Φ(*Tc*+)/*R*	0.693	0.633	0.628	0.626	0.652	0.650	0.562	0.46
$\Phi_c(\sigma)/R$	0	0.0604	0.065	0.067	0.0411	0.043	0	0.10
Φ(∞)/*R*	0.693	0.693	0.693	0.693	0.693	0.693	0.562	0.562
C(*Tc*−)/*R*	1.50	1.90	2.14	4.233	1.78	2.207	2.36	——
C(*Tc*+)/*R*	0	0.119	0.203	0.134	0.081	0.0858	0	0.16

atoms. We take the *a priori* probability of the state with order S to be proportional to $W(S)$, the number of ways. We shall then obtain the relationship:

$$\Phi = k \ln W(S). \tag{1.21}$$

To find the number of ways consider the $F_A N$ atoms on the α-sites. Of these $r_\alpha F_A N$ are A atoms and $w_\alpha F_A N$ are B atoms. The number of distinct ways of arranging them, (considering arrangements which differ only by permutations of the A atoms among themselves and the B atoms among themselves as not distinct) is given in a well-known way by the binomial coefficient:

$$W_\alpha = \binom{F_A N}{r_\alpha F_A N} = \frac{F_A N!}{(r_\alpha F_A N)!(w_\alpha F_A N)!}. \tag{1.22}$$

A similar expression gives the number of ways of arranging the atoms on the β-sites. The *a priori* probability of the state S is given by

$$W(S) = W_\alpha \times W_\beta \tag{1.23}$$

and the application of Stirling's formula for the factorials gives:

$$\Phi(S) = k \ln W(S) = -kN[F_A(r_\alpha \ln r_\alpha + w_\alpha \ln w_\alpha) + F_B(r_\beta \ln r_\beta + w_\beta \ln w_\beta)]. \tag{1.24}$$

This can be expressed in terms of S and becomes:

$$\begin{aligned}\Phi(S) = k \ln W(S) = \\ -R[F_A[1-F_B(1-S)] \ln [1-F_B(1-S)] \\ + F_A F_B(1-S) \ln F_B(1-S) \\ + F_B[1-F_A(1-S)] \ln [1-F_A(1-S)] \\ + F_B F_A(1-S) \ln F_A(1-S)].\end{aligned} \tag{1.25}$$

The reader will recognize that each expression of which the logarithm is taken is positive and not greater than unity; hence each term in the sum is negative and Φ is positive. A further consideration will show that the limits for $S=1$ and $S=0$ are

$$\begin{aligned}\Phi(1) &= 0, \\ \Phi(0) &= -R[F_A \ln F_A + F_B \ln F_B].\end{aligned} \tag{1.26}$$

This gives for the entropy changes from order to disorder the values

$$AB \quad \Delta\Phi = R \ln 2 = 0.693R = 1.37 \text{ cal./°C g atom}, \tag{1.27}$$

$$AB_3 \quad \Delta\Phi = R\tfrac{1}{4}[4 \ln 4 - 3 \ln 3] = 0.562R = 1.11 \text{ cal./°C g atom}. \tag{1.28}$$

These two values must be obtained for *any* theory which assumes that at the lowest temperature the arrangement is perfect and that at the highest temperature the arrangement is random.

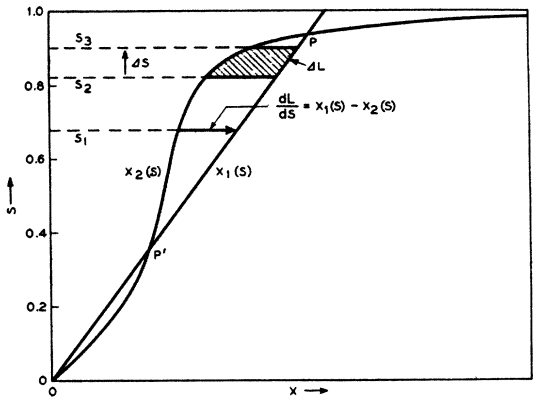

FIG. 15. Comparing the free energy method with the $V(S)$ and $S(X)$ method.

They are not restricted merely to application with the Bragg-Williams approximation.

We can also calculate the entropy just below the critical temperature; putting $S=0.467$ in Eq. (1.25) we obtain $\Phi(0.467)=0.462R$. In this case we can calculate the entropy easily in another way. The entropy above the critical temperature where $S=0$, has already been calculated and is $0.562R$. Also the latent heat is $0.100RT_c$ so that the change in entropy at T_c is $0.100R$. Hence the entropy just below T_c is

$$0.562R-0.100R=0.462R. \qquad (1.29)$$

The fact that the Bragg-Williams treatment gives this thermodynamic consistency is a consequence of the theorem proved in the following paragraphs: that the Bragg-Williams method is equivalent to a statistical mechanical free energy treatment; and it is known that such treatments are always thermodynamically consistent and in fact can be made to yield demonstrations of the basic thermodynamic principles.

Derivation of the Bragg-Williams equations from the free energy principle.

We shall now utilize the expression for entropy obtained in the last section in order to derive afresh and more rigorously the principles of the Bragg-Williams theory. This treatment follows that given by Williams[35V] and by Fowler.[36J]

The statistical mechanical weight of a given state of a system is equal to the product of the *a priori* probability times the Boltzmann factor. Thus the weight of the state of order S is

$$\gamma(S)=W(S)\exp(-E(S)/kT), \qquad (1.30)$$

where $W(S)$ has been calculated above, Eq. (1.25), and $E(S)$ is given by Eq. (1.13):

$$E(S)=\tfrac{1}{2}NV_0F_AF_B(1-S^2). \qquad (1.31)$$

The equilibrium state at a given temperature is that with the largest value of $\gamma(S)$. In order to determine this state we shall maximize not $\gamma(S)$, but instead the equivalent quantity $\ln\gamma(S)$, in respect to S. The expression for $\ln\gamma(S)$ is

$$\ln\gamma(S)=\ln W(S)-E(S)/kT. \qquad (1.32)$$

Although we shall deal with $\ln\gamma(S)$ in the form just given, we shall write it once more in an interesting variation:

$$\begin{aligned}-kT\ln\gamma(S)&=E(S)-Tk\ln W(S)\\&=E(S)-T\Phi(S)\\&=F(S).\end{aligned} \qquad (1.33)$$

As the above sequence of equalities shows, $\ln\gamma(S)$ is simply related to the free energy F. Thus our argument presents a somewhat simplified proof that the thermodynamic equilibrium requirement of minimum free energy is a consequence of the statistical mechanical demand for maximum probability.[2]

We shall now maximize $\ln\gamma(S)$ in respect to S. The expressions appearing on the right of equation (1.32) are known functions of S given in Eqs. (1.25) and (1.13). Carrying out the process gives:

$$\begin{aligned}0=\frac{d\ln\gamma(S)}{dS}&=\frac{d\ln W(S)}{dS}-\frac{1}{kT}\frac{d\ln E(S)}{dS}\\&=NF_AF_B\left[-\ln\left(\frac{1}{F_A(1-S)}-1\right)\right.\\&\quad\left.-\ln\left(\frac{1}{F_B(1-S)}-1\right)\right]+\frac{1}{kT}NV_0F_AF_BS\\&=NF_AF_B\left[-\ln\left(\frac{1}{F_A(1-S)}-1\right)\right.\\&\quad\left.-\ln\left(\frac{1}{F_B(1-S)}-1\right)+\frac{V_0S}{kT}\right].\end{aligned} \qquad (1.34)$$

The factor NF_AF_B may well be removed to the other side and we write

[2] Since a rigorous discussion of thermodynamic analogs has no place in this review, we shall be content with this rough demonstration. For a comprehensive treatment of such questions, the reader should consult 36J.

$$L(S)=\ln \gamma(S)/NF_AF_B, \tag{1.35}$$

$$X_1(S)=(V_0/kT)S, \tag{1.36}$$

$$X_2(S)=\ln\left[\frac{1}{F_A(1-S)}-1\right]\left[\frac{1}{F_B(1-S)}-1\right]. \tag{1.37}$$

The condition of equilibrium is then equivalent to making L a maximum

$$dL/dS=X_1(S)-X_2(S)=0. \tag{1.38}$$

In order to solve this equation we plot $X_1(S)$ and $X_2(S)$ as functions of S. The results for the case of AB_3 are shown in Fig. 15. For reasons which will soon be apparent we plot S as ordinate and X_1 and X_2 as abscissae. We see then that the curves appear to be the same as those we drew in Fig. 8 in connection with $S(X)$ and $V(S)$. We shall postpone a proof of this identity for a few lines and instead study this figure in its new aspect.

For any given value of S, say S_1, dL/dS is equal to the horizontal difference between the two curves (X_1-X_2). When this is positive a larger probability will be found by increasing S; and the change in L in going from S_2 to S_3, for example, will be represented by the area between the curves indicated by shading. A simple continuation of this argument shows that P' always gives a smaller value of L and hence of $\ln \gamma(S)$ than $S=0$ or P and that $S=0$ and P have the same value for $\ln \gamma(S)$ only when T is so chosen that the areas in the two loops between X_1 and X_2 are equal. When T is less than this critical temperature P is more probable and when it is greater $S=0$ is more probable.

We must next verify that these curves are really the same as those known as $S(X)$ and $V(S)$. Recalling the previous definition, Eq. (1.10), of X:

$$X=V/kT$$

we see that $V(S)$ which is

$$V=V_0S=kTX$$

is the same as

$$X=X_1(S)=(V_0/kT)S.$$

The old equation, (1.8), from which the relation $S(X)$ was derived read

$$\left(\frac{1}{F_A(1-S)}-1\right)\left(\frac{1}{F_B(1-S)}-1\right)=e^{V/kT}=e^X.$$

The logarithm of this equation clearly gives the relationship between S and X implied by $X_2(S)$.

Thus we see that the equal area statement about the $V(S)$ and $S(X)$ curves is equivalent to requiring that $\ln \gamma(S)$ be a maximum or that the free energy be a minimum.

2. The Theory of Bethe[35B]

Introduction

A weakness of the Bragg-Williams attack is its rather macroscopic character. The ordering energy acting upon any particular atom is assumed to depend upon the distribution of all the other atoms in the crystal and not, as one would intuitively feel, upon only its immediate surroundings. It would be expected that more adequate theories would be developed by considering the atoms in detail and inquiring into the forces acting between them. Considerable progress in this direction has been made by Bethe,[35B] whose work has since been extended by Peierls[36G] and others. Bethe assumed that the atoms interact in pairs, so that every two atoms have a mutual potential energy, which, however, falls off rapidly with increasing separation of the atoms. He assumed this falling off to be so rapid that potential energies are appreciable only for those pairs of atoms which are nearest neighbors in the lattice. (Bethe's theory can be generalized by considering interactions between next nearest neighbors as well. This possibility has been investigated by Chang.[37Y])

The alloys which we consider in this section have simple lattices for which it is easy to recognize the nearest neighbors of each atom. (We shall here neglect the effects of slight distortions of the lattice which occasionally transform some nearest neighboring positions into next nearest neighboring positions.) The number of nearest neighbors of each atom in the lattice depends upon the type of lattice. We denote this number by z. The following tabulation shows its dependence on lattice type.

Lattice Type	z
Simple cubic	6
Body-centered cubic	8
Face-centered cubic	12
Hexagonal close packed	12
Two dimensional square net	4

The assumption as to energy

Thus each atom is surrounded by z nearest neighbors and hence has z non-negligible potential energies. Since each of these is shared between a pair of atoms, there will be in all $z/2$ potential energies per atom. The value of each potential energy will be determined by the nature of the atoms constituting the pair to which it belongs. If the atoms are both A atoms the potential energy will be denoted by v_{AA}; if both are B, v_{BB}; if one is A and one B, v_{AB}. In this work it will be assumed that these energy values are characteristic constants of the two metals; and no variations in their magnitudes, due to change in order, composition, or state of strain, will be admitted. This assumption (which differs from Bethe's only in regard to the explicit statement of its assumed range of application), will be referred to as the "nearest neighbor assumption."

In terms of the nearest neighbor assumption a formally simple expression for the energy of the alloy can be obtained. Let the number of pairs (henceforth we shall refer to a pair of nearest neighboring atoms merely as a pair) which are AA, BB, and AB be denoted by Q_{AA}, Q_{BB}, and Q_{AB}, respectively. Then associating with each pair its potential energy and summing these for all pairs in the lattice, we obtain for the total energy:

$$E=v_{AA}Q_{AA}+v_{BB}Q_{BB}+v_{AB}Q_{AB}. \tag{2.1}$$

It would now appear that Bethe's theory has the advantage of having three adjustable parameters, v_{AA}, v_{BB}, and v_{AB} whereas the Bragg-Williams theory had only one, V_0. This appearance, however, as will be shown below is only delusive and actually no one of Bethe's parameters is important by itself but only a certain linear combination denoted by v

$$v=\tfrac{1}{2}(v_{AA}+v_{BB})-v_{AB}. \tag{2.2}$$

The reason for the importance of v is that the interchange of any two atoms in the crystal always changes the energy in units of v. For example, consider the interchange of an A atom and a B atom which are not nearest neighbors in the lattice.[3] Let a of the neighbors of the first atom be A atoms and $(z-a)$ be B atoms, and let the B atom have a' A neighbors and $(z-a')$ B neighbors. The total energy associated with these two atoms is

$$av_{AA}+(z-a+a')v_{AB}+(z-a')v_{BB}. \tag{2.3}$$

If the two atoms are interchanged, the new energy will be

$$a'v_{AA}+(z-a'+a)v_{AB}+(z-a)v_{BB} \tag{2.4}$$

and the change in energy is seen to be

$$(a'-a)v_{AA}+(a'-a)v_{BB}-2(a'-a)v_{AB}=2(a'-a)v. \tag{2.5}$$

This is a particular example of a general result given in Appendix 1. It is there shown that for an alloy of given fixed composition,

$$Q_{AB}=\text{const.}-2Q_{AA}=\text{const.}'-2Q_{BB}. \tag{2.6}$$

Utilizing these equations, we see that E can be expressed by any of the three forms

$$E=\begin{cases}2vQ_{AA}+\text{const.}\\ 2vQ_{BB}+\text{const.}\\ -vQ_{AB}+\text{const.}\end{cases} \tag{2.7}$$

In these the values of "const." are different but need not concern us here, since they do not contribute to *changes* in configurational energy.

We see now that if v is positive, lower energies are obtained by creating unlike pairs of atoms at the expense of like pairs. This is in accord with the observed fact that in ordered structures like atoms tend to keep apart. A negative value of v will lead to like atoms keeping together and will result in segregation into pure metals at low temperatures. We shall return to this case very briefly in Section 8.

A practical feature of the forms should be pointed out. In carrying out calculations it is sometimes much easier to count the AA pairs than the AB pairs. We see that we need count only the AA pairs if we use the first of the three forms of E, or only the AB pairs if we use the third. This result can be seen in another way: since v only is important, the results obtained for v_{AA}, v_{BB}, and v_{AB} will also be obtained if we make $v_{AB}=v_{BB}=0$ and $v_{AA}=2v$. In the case thus obtained the interaction exists only between AA pairs and the other types can be disregarded. A similar process can be used to eliminate other sets of pairs.

[3] As the reader may verify, this restriction is not essential to the obtaining of the result.

The short range order σ

In order to discuss the consequences of his theory, Bethe introduces a new order parameter σ. This parameter is defined like that of Bragg and Williams insofar as it is unity for perfect order and zero for randomness. It is different, however, in not being connected with the α- and β-sites but with the behavior of the nearest neighbors. Let Q be the total number of pairs in the lattice. In terms of N and z it is

$$Q=(z/2)N. \tag{2.8}$$

Then the fraction of pairs which are unlike is

$$q=Q_{AB}/Q. \tag{2.9}$$

In the state of perfect order q has a maximum value q(max.) (which is unity for some simple cases) and for randomness a smaller value q(rand.). Bethe's parameter σ is defined by

$$\sigma=\frac{q-q(\text{rand.})}{q(\text{max.})-q(\text{rand.})} \tag{2.10}$$

so that the limits unity and zero are properly attained for order and randomness.

The parameter σ indicates how on the average each atom is surrounded by its neighbors; that is, it is a measure of the average order immediately about each atom. For this reason it is termed the "short range order" or "local order," in contrast to the long range order S which gives the order upon the α- and β-sites over the entire lattice.

Limitations imposed on the present application

For our discussion of Bethe's theory we shall, as he did in his original paper, limit ourselves to alloys of the AB type. For these it will be further supposed that all the nearest neighbors of a given α-site are β-sites and that all nearest neighbors of a β-site are α-sites. This is true for the simple cubic lattice, the body-centered cubic lattice, and the two-dimensional square net. The ordered structure of the simple cubic lattice is exemplified by the sodium chloride structure in which the α-sites form a face-centered lattice occupied by the ions of one sign and the β-sites are occupied by the ions of the other sign. The caesium chloride structure is a corresponding example for the body-centered lattice. The ordered structure of the two-dimensional square net is indicated in Fig. 16(a), and we may regard the positions occupied by A atoms as α-sites and those by the B atoms as β-sites.

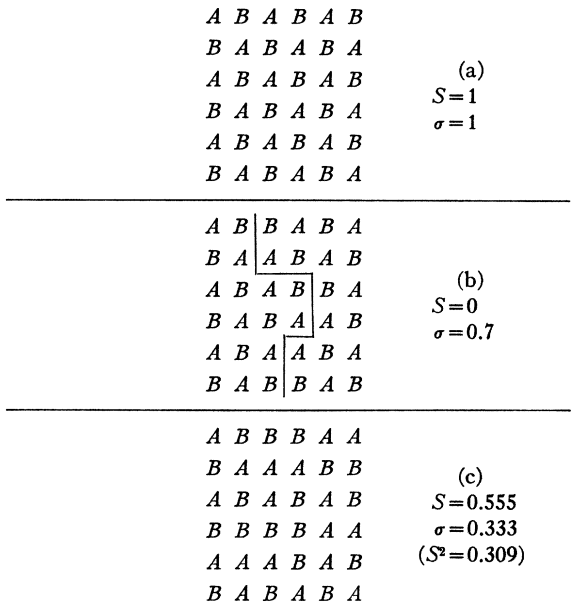

FIG. 16. Illustrating several degrees of long and short range order.

For these simple cases the limiting values q(max.) and q(rand.) are easily found. For perfect order all pairs are of type AB and q(max.)$=1$. For randomness the probability is one-half that any particular neighbor of a given atom is unlike the given atom; hence one-half the pairs are of AB type and q(rand.)$=\frac{1}{2}$. Thus we find

$$\sigma=2(q-\tfrac{1}{2}). \tag{2.11}$$

According to the third form for the energy equation, the energies of the best ordered and random states are:

Best ordered

$$-vQ_{AB}(\text{max.})=-vQ1=-\tfrac{1}{2}Nzv. \tag{2.12}$$

Random

$$-vQ_{AB}(\text{rand.})=-vQq(\text{rand.})=-\tfrac{1}{4}Nzv. \tag{2.13}$$

Hence the energy of transformation, which is denoted by the same symbol here as in the Bragg-Williams theory, is

$$E_0=\tfrac{1}{4}Nzv \tag{2.14}$$

and the energy of intermediate states is given in terms of σ by

$$E=E_0(1-\sigma). \tag{2.15}$$

In comparing various theories with each other, we shall assign to each the same value for E_0. Equating values of E_0 for the Bragg-Williams and Bethe theories we find

$$V_0 = 2zv. \tag{2.16}$$

This equation has a physically satisfying significance. Consider the state of nearly perfect order in which only two atoms are wrong. Although such a state must come into being by interchange of nearest neighbors, it is actually much more probable that the two wrong atoms are not nearest neighbors: there are only $\frac{1}{2}Nz$ ways of having two wrong atoms which are nearest neighbors but there are $\frac{1}{4}N^2$ ways of having two wrong atoms. Hence the "first excited state" of the alloy corresponds to two wrong atoms in different parts of the lattice. By definition its energy is V_0 in the Bragg-Williams theory; in the Bethe theory each atom reduces the number of unlike pairs by z, hence the energy is $2zv$, which is the same if the two theories have the same E_0. We see, therefore, that equating the over-all change in energy for the two theories makes them agree near the state of perfect order. We shall see later that, as follows from these ideas, the theories do converge in the low temperature range.

The relationship between S and σ

In Fig. 16(a) the order is perfect and there are as many AB pairs as possible. Hence both S and σ are unity. It will readily be appreciated that for this lattice these two conditions are equivalent: perfection of either long or short range order implies perfection of the other. In Fig. 16(b), however, we see that half the atoms are right and half are wrong in respect of long range order and hence that $S=0$. This represents a situation which is discussed in more detail in Part II. It can be described by saying that the crystal consists of two domains which are out of step with each other. In each the order is perfect; however, for the crystal as a whole $S=0$. The situation is somewhat different for σ; in the case indicated $\sigma=0.7$. The defect in σ arises, obviously, from the interface or "change-step" boundary between the out-of-step domains. The larger the domains, the smaller is the relative importance of the interface and the nearer σ approaches unity although S remains zero.

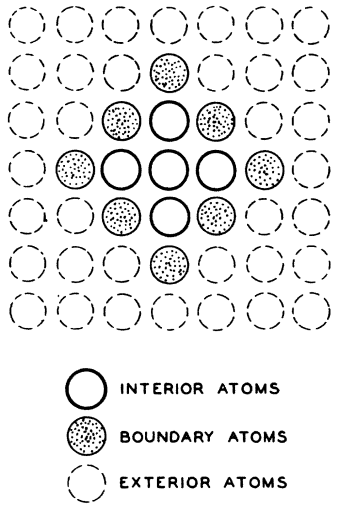

FIG. 17. Selection of a group of sites for Bethe's indirect method.

In the Bragg-Williams theory, low energy corresponds to a high degree of long range order and hence at low temperatures the stable state is one with long range order. In Bethe's theory, the connection between energy and long range order is not so close, in fact we have just exhibited the possibility of achieving nearly the minimum energy, i.e., $\sigma=1$, while having no long distance order. These considerations raise the question: will Bethe's assumptions, after the mathematical deductions from them shall have been completed, ever predict a state with long range order? This difficulty he resolves by a consideration of the probability of occurrence of a change-step boundary. The probability of having a boundary as compared to not having any is given by the number of ways of putting in such a boundary times the Boltzmann factor associated with the extra energy owing to its presence. When the magnitude of this probability is estimated, two conclusions can be drawn: the probability of a change-step boundary is negligible at low temperatures; it becomes large at a certain critical temperature which is independent of the size of the crystal provided only that the number of atoms is large. This type of calculation constitutes a sort of existence proof of a critical temperature for Bethe's theory. However, in order to evaluate the critical temperature, one must go over to the indirect method of Bethe.

In general, S and σ will be less closely related than in Fig. 16(a) and more closely related than in 16(b). Fig. 16(c) indicates such a case. If the Bragg-Williams and Bethe theories agreed, we should be able to derive the energy of the former expression, Eq. (1.13), from that of latter, Eq. (2.15), and write

$$E=E_0(1-\sigma)=E_0(1-S^2) \quad \text{or} \quad \sigma=S^2.$$

Actually we shall find that $\sigma>S^2$ (above T_c for example $\sigma>0=S$) except for $T=0$ with $S=\sigma=1$ and $T=\infty$ with $S=\sigma=0$. Thus less energy is required to attain a state of given long distance order, specified by S, in the Bethe than in the Bragg-Williams theory.

Bethe's indirect method of solution

Next the ideas of energy of nearest neighbors, short range order and long range order must be combined to give an equilibrium theory. In order to do this, we arbitrarily select a group of sites, as indicated in Fig. 17 for detailed consideration. We further distinguish between two parts of the group: an interior, which may consist of one site or of several, and a boundary. The selection is so made that the nearest neighbors of interior sites which are not themselves of the interior constitute the boundary. All the remaining sites of the lattice constitute the exterior. Bethe has carried out his calculations for groups of two sizes. In the smaller group, Fig. 18(a), dealt with in his first

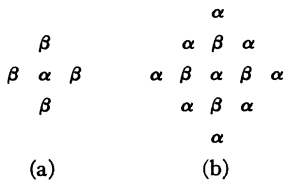

FIG. 18. Bethe's two approximations: (a) first; (b) second.

approximation, the interior consists of one α-site, and the boundary consists of the z neighboring β-sites. In the larger, Fig. 18(b), dealt with in his second approximation, the interior consists of the whole smaller group, and the boundary of the neighboring α-sites.

The particular group of sites selected for consideration is in no way physically different from any other similar group in the lattice. Hence conclusions drawn from a consideration of it can be applied to sites of other groups as well. Furthermore, according to the limitations of the present application, there is physical symmetry between the A and B atoms and between the α- and β-sites. Consequently if any statement regarding the distribution of A atoms upon α-sites is true, then a similar statement regarding B atoms on β-sites must also be true. However, in the groups considered by Bethe, an α-site has been given the special distinction of being at the center of the group. For this reason consideration of the arbitrarily selected group, unless tempered by a proper realization of the arbitrariness, can lead to conclusions which are inconsistent with the physical symmetry between α- and β-sites. As we shall see below, from the requirement that such inconsistency does not arise, we obtain the basic equation of Bethe's solution.

Now if atoms are allocated in some definite way to the boundary sites, it is possible to calculate the probability of any given arrangement in the interior. This is a consequence of the fact that since all the nearest neighbors of the interior atoms (or atom for the first approximation) are known, the energy can be found and the Boltzmann factor calculated. Since the number of available atoms in the entire crystal is very large, the *a priori* probability of any given atom being an A atom or a B atom is $\frac{1}{2}$, irrespective of how many other A or B atoms have already been chosen. Thus the probabilities are entirely determined by the Boltzmann factor discussed above. However, we do not know what arrangement to assume for the boundary atoms.

Let us suppose that there is a state of long distance order in the exterior. This will affect what happens upon the boundary by tending to make A atoms go to α-positions and B atoms to β-positions. We shall represent this tendency by an ordering energy "u," the magnitude of which we shall determine later, such that the energy of a wrong atom in the boundary is greater by u than that of a right atom because of the influence of the exterior. We can now carry out calculations of the probability of various situations for both the boundary and the interior because now all of the energy terms can be included. The results of such calculations will be expressed as functions of three variables: two of these, v and T, are regarded as known and the third, u, as unknown.

It would appear at first that many values of u could be assumed and that there would be no

way of telling which was right. Nevertheless we shall see that unless a particular value of u is chosen, the assumptions prove to be inconsistent. This particular value of u is then the one which must correspond to the equilibrium degree of long range order in the exterior; and in terms of it we can calculate all pertinent information about the equilibrium state.

In order to find the correct value of u we proceed by noting that the center site of the group is an α-site and has as its nearest neighbors z β-sites. In this treatment we supposed that there were in the crystal as a whole equal numbers of A and B atoms and equal numbers of α- and β-sites. Thus any satisfactory theory should treat the α- and β-sites in a symmetrical way and we should find that the probability, denoted by r_α, of having a right atom on the α-site in the center would be equal to the probability, denoted by r_β, of having a right atom on one of the neighboring β-sites. Now in terms of the known quantities v and T and the unknown u we can calculate $r_\alpha(v, T, u)$ and $r_\beta(v, T, u)$. The equation

$$r_\alpha(v, T, u) = r_\beta(v, T, u) \qquad (2.17)$$

becomes a means of determining u as a function of the other two variables.

Thus starting with definite values of v and T, we can use Eq. (2.17) to determine u. For Bethe's first approximation, each boundary atom has one neighbor in the interior and $(z-1)$ in the exterior. The theory shows that at low temperatures, the value of u is $(z-1)v$, corresponding to the influence of $(z-1)$ right neighbors in the exterior. As the temperature rises, u decreases finally vanishing at a certain critical temperature. Similar results follow from the second approximation.

In terms of v and T and the now known value of u, the probability of any situation in the interior and the boundary becomes perfectly definite. Because of this, we can determine the long range order over the entire lattice; let us denote by r the common value of the two expressions $r_\alpha(v, T, u)$ and $r_\beta(v, T, u)$. Then r is the probability that the center site or any of its nearest neighboring sites be rightly occupied. Since, as we know, the group under consideration is typical of the entire lattice, the probability that any site whatever is correctly occupied is r. Hence from the definition of long-distance order, Eq. (1.3), we find $S=2(r-\frac{1}{2})$. We can also calculate the probability that any particular pair consists of unlike atoms; this probability is q by definition (2.9), and in terms of it and Eqs. (2.11) and (2.15) we can calculate $\sigma=2(q-\frac{1}{2})$ and $E=E_0(1-\sigma)$. These quantities, like S, apply to the entire lattice.

The results of Bethe's two approximations differ only slightly. The second approximation is regarded as the more accurate because for it the boundary is farther away from the central atoms. Hence any errors introduced by the rather simplified assumption regarding the influence of the exterior will have a diminished effect upon the central atoms, to which we apply Eq. (2.17), because of the exact treatment of the intermediate atoms. The rather small difference between the first and second approximation, shown in the results, makes one believe that the effect of such errors is small and that both approximations are quite accurate.

Results of Bethe's theory for the AB alloy

By means of the method described above, Bethe has calculated the dependence upon temperature of S and σ for the first and second approximations in the simple cubic lattice. The results are shown in Figs. 9, 11, and 13 and Table I. Some of the details of the first order approximation are given in Appendix 2.

Bethe's theory predicts for the AB case, as does that of Bragg and Williams, that S vanishes at a certain critical temperature T_c without, however, suffering any discontinuous change. For this reason there is no latent heat of transformation at T_c. In Bethe's theory the critical temperature is represented by the vanishing of u which implies that the exterior is no longer capable of differentiating the A from the B atoms. Hence there is equal likelihood of finding either type of atom on the boundary and $S=0$. However, owing to the interaction between atoms of the group, each atom is even then more likely to have an unlike atom than a like atom as its neighbor; and although S vanishes, σ does not. Hence only a certain part of the energy E_0 is required to get the alloy to T_c; since there is no latent heat in this case, the energies just above

and just below T_c are equal and the energy in question is represented by $E(T_c-)=E(T_c+)$. This quantity bears nearly the same relationship to the critical temperature as in the Bragg-Williams theory, as may be seen from the row $RT_c/E(T_c+)$ in Table I.

Additional energy is required to heat the alloy above T_c and destroy the short range order. This gives rise to the anomalous specific heat above the critical temperature. In this respect, Bethe's theory is a considerable improvement over that of Bragg and Williams in which there is no anomalous specific heat above the critical temperature; as we shall see in Part II, Section 14, experiment shows an appreciable anomalous specific heat above T_c. Just below the critical temperature the specific heat has a peak, as was the case in the Bragg-Williams theory, owing to the rapidity of the disappearance of long distance order. Just above the critical temperature its value is much smaller, corresponding to the steady decrease in short range order above T_c. The limiting values just below and above the discontinuity are shown in Table I.

Entropy changes

So far, we have presented no justification, save its intrinsic reasonableness, for Bethe's method of approximation. The $V(S)$ and $S(X)$ procedure of Bragg and Williams has been shown to give the mathematically exact solution corresponding to the physical assumptions; this followed from the free energy treatment at the end of Section 1. Bethe's method of approximation does not appear to possess any such simple free energy analog and we must adopt different means for testing its exactness as a mathematical solution of the problem defined by the nearest neighbor assumption. Since there is no free energy analog for Bethe's method, the results are not consistent with thermodynamics. Hence a satisfactory numerical agreement of Bethe's theory with thermodynamic predictions, instead of being merely an identity as for the Bragg-Williams theory, is more or less a measure of the absolute accuracy of his method of approximation.

The thermodynamic test of Bethe's theory is made by computing the entropy change from perfect order to randomness. As was pointed out in Section 1 this value should be given by Eq. (1.27)

$$\Delta\Phi = R \ln 2 = 0.693R \text{ (correct)}. \quad (2.18)$$

For Bethe's theory this is found by integrating the specific heat.

$$\Delta\Phi = \int_0^\infty C\, dT/T. \quad (2.19)$$

His calculations based on the results of his second approximation give the value

$$\Delta\Phi = 0.698R \text{ (Bethe)}. \quad (2.20)$$

This good agreement, together with the small difference between the first and second approximations, tend to make one believe that the final approximation is rather good.

It would also be of interest to know the change in entropy from perfect order to the critical temperature. Unfortunately Bethe does not give this. However, an estimate can be made from his data for the change in entropy between the critical temperature and the random state. Combining this with the correct value for the entropy of the random state, we have computed the entropies in Table I.

Peierls' application of Bethe's theory to the case of AB_3[36G]

Peierls has applied the nearest neighbor assumption to alloys having unequal numbers of A and B atoms. His results are designed to apply to Cu_3Au. There are two features which greatly increase the computational difficulties of his work as compared to that of Bethe. In the first place there are three times as many B atoms as A atoms and consequently the symmetry between α- and β-sites postulated in Bethe's theory is destroyed. Also the face-centered lattice of the Cu-Au system does not have the simplifying feature of the simple cubic or body-centered cubic lattices. For them the nearest neighbors of any atom were never nearest neighbors of each other; for the face-centered lattice, however, each nearest neighbor of a given atom has among its nearest neighbors four which are also nearest neighbors of the given atom.

These difficulties are of an entirely mathematical character. It is necessary to introduce more than one new energy "u" and consistency relationships more complicated than $r_\alpha = r_\beta$ are needed. Physically the assumptions and process

of solution are the same as for the case discussed by Bethe. For the details of Peierls' work the reader is referred to references 36G and 37G. The results will be given below.

Like Bragg and Williams, Peierls finds that for the case AB_3 there is an abrupt change in state of order at a certain critical temperature and with it there is associated a latent heat. Like Bethe, he finds that the state above the critical temperature is not truly random and that a relatively high degree of local order prevails. The decrease with increasing temperature of this local order gives rise to an anomalous specific heat above the critical temperature.

The dependence of long range order and energy upon temperature for Peierls' theory are shown in Figs. 10 and 12. It will be noted that there are two vertical dotted lines in these figures. Peierls' calculations are not sufficient to enable him to give the critical temperature precisely; however, he computes that it must lie between the two dotted lines. The same computational obstacles have prevented him from giving curves of specific heat. A rough estimate from his data gave the values in Table I.

It would also be of interest to have an entropy calculation from Peierls' theory in order to check its accuracy as was done with the Bethe theory. Owing to the computational difficulties involved, this has not been done. We have estimated from Peierls' tables the entropy change from $T_c(RT_c/E_0=1.33$ was arbitrarily chosen for this purpose) to $T=\infty$ due to decreasing short range order. The entropy change at the critical temperature can also be estimated. These can then be combined with the theoretical value for the entropy of the random state to give the values in Table I.

3. The energy *versus* entropy representation[4]

Let us now analyze afresh the order-disorder problem with a view to finding what really constitutes a solution. In the results given in the previous section, variations of energy, specific heat and state of order, have been given. However, none of these quantities appear to be particularly fundamental by themselves and we are interested in something which is as nearly self sufficient as possible.

A good answer, and the one which we shall use, is suggested by the relative probability in statistical mechanics; namely the product of the *a priori* probability times the Boltzmann factor which was before discussed in connection with the free energy treatment at the end of Section 1. For our case the *a priori* probability is given by the number of ways of arranging the atoms. Let us disregard the value of the long distance order parameter, S, for the moment and concentrate upon the energy. According to Bethe's assumptions, which we shall take as the basis of this section, the energy changes in steps of v. The lowest energy, corresponding to perfect order can be chosen as zero and then all other possible energies will be multiples of v. For each possible energy, E, there will be a certain number of ways, $W(E)$, of arranging the system so that it will have this energy E. The relative probability of finding the system with this energy is $\gamma(E)$ where we have

$$\gamma(E)=W(E)\exp(-E/kT)$$
$$=\exp(\ln W(E)-E/kT). \quad (3.1)$$

If $W(E)$ were a known function of E, it would be possible to maximize $\gamma(E)$ and thus find the most probable, or equilibrium, state for each temperature. Or alternatively we could compute the partition function

$$\Gamma=\Sigma_E\gamma(E) \quad (3.2)$$

and in terms of it calculate by known means[5] all the equilibrium properties of the system.

Thus a knowledge of the functional dependence of $W(E)$ upon E is equivalent to a solution of the problem. Let us therefore assume divers forms for $W(E)$ and see how they lead to various types of temperature dependence for the system. In doing this it is most convenient to deal with the entropy $\Phi(E)$ related to $W(E)$ by the Boltzmann equation:

$$\Phi(E)=k\ln W(E). \quad (3.3)$$

Utilization of this expression in the equation for γ gives

$$\gamma(E)=\exp(\ln(W(E)-E/kT))$$
$$=\exp\{[T\Phi(E)-E]/kT\}=\exp(-F/kT), \quad (3.4)$$

[4] The writers are indebted to Dr. F. Seitz for suggesting the energy *vs.* entropy type of plot as a convenient means of expression.

[5] See for example R. H. Fowler, 36J.

thus showing that maximum probability corresponds to a minimum of the free energy

$$F=E-T\Phi. \tag{3.5}$$

Graphical presentation

On Fig. 19, curve C represents the type of behavior to be expected for the configurational energy and entropy of an alloy. The lowest energy corresponds to a high degree of order and hence to only a few arrangements and a small entropy. For higher energies there are more ways of arranging the atoms and the entropy increases. The maximum entropy corresponds to the energy of the random state which energy can be achieved in more ways than any other. However, we can produce arrangements having energies greater than E_0 by arbitrarily clustering like atoms together. The limit of this process is reached when all the A atoms are clustered together forming a crystal of pure A leaving the B atoms as pure B. This arrangement can be obtained in only a few ways and has a low entropy. This explains the turning back of the curves above E_0.

The slope of the curve at any point is

$$\frac{dE \text{ cal.}}{d\Phi \text{ cal./°K}}=\frac{dE}{d\Phi} \text{ °K.} \tag{3.6}$$

It is seen to have the dimensions of temperature, and we shall use this fact to analyze the equilibrium conditions.

Each point on the curve corresponds to a pair of values of E and Φ which represent some state of the system. To discover which point corresponds to equilibrium at any temperature T, we proceed as follows. Draw a line having slope equal to T, and traversing the curve at any point P' for which E and Φ have the values E' and Φ', respectively. It is readily seen that the intercept of this line upon the E axis is equal to $(E'-T\Phi')$, *viz.* to the free energy which the system would possess, if the energy E' and the entropy Φ' coexisted at the temperature T. Now among all the possible value-pairs of E' and Φ' which are represented by the points of the curve, that one which is in thermal equilibrium at T is that one for which the free energy is least. It is consequently represented by the point of tangency, P, between the curve and the line of slope T. At it we have

$$dE/d\Phi=T. \tag{3.7}$$

This condition is also obtained at once by setting the derivative of Eq. (3.5) equal to zero.

The temperature behavior of the system represented by curve C of Fig. 19 can easily be visualized. At $T=0$, the stable state corresponds to the origin with $E=\Phi=0$. For higher values of T, intermediate points like P are obtained. Finally as T approaches ∞, and the entropy becomes the dominant term in F, point G at which the entropy is a maximum is approached. The portion of the curve above G will obviously never give rise to stable states.

Latent heat

Curve D represents a qualitatively different situation; it has a reentrant portion between P_1 and P_2 and because of this it may have the same slope at as many as three points. In general one of these will have a lower free energy than the other two and will give a unique stable state. However, there is one particular slope T_c for which the free energies are the same for two points, P_1 and P_2. For temperatures below T_c, the stable state corresponds to a point below P_1 while above T_c points above P_2 are stable. Thus T_c marks a transition temperature and at it there are discontinuous changes of ΔE in energy and of

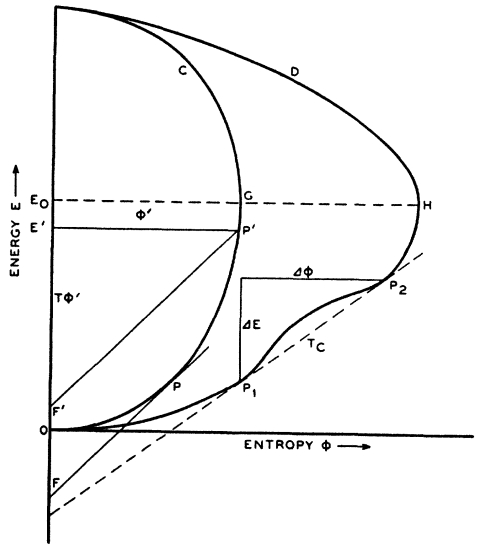

FIG. 19. Illustrative inexact plots of configurational energy *versus* configurational entropy.

$\Delta\Phi$ in entropy. These quantities are related by the equation

$$\Delta E = T_c \Delta\Phi. \tag{3.8}$$

Specific heat

The smooth increase in energy and entropy with rising temperature leads to a specific heat. This is easily evaluated in terms of derivatives on the curve. Denoting the equation of C as $E=E(\Phi)$, we have

$$\frac{dE}{d\Phi}=T, \quad \frac{d^2E}{d\Phi^2}=\frac{dT}{d\Phi}. \tag{3.9}$$

Hence the specific heat is

$$C=\frac{dE}{dT}=\frac{Td\Phi}{dT}=\frac{dE}{d\Phi}\Big/\frac{d^2E}{d\Phi^2}. \tag{3.10}$$

Connection between the assumptions of Bragg and Williams and of Bethe as to energy

Let us suppose that the system has a definite value S of long range order. The number of ways of obtaining any allowed value of E is denoted by $W(E, S)$ and is less than $W(E)$. Now according to the Bragg-Williams theory all the arrangements of the atoms with given order S had a common energy $E(S)$. However we know that for Bethe's assumption the energy depends entirely upon how the atoms are arranged locally and that the energy can be expressed in terms of this local or short range order σ by Eq. (2.15)

$$E=E_0(1-\sigma).$$

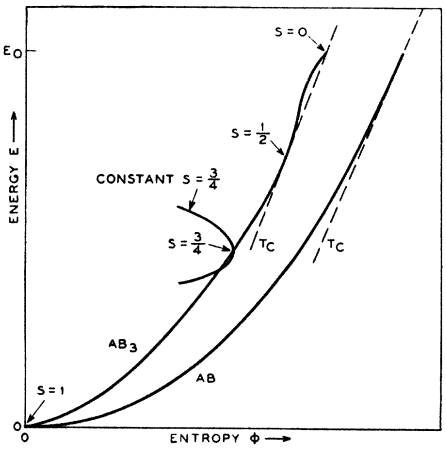

FIG. 20. Illustrating energy *versus* entropy according to the Bragg-Williams theory.

We have adopted Bethe's assumption and shall try to interpret the Bragg-Williams formulation in terms of it.

Among the various ways of arranging the atoms with order S, some will correspond to high and some to low values of σ. There will then be some average value of σ; and since the number of atoms is to be supposed very large, the probability of an appreciable deviation of σ from this average value is small. In this paragraph we mean by average a purely statistical process; no connection with the Boltzmann factor is implied.

For the simple AB lattice discussed in connection with Bethe's theory, the relationship between S and the average value of σ is simply found. Consider any pair composed of an α-site and a nearest neighboring β-site; the probability that the two atoms upon these sites are both right is $r_\alpha r_\beta$ and the probability that both are wrong is $w_\alpha w_\beta$. Hence the probability that this pair is composed of unlike atoms is $r_\alpha r_\beta + w_\alpha w_\beta$. This quantity is the average value of q; q was defined in Eq. (2.9) as the fraction of the pairs which are of AB type. From the relationship (1.3) between the r's and the w's and S we find

$$\text{average of } q = q_{Av} = (1+S^2)/2 \tag{3.11}$$

and in terms of Eq. (2.11) for σ

$$\text{average of } \sigma = \sigma_{Av} = S^2. \tag{3.12}$$

Hence the average value of the energy when the system has order S is

$$E_{Av}(S) = E_0(1-\sigma_{Av}) = E_0(1-S^2). \tag{3.13}$$

The above result shows quite clearly the relationship between the Bragg-Williams and Bethe theories. In the former the energy is supposed to have a certain definite value when S is specified; in the latter this energy is not definite but may fluctuate about a mean value, this mean value being that assumed as definite in the former.

The entropy of the state of order S was found in Section 1 by counting the number of ways of arranging the atoms for this fixed order and the mathematical formula for $\Phi(S)$ was given in Eq. (1.25). Since both $E_{Av}(S)$ and $\Phi(S)$ are known functions of S, they can be plotted against each other with S as a parameter. The results are shown in Fig. 20 in an inexact form, the concavity

of the re-entrant portion of the AB_3 curve being greatly exaggerated. These curves terminate abruptly with the random state $S=0$, which gives the highest possible energy on the Bragg-Williams theory. The critical temperatures are given by the slopes of the dashed lines and the values of S are indicated on one of the curves. For temperatures above the critical temperature the stable state has $E=E_0$ and $S=0$, and hence there is no increase in energy above T_c and the anomalous specific heat vanishes. In this respect these curves differ from those of Fig. 19, for which the state with $E=E_0$ is not reached until T goes to infinity. An analytical treatment of the AB_3 curve can determine the exact slope of the dashed line which is tangent to the curve near $S=\frac{1}{2}$ and also passes through the $S=0$ point. The result of this calculation has already been given in Section 1.

Constant S curves

The Bragg-Williams theory curves were constructed by assigning to each value of S a definite energy and entropy, thus obtaining a point on the curve. Actually, as explained above to each value of S there corresponds a variety of values of the energy each with its own entropy, $\Phi(E, S)=k \ln W(E, S)$. Hence each value of S gives not a point on the figure but instead a curve. This curve will have its maximum entropy at the most probable or average energy for that value of S, and thus at the same value $E_{Av}(S)$ as occurs on the Bragg-Williams curve. Furthermore, as we shall show below, the value of this maximum entropy is $\Phi(S)$. Hence the curve for a fixed value of S, hereafter referred to as a "constant S curve," has its maximum entropy at the point on the Bragg-Williams curve corresponding to the same value of S. A portion of the constant S curve for $S=\frac{3}{4}$ is indicated on Fig. 20 for the AB_3 case.

At first it seems surprising that the maximum entropy on a fixed S curve is the same as the Bragg-Williams entropy for that value of S; because for the Bragg-Williams case the entropy corresponds to all arrangements with order S while for the constant S curve the maximum entropy corresponds to only the fraction of these having the average energy $E_{Av}(S)$ (or the nearest allowed value of energy). We should therefore expect the maximum entropy of the fixed S curve to be somewhat less than the Bragg-Williams value. Actually the difference is negligible owing to the fact that we are dealing with a large number of atoms. Because of this the number of ways of arranging the atoms for order S is given according to Eq. (1.25) by an expression like

$$e^{Nf(S)}, \tag{3.14}$$

where $f(S)$ is of the order of unity. The number of allowed energy values for the system is of the order of N. Hence the most popular energy value must be obtainable in at least

$$e^{Nf(S)}/N \tag{3.15}$$

ways. Its entropy will be

$$\Phi=kNf(S)-k \ln N. \tag{3.16}$$

The second term is negligible compared to the first and hence the entropy is practically as great as that corresponding to all arrangements having order S.

In the next section we shall discuss a method of dealing with order-disorder problem developed by Kirkwood, and shall see how his results can be utilized in order to obtain information about the constant S curves.

4. The method of Kirkwood[6]

Kirkwood has devised a particularly ingenious and elegant method which can be used to determine the shape of the constant S curve. Since, however, the effectiveness of the method lies in the utilization of certain mathematical tricks, we shall present only the results here and give the details in Appendices 3, 4, and 5.

As was explained in the last section, there is no definite energy for a state of order S but instead a wide distribution of energies. When we averaged over these statistically (considering only the *a priori* probability and not the Boltzmann factor) we found a certain average energy, $E_{Av}(S)$. Other energies will be possible also and what we really desire is the distribution in energy of these other energies; having, this is equivalent to knowing the constant S energy-entropy curve.

[6] J. G. Kirkwood, 38B. The writers are very greatly indebted to Professor Kirkwood for several discussions of his method and for the privilege of seeing an advance copy of his paper.

Now no methods have been devised for finding this distribution directly;[7] however, we can find various quantities more or less intimately related to it. One of these is Δ_2, the mean square deviation of the energy from the mean value:

$$\Delta_2=\langle(\Delta E)^2\rangle_{Av}=\langle(E-E_{Av})^2\rangle_{Av}$$
$$=\Sigma(E-E_{Av})^2/W(S). \quad (4.1)$$

Here $W(S)$ represents the total number of ways of arranging the atoms with order S (derived in Eq. (1.25)) and the Σ extends over all of these arrangements. Δ_2 is a measure of the width of the distribution. It can be evaluated for any particular lattice and any particular state of order by straightforward but rather laborious calculations of the nature met with in statistics. A simple case is treated in Appendix 4.

In order to apply Kirkwood's method generally we should calculate all quantities like $\langle(\Delta E)^2\rangle_{Av}$; such as $\langle(\Delta E)^3\rangle_{Av}$; $\langle(\Delta E)^4\rangle_{Av}$, etc. These quantities are customarily known as moments of the deviations and we shall designate them symbolically as

$$\Delta_n=\langle(E-E_{Av})^n\rangle_{Av}. \quad (4.2)$$

They are, like E_{Av}, functions of S. When these moments are known it is then possible to obtain an expansion of the free energy in terms of them and the temperature. The result, derived in Appendix 3, reads

$$F=E_{Av}-T\Phi(S)-\frac{\Delta_2}{2!kT}+\frac{\Delta_3}{3!(kT)^2}$$
$$-\frac{\Delta_4-3\Delta_2^2}{4!(kT)^3}+\cdots. \quad (4.3)$$

Here $\Phi(S)=k\ln W(S)$ is the entropy calculated on the basis of the Bragg-Williams theory. The numerators of the higher terms are not the simple "moments" but are instead the so-called "semi-invariants" of Theile.[22A]

As was indicated in the last section we regard the energy-entropy curve as the fundamental desideratum, and we shall convert Kirkwood's result into it. For the solution of any practical problem this transformation is not necessary and may even lead to more complicated results; our principal aim in making the transformation here is one of presentation. By a general equation given in Appendix 5 it is shown that an expression of the free energy as a power series in $(1/T)$ can be transformed to give the entropy as a power series in E. When the details are carried out we find that Eq. (4.3) becomes

$$\Phi=\Phi(S)+k\left(-\frac{1}{2!\Delta_2}(E-E_{Av})^2+\frac{\Delta_3}{3!\Delta_2^3}(E-E_{Av})^3\right.$$
$$\left.+\frac{\Delta_4\Delta_2-3\Delta_2^3-3\Delta_3^2}{4!\Delta_2^5}(E-E_{Av})^4\cdots\right). \quad (4.4)$$

We see here in analytic form the result given in the last section that the entropy on the constant S curve is $\Phi(S)$ when $E=E_{Av}(S)$.

Thus in principle if we are willing to calculate enough moments, we can get the fixed S curve with arbitrary accuracy. Actually the calculation of the moments is very tedious and work has been done including only the second, Δ_2, although Kirkwood has calculated them up to the third for a simple type of lattice.

An important feature of Kirkwood's method is its generality of application. It need not necessarily be applied to the simple lattices of the type considered by Bethe. Also there is no reason why it should be restricted to stoichiometric ratios of the elements: it is very little more difficult to find the deviations when the ratio of the elements are not 3 : 1 but say instead 3.1 : 1.

Results from Kirkwood's method

We shall here restrict the discussion to the AB case of the simple cubic lattice. Fig. 21 shows the constant S energy *vs.* entropy curves and also the Bragg-Williams curve. Only the first two terms of Eq. (4.4) were used for this figure and consequently the fixed S curves are parabolas with their vertices on the Bragg-Williams curve. This means that the distribution in energy, $W(E, S)=\exp[\Phi(E, S)/k]$, has the form of a Gauss error function. This degree of approximation has been discussed in cooperative phenomena before: in the theory of ferromagnetism[32K] and in treatments of rotation of polar molecules in solids.[37S]

Stable states always correspond to maximum entropy for fixed energy and hence to points on

[7] See, for example, a discussion by R. Becker, reference 37A.

the envelope of the fixed S curves. This envelope is seen nearly to coincide with the Bragg-Williams curve for low energies and entropies. This is because at low energies only a few atoms are wrong and, as we pointed out in discussing the relationship $V_0 = 2zv$ in Section 2, the probability that they come together and produce fluctuations in energy are so small as to be negligible. Hence the Bragg-Williams representation is adequate. At higher energies the envelope diverges more from the Bragg-Williams curve and we find that for each energy the maximum entropy occurs for a smaller value of S than that given by the Bragg-Williams curve. As the envelope is followed higher up, the values of S are bunched more closely together until finally $S=0$ is reached. The last portion of the curve is not truly an envelope but merely a section of the $S=0$ parabola.

There is no abrupt change in slope or reentrant portion of the curve at or near the point where $S=0$ joins the envelope. Hence there is no discontinuity in energy giving rise to a latent heat. The theory therefore predicts the same continuous type of vanishing order as was given by Bragg and Williams and by Bethe for the AB case of the simple cubic lattice. However, near the point where the $S=0$ curve joins the envelope, the latter has a very small curvature; hence a small change in slope requires a large change in energy and gives a large specific heat. Immediately above the point of juncture the $S=0$ curve has much greater curvature and gives a smaller specific heat. The mathematical significance of this situation is represented by the $d^2E/d\Phi^2$ term in Eq. (3.10).

Kirkwood's method being built upon free energy considerations is automatically thermodynamically consistent. Hence a check such as that applied to Bethe's theory is merely an identity for it.

The results of Kirkwood's method for the simple cubic lattice are given in Figs. 9, 11 and 13 and Table I. For his theory, as for that of Bragg and Williams, $RT_c/E(T_c\pm)=2$. We have also calculated the data in Table I for the body-centered lattice. We have been informed[38D] that the value 4.23 for the specific heat just below T_c is reduced to 1.7 by including the Δ_3 term in Eq. (4.3).

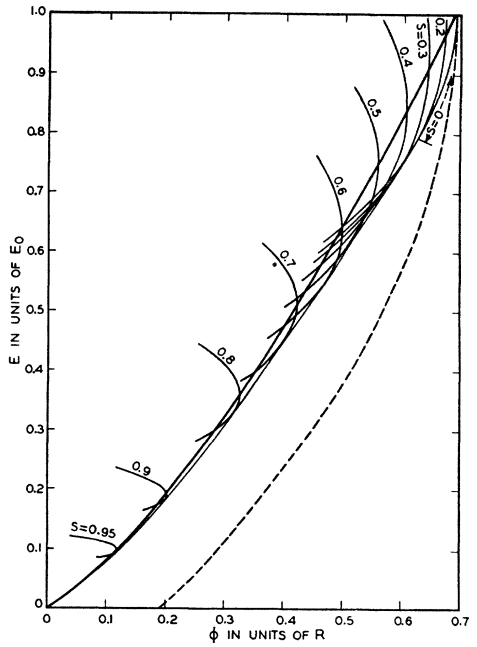

FIG. 21. Energy *versus* entropy for the simple cubic lattice AB case as given by Kirkwood's method. Dashed line, $S=0$ curve for face-centered lattice AB case.

Further application of Kirkwood's method

It would be of considerable interest to apply Kirkwood's method to the case of AB_3 and to compare the results with Peierls' work. This would involve treating the face-centered lattice, for on the basis of the nearest neighbor assumption no superlattice would form in the simple cubic or body-centered cubic lattice at this composition. The writers have attempted such an application taking into account the second moment. It proves that the second moment approximation is not good enough for the face-centered lattice and instead of obtaining an envelope for the Φ *versus* E parabolas it is found that the fixed S parabola for $S=0$ lies outside of all the others as indicated by the dashed curve of Fig. 21. This would predict no formation of a superlattice at all, and in order to apply the method further moments, which can be obtained only with considerable effort, would be needed.

A fundamental difficulty connected with the definition of long range order

We are now in a position to consider a fundamental difficulty connected with long range order and energy *versus* entropy plots. It is

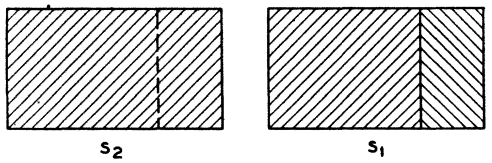

FIG. 22. Reduction of order from S_2 to S_1 by means of change-step boundary.

inherent in the nature of the problem and not restricted to Kirkwood's method. In Fig. 21 a constant S curve starts at energies higher than $E_{Av}(S)$, proceeds downward until it touches the envelope and then turns inward. This value of S is then attained for a temperature given by the slope of the envelope where the constant S curve touches it. The fundamental difficulty is that in actuality the constant S curve does not turn inward after striking the envelope from above but instead follows it downward to the point $E=\Phi=0$. This conclusion is drawn from the following reasoning. Consider two values of S, $S_1<S_2$. Suppose the crystal can be set up in $W(E, S_2)$ ways so as to have energy E and order S_2. Now suppose that the crystal consists of a rectangular block as indicated in Fig. 22. Then for each arrangement having order S_2 we can find a dividing line as indicated such that if the two parts of the crystal are displaced one lattice spacing in respect to each other across this plane, the order is reduced to S_1. There is in general an increase in energy in this process corresponding to the introduction of the "change-step" boundary, but this is negligible on the scale of Fig. 21. Hence we see that there are essentially at least as many ways of achieving energy E with order S_1 as with S_2. Thus we conclude that $W(E, S_1)\geqq W(E, S_2)$. This shows that in an exact figure, drawn on the axes of Fig. 21 there would never be any turning in from the envelope.

However, this reasoning should not be construed to imply that long range order is merely a fiction and that Kirkwood's method, if exactly carried out, would yield no answer. An exact plot, such as discussed above, would give correctly all theoretical predictions concerning energy and entropy changes. The long range order would be implied in these predictions and it would arise from the change in energy due to the change-step boundaries, which, although negligible on the scale of such a figure, can bring about order in the manner described in Section 2. Due to this effect there would be a turning in from the envelope, invisible on any plot of practical size, and a definite value of order for each point on the envelope. This is just the result obtained by the very incomplete application of Kirkwood's method. We see now that it was the roughness of the approximation which led so simply to this result and that with improvement it would be more difficult to tell how the values of S were arranged on the envelope. The situation is reminiscent of many problems in quantum mechanics where although satisfactory results are obtained by first-order perturbations higher order approximations lead to difficulties.

Some ideas which may be of importance in clearing up the situation just described have been mentioned by Slater.[37ZZ] He points out that both short range and long range order are simplified concepts, a complete description of the state of order requiring more complicated variables. For these reasons it may be that definitions of "intermediate range" order will prove helpful in further developments of the theory.

B. Equilibrium theories for alloys of arbitrary composition

The theories discussed above have been limited to very simple alloys: those for which the concentration of the metals is such that there are just enough atoms of each type to fill up some simple fraction of the lattice sites, one-half in the case of AB, and one-quarter and three-quarters in the case of AB_3. In metallurgy, these are very special cases; in general wide ranges of composition must be considered.

Not very much thorough theoretical work has been done for the case of arbitrary composition. Borelius[35C] has given a description of the type of results to be expected which is helpful in understanding the problem in general. Two writers have recently given treatments utilizing the nearest neighbor assumption: Easthope[37G] has used Bethe's first approximation to find the dependence of critical temperature upon composition, with especial emphasis on the compositions close to AB_3; and Shockley[38C] has used the

Bragg-Williams approximation to discuss order-disorder phase diagrams for alloys which, like Cu-Au, form face-centered lattices.

5. The energy of formation of alloys

In this section we shall consider alloys which do not modify very greatly their lattice structure as the composition is varied. Thus a change from a face-centered cubic to a body-centered cubic lattice will be excluded. The change from face-centered cubic to a slightly distorted tetragonal form will be included, but the effect of this distortion in dividing nearest neighboring sites of a given site into nearest neighbors and next nearest neighbors will be neglected. This simplification permits an easy application of the nearest neighbor assumption because the number of nearest neighbors of a given site is constant and only the variation in the numbers of like and unlike pairs need be considered. In dealing with the energy of an alloy it is convenient to take as zero the energy of the constituent metals when pure. When this is done, the expression (2.1) for the energy of a sample of alloy of arbitrary composition and state of order may be simplified by methods given in Appendix 1 to the form:

$$E = -vQ_{AB}, \tag{5.1}$$

where Q_{AB}, as defined in Section 2, is the total number of AB pairs in the alloy.

Energy of best ordered and random states as functions of composition

The energy of the random state may be very easily calculated in the manner used in Section 3 and leads to the smooth curves of Fig. 23, for the body-centered and face-centered cubic lattices. It is essentially a more complex problem to determine the lowest possible energy for each composition, for it is necessary both to find an arrangement of atoms which gives this lowest energy and to prove that no other arrangement can give a lower one. The solution of this problem is outlined in Appendix 1 and gives the lines consisting of straight segments of Fig. 23. For later reference to experimental work we point out that the best arrangement for 50 atomic percent on the body-centered lattice corresponds to the CsCl type structure with each atom having eight unlike nearest neighbors, as shown in Fig. 40(C). For the corresponding best arrangement of the face-centered lattice, the structure is as shown later for the CuAu alloy, Fig. 40(B), and each atom has eight unlike and four like neighbors. For the composition AB_3 in the body-centered cubic lattice the condition of minimum energy implies no unique lowest energy state, and there are many ways of arranging the atoms with the lowest possible energy; for the face-centered cubic lattice, however, a definite superlattice, as shown in Fig. 40(A), is implied with each A atom surrounded by twelve B atoms. In Part II we shall see that in several cases these three ordered structures actually occur but that in other cases structures in definite disagreement with the nearest neighbor assumption are found.

A striking feature of the diagram is its symmetry about 50 atomic percent. This is an evident consequence of Eq. (5.1) and emphasizes again the fact that only one parameter v—rather than three, v_{AA}, v_{BB}, v_{AB}—is important. It is also evident that Eq. (5.1) will give predictions which are symmetrical about 50 atomic percent for all properties having to do with superlattice formation.* Experiment does not confirm this prediction and thus shows that the nearest neighbor assumption does not represent the whole story.

It is a little difficult to see why there should be a state of long range order for compositions differing appreciably from simple ratios like 1 : 1 and 1 : 3. Thus as soon as there are enough extra atoms to complete a plane bisecting the alloy crystal (i.e., to have one plane through

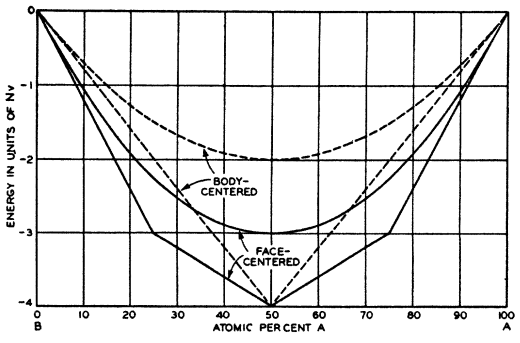

FIG. 23. Energy of formation from pure A and pure B of random alloys (smooth curve) and best ordered alloys (straight lines).

*This situation is unaltered by considerations of next nearest neighbor interactions, etc.

the alloy which does not divide AB pairs), it is possible to have the atoms on one side of the plane out of step with those on the other and to obtain the state of lowest possible energy with zero long distance order. However, there are relatively few ways of bringing this about compared to the large number of ways of having one coherent scheme of order through the crystal with the extra atoms distributed at random in wrong positions, a situation which also gives the minimum energy. For any particular lattice, there will be a certain minimum percentage of A below which the lowest energy can be obtained in more ways without long distance order than with it. According to the theory of Easthope, who uses Bethe's first approximation, alloys having as little as $1/z$th (z is the number of nearest neighbors of each atom) of their atoms of type A may still form a superlattice. This figure seems somewhat small—it implies that when each B atom has on the average only one A neighbor, there will still be enough A atoms to form a superlattice. In the work of Shockley treating the face-centered lattice by the Bragg-Williams approximation, the lowest energy always corresponds to the best possible order and, hence, a superlattice is predicted for all compositions. However, we do not think that this unreasonable prediction invalidates any of the more important conclusions at which Shockley arrived.

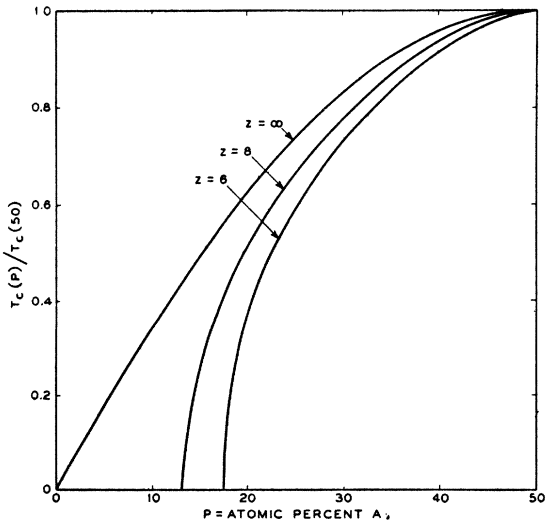

FIG. 24. Critical temperature as a function of composition.

6. The dependence of critical temperature upon composition

The theory of Bethe and the extension by Peierls can be perfectly well applied to arbitrary compositions and the critical temperature calculated. It is merely necessary in calculating the probability of any given configuration of atoms to weight the *a priori* probability of atoms in accord with their relative abundance. The calculations are, however, quite complicated and considerable computational work is demanded.

Easthope has carried out calculations for two cases.[37G] The first of these is for a lattice like the body-centered or simple cubic for which we can choose a set of α-sites and a set of β-sites so that all the nearest neighbors of each α-site are β-sites and *vice versa*. (For cases of arbitrary composition there will not in general be equal numbers of A atoms and α-sites or of B atoms and β-sites and for even the best ordered arrangements there will be some "wrong" atoms.) He has furthermore made his calculations as if there were no latent heat to be expected during the transformation for any composition. As he points out, this will probably introduce a small error into his results. With this restriction he has given an accurate treatment by Bethe's first approximation ("interior" composed of one atom only) for all compositions. His plot of critical temperature *versus* composition is shown in Fig. 24. The limiting case, $z=\infty$, for which the Bethe and Bragg-Williams approximations converge is also shown. In the Bethe theory, only part of the energy of transformation is used up in getting to the critical temperature. This part is plotted in Fig. 25. Here the unit of energy is that required to bring the 50 atomic percent alloy to the critical temperature; it is $(z-2)/(z-1)$ times the total energy of transformation of the 50 percent alloy, that is $0.800(\frac{1}{4}Nzv)(=0.800E_0)$ for the simple cubic, $0.855(\frac{1}{4}Nzv)(=0.855\ E_0)$ the body-centered and $\frac{1}{4}Nzv(=E_0)$ for the Bragg-Williams approximation. Since Easthope disregards the possibility of a latent heat, this energy is denoted not by $E(T_c+)_P$ but by $E(T_c)_P$. For the Bragg-Williams approximation, the entire energy of transition is used up in getting to T_c. Hence the Bragg-Williams curve is the difference be-

tween the best ordered and random curves of Fig. 23.

Easthope's second calculation is for the face-centered lattice for compositions near AB_3. It has been observed in some experiments that the critical temperature has a maximum at the stoichiometric ratio of 3 : 1. Easthope does not calculate a curve of T_c *versus* composition for this case but instead calculates the derivative of T_c in respect to composition at this point. He finds that the derivative is not zero, as it should be for a maximum, and that higher critical temperatures are to be expected towards the 1 : 1 ratio.

7. Phase diagrams for the order-disorder phenomenon

The similarity between the disappearance of long range order and the melting of a solid has been pointed out by various writers. E. J. Williams[35V] even refers to the state above T_c as having "liquid order." In accordance with these ideas we may think of the solid solution of two metals as having an ordered phase and a random phase. It is then natural to inquire into the phase diagram for an alloy system.

Shockley has done so for the Bragg-Williams approximation and the face-centered lattice. The copper-gold system has a face-centered lattice and possesses ordered structures for Cu_3Au and CuAu. The first of these is cubic and the second tetragonal. Shockley's work shows that these are special cases of two ordered phases, so that the problem actually involves three phases: a random phase denoted by ξ, an ordered cubic phase η and an ordered tetragonal phase ζ. The phase diagram for these three phases is shown in Fig. 26. The relationship between critical temperature, T_{50} percent, and ordering energy for 50 atomic percent is that given by the Bragg-Williams theory for case AB; in accord with Fig. 23, the energy of transformation E_0 is Nv.

In discussing this system Shockley finds it necessary to generalize the definition of order. This is done by dividing the face-centered lattice into four simple cubic sublattices as is indicated in Fig. 27. For each of these sublattices there is an order parameter defined in terms of the fraction of the sites of the sublattice

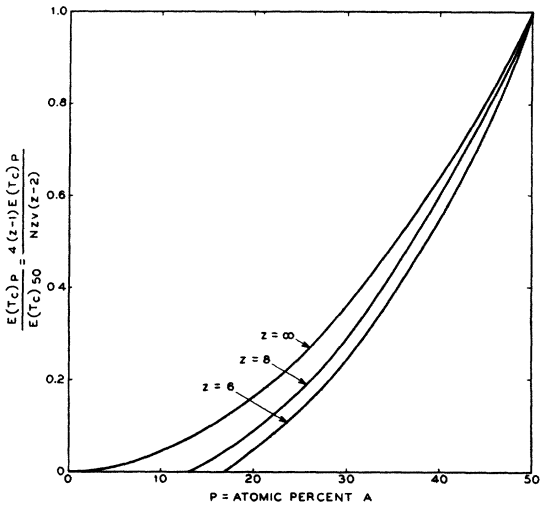

FIG. 25. Energy required to destroy superlattice as a function of composition.

which are occupied by A atoms. Numbering the sublattices from 1 to 4 and denoting the fractions by f_1, f_2, f_3, f_4 the order parameters are defined by

$$\begin{aligned} S_1 &= 2(f_1 - \tfrac{1}{2}) \\ &\cdots \\ S_4 &= 2(f_4 - \tfrac{1}{2}). \end{aligned} \tag{7.1}$$

These expressions were chosen in analogy with the expression

$$S = 2(r_\alpha - \tfrac{1}{2})$$

which was used in Section 1 for the AB case. In terms of these order parameters the ordered and random states of AB and AB_3 correspond to the values tabulated below. The values of $+1$ and

	S_1	S_2	S_3	S_4
AB ordered	1	1	-1	-1
AB random	0	0	0	0
AB_3 ordered	1	-1	-1	-1
AB_3 random	$-\frac{1}{2}$	$-\frac{1}{2}$	$-\frac{1}{2}$	$-\frac{1}{2}$

-1 imply sublattices of pure A and pure B, respectively. Thus for AB ordered, two of the sublattices are pure A and two are pure B; it is immaterial which two are chosen and the values of the S_i may be permuted. This structure is just that observed for CuAu and is shown in Fig. 40(B). Similarly the ordered AB_3 corresponds to three sublattices of pure B and one of pure A and conforms to the experimentally known structure

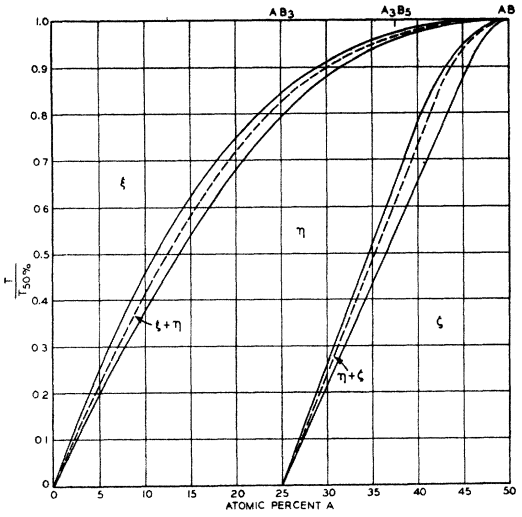

FIG. 26. Phase diagram for face-centered cubic lattice, solid lines. Critical temperature for an alloy of homogeneous composition, dashed lines.

of Cu_3Au, Fig. 40(A). This scheme may easily be applied to arbitrary composition; for example the composition A_3B_5, halfway between AB and AB_3, gives

A_3B_5 best ordered	1	0	−1	−1
A_3B_5 random	$-\frac{1}{4}$	$-\frac{1}{4}$	$-\frac{1}{4}$	$-\frac{1}{4}$

The treatment involving these order parameters is like that described in the last paragraphs of Section 1. The entropies for all of the sublattices are calculated and added to give the total entropy, and the average energy is determined. Both of these quantities are explicit functions of the state of order, as expressed by the four variables S_1, S_2, S_3, S_4. Hence the free energy $F-T\Phi$ is a known function of the state order and may be minimized by known mathematical processes. The fact that the state of order cannot be expressed by a single parameter considerably increases the labor involved. The results show that the free energy depends in a distinct way on composition for three phases which are characterized by certain relationships between the parameters:

phase ξ, random cubic, $S_1=S_2=S_3=S_4$ (7.2)
phase η, ordered cubic, $S_1\neq S_2=S_3=S_4$ (7.3)
phase ζ, ordered tetragonal, $S_1=S_2\neq S_3=S_4$ (7.4)
and $S_1\neq S_2\neq S_3=S_4\neq S_1$ (7.5)

When plots at constant temperature of free energy for each of the three phases *versus* composition are made, results like that indicated in Fig. 28 are obtained. (This figure is not quantitative; the reentrant portions near the crossing points being greatly exaggerated.) It is seen that in different composition ranges different phases have the least free energy and are stable. In the neighborhood of the intersection points of the free energy curves, common tangents can be drawn as are indicated in the left half of the figure. For compositions between the points of tangency, the most stable state of the alloy will

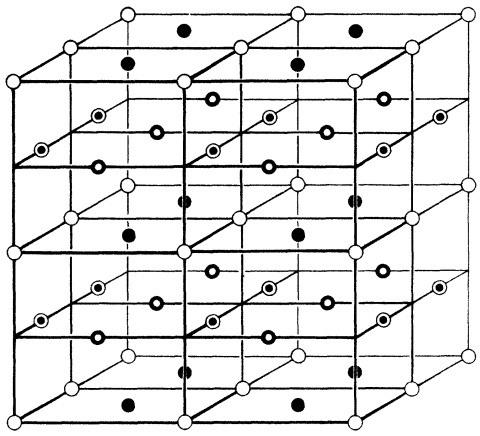

FIG. 27. Resolution of face-centered cubic lattice into four simple cubic sublattices; all points of each sublattice are indicated by same symbol.

be a mixture of two phases having compositions corresponding to the points of tangency.[8] After similar curves are found for other temperatures, the phase diagram, Fig. 26, can be constructed.

No experimental work has as yet shown the occurrence of two phases with different compositions, one ordered and one not, in equilibrium with each other. Although such situations seem inevitable on basic thermodynamic grounds, they may be very difficult to realize in practice owing to the slowness of obtaining equilibrium.

If the segregation into two phases does not have time to occur, then the temperature composition diagram should be constructed as indicated on the right of Fig. 28 where the stable phase for each composition is given. The result of this process is represented by the dashed lines in Fig. 26. They correspond to Easthope's curve

[8] For a discussion of this thermodynamical question see, for example, N. F. Mott and H. Jones *The Theory of the Properties of Metals and Alloys* (Oxford 1936) p. 24 and various texts of physical chemistry.

for $z=\infty$, Fig. 24, save that a different type of lattice is present. We see that there is no maximum in the critical temperature at the atomic ratio 3 : 1.

The writers believe that there is no theoretical basis for expecting a maximum or minimum of the critical temperature at any particular atomic ratio save 1 : 1. Here the curve must be flat because of the symmetry about this point. This belief is based on the following reasoning. At the critical temperature there is only a small amount of order present. Consequently an excess or defect of one species of atom represents a continuous change in the state of affairs and there seems no reason for a particular ratio of abundance, like 3 : 1, having special significance. This is very different from the situation at low temperatures; then it will be quite important to have just the right proportion of atoms and an excess and a defect will change the energy in quite different ways; note the kink in the energy *versus* composition curve for the ordered face-centered cubic lattice in Fig. 23.

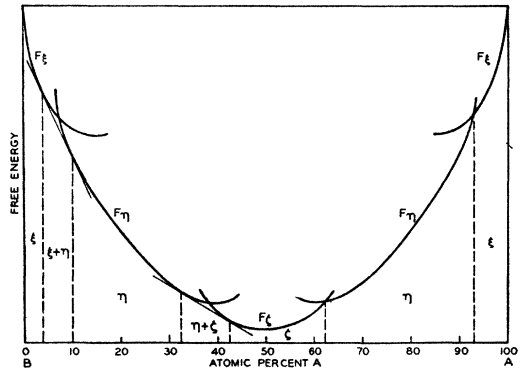

FIG. 28. Free energy *versus* composition for the three phases of the face-centered cubic lattice.

We see furthermore that between ratios of 3 : 1 and 1 : 1 there are two critical temperatures: one corresponding to a transition from tetragonal ordered to cubic ordered, the other from cubic ordered to cubic random. For the Cu-Au alloy system, as described in Part II, Section 16, two phase changes for a single composition have been observed.[36E] However, one of the two observed ordered structures is orthorhombic rather than cubic. Each of these transitions has in general an associated latent heat and a kink in the specific heat curve. Fig. 29 shows the latent heat as a function of composition and Fig. 30 represents the specific heat curve corresponding to A_3B_5. The prediction based on the work of Bragg-Williams, Bethe, and Peierls that only the ratio 1 : 1 has no latent heat is confirmed. We shall return to this point briefly in Section 13.

8. Treatments not using the nearest neighbor assumption

Borelius does not utilize the nearest neighbor assumption but assumes instead a more general form for the energy. In terms of our expressions it amounts to assuming that the energy is

$$E=E_0(a+bS^2+cS^4+dS^6+\cdots) \qquad (8.1)$$

and the entropy is

$$\Phi=\Phi(S), \qquad (8.2)$$

where $\Phi(S)$ is the Bragg-Williams approximation expression. The constants in the energy form are to be determined by experiment. This formulation allows Borelius to give a discussion in terms more general than are permitted by the nearest neighbor assumption; however, it has the simultaneous disadvantage of restricting most of the results to generalities and thus not giving material which can be directly compared with experiment.

Energy-entropy-composition surface

Borelius discusses the problem by using a generalization of the energy-entropy curves discussed in Section 3. These curves corresponded

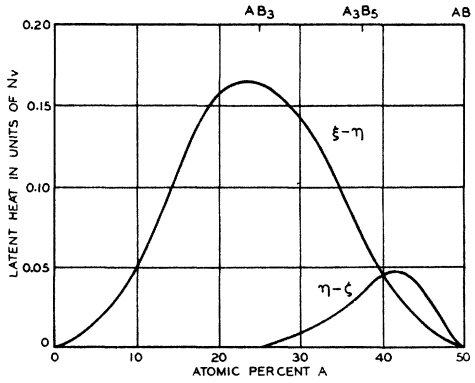

FIG. 29. Latent heats of transformation for face-centered cubic lattice.

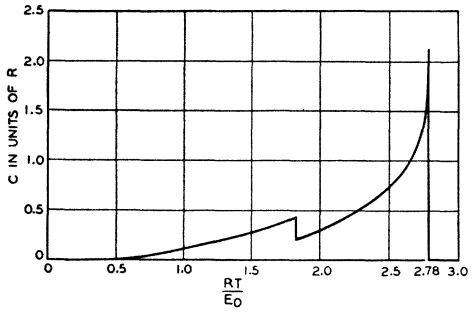

FIG. 30. Specific heat *versus* temperature for face-centered cubic lattice A_3B_5 case.

to a single composition; if a composition axis is constructed at right angles to the entropy and energy axes, then the family of energy-entropy curves for various compositions will constitute a surface. Just as a complete knowledge of the energy-entropy curve was equivalent to a solution of the case of fixed composition, so is a complete knowledge of this surface all that is needed for the alloy system.

Borelius gives a general discussion of this type of surface even including the case for which the random state, rather than the ordered state, has the lower energy. This interesting case corresponds to metals which have limited solid solubilities in each other at low temperatures. It has recently been discussed by R. Becker[37Z] using the nearest neighbor assumption with a negative value of v. A further discussion of this topic would be out of place in this review; and it has been mentioned only as an example of the utilization of ideas developed in the order-disorder theory in other branches of metallurgy.

9. The thermodynamic potentials of ordered phases

Tammann based his early prediction of ordered structures upon chemical evidence in the Cu-Au system. We discussed these ideas briefly in the introduction. He found two concentration limits for the action of Cu dissolving solvents, one at Cu_3Au and one at CuAu. These correspond to the abrupt changes of slope near Cu_3Au and CuAu of the free energy *versus* composition curve, which for low temperatures is very nearly like the curve for best order of Fig. 23. From the "slope-intercept" method of finding thermodynamic potentials, we can easily see that there will be a sudden change of the thermodynamic potential of Cu for these compositions, of a nature to make it more difficult to extract Cu from the less Cu rich alloys.

This means of investigating superstructures has not been very active recently. For a further discussion the reader is referred to the works of Tammann.[19A, 21A]

C. *Theories for alloys which are not in thermal equilibrium*

Not very much work of a theoretical nature has been done as yet upon the behavior of alloys which are not in equilibrium. The two principle contributions concern rather different aspects of the question. Bragg and Williams have investigated the rate of approach to equilibrium of alloys which are almost in equilibrium; and Borelius has dealt primarily with questions of temperature hysteresis: that is, with effects connected with order which are very much like the supercooling of liquids or the lag in phase change between white and grey tin.

The rate of approach of the alloy to equilibrium is governed by the frequency with which atoms change places. This interchanging is in turn associated with an activation energy and, like many chemical processes having an activation energy, it "freezes out" at a certain temperature: that is, at this temperature the time of relaxation is of the order of years and somewhat above it, of the order of hours. For some alloys, β-brass for example, the "freezing out" temperature, T_f, is considerably below the critical temperature of ordering, T_c. These alloys usually order upon cooling from temperatures above T_c: during the process of cooling, they pass through temperatures below T_c, for which a superlattice should form, while they are still hot enough to possess a short relaxation time; this favorable situation produces a superlattice. On the other hand if T_f is much above T_c, no superlattice can be produced by heat treatment: at temperatures where a superlattice would be thermodynamically stable, the relaxation time is so great as effectively to prevent ordering: while at temperatures giving a short relaxation time, the superlattice is not stable. The freezing out effect just discussed probably prevents the formation of a considerable number of otherwise to be expected superlattices.

10. The time of relaxation

Bragg and Williams, using the ideas presented in Section 1, have developed a theory describing the relaxation of an alloy toward its state of thermal equilibrium. The following discussion follows closely their presentation of reference 34C.

As we discussed in connection with the $S(X)$ and $V(S)$ curves of Section 1, when the alloy is not in equilibrium the degree of order is not what it should be for the ordering force which is present. Let us once more concentrate upon the A atoms and see how they change places between α- and β-sites.

Denote by n_w the number of A atoms on α-sites which displace B atoms on β-sites per second, that is the number going wrong, and by n_r the corresponding number of A atoms returning from β-sites and displacing B atoms on α-sites. Under equilibrium conditions, these processes will of course balance and we shall have

$$n_w = n_r. \tag{10.1}$$

When we do not have equilibrium these will not be equal and consequently the total number of right A atoms will be changing.

According to the definitions and limitations of Section 1, the total number of right atoms is $F_A N r_\alpha$, and the rate of change of this is

$$F_A N(dr_\alpha/dt) = n_r - n_w. \tag{10.2}$$

Let the temperature now be considered constant with value T; let $r_{\alpha e}$ signify the corresponding equilibrium value of r_α and let the instantaneous value of r_α be

$$r_\alpha = r_{\alpha e} + \delta, \tag{10.3}$$

where δ represents the deviation from equilibrium. When δ is zero, we have equilibrium and $n_r - n_w$ vanishes. If δ is positive, there are more right atoms than there should be and there is a net change towards wrong positions. At the constant temperature, T, n_w and n_r are both functions of r_α, and the value of their difference for the small deviation δ will be

$$n_w - n_r = [(d/dr_\alpha)(n_w - n_r)]_e \delta = C\delta, \tag{10.4}$$

where the subscript e means that the derivative is evaluated at $r_\alpha = r_{\alpha e}$ and

$$C \equiv [(d/dr_\alpha)(n_w - n_r)]_e. \tag{10.5}$$

Putting this in Eq. (10.2) we find

$$\frac{d\delta}{dt} = -\frac{C}{F_A N}\delta. \tag{10.6}$$

This is the conventional equation of an exponentially decaying disturbance. In terms of the relaxation time τ,

$$\tau = F_A N / C, \tag{10.7}$$

the solution is

$$\delta = \delta_0 e^{-t/\tau}, \tag{10.8}$$

where δ_0 is the deviation from equilibrium at $t = 0$. The problem of Bragg and Williams was to estimate the value of C.

Consider an adjacent pair of A and B atoms. Owing to the temperature agitation there is a probability that these two atoms will acquire sufficient energy and appropriate directions of motion and will change places. In making this change with the A atom going from the α- to the β-site, the atoms must climb over a potential barrier of height W, hence their thermal energy at the beginning of the interchange must be at least W. When returning they must again climb over this barrier but since initially they had potential energy $V = V_0 S$ due to the fact that both atoms were wrong, an initial thermal energy of only $W - V$ is needed. We approximate the condition necessary for two adjoining A and B atoms to change places and become wrong atoms by the three conditions:

(1) When A crosses the plane which passes through the α-site and is perpendicular to the line connecting the pair of sites, it does so with kinetic energy greater than $W/2$ and in a direction which lies within a certain solid angle $4\pi\omega$.

(2) The same condition (with B and β replacing A and α) applies to B.

(3) These events agree in time within a fraction φ of the period of oscillation which may be taken to be the same for both.

"In other words an interchange will take place during a period of oscillation if both atoms have sufficient energy, are aimed correctly, and approach the barrier nearly simultaneously." Denoting the frequency vibration by ν and denoting by $F_{\alpha\beta}$ the probability that the two adjoining A and B atoms go wrong per unit time, we find

$$f_{\alpha\beta} = 16\nu\varphi\omega^2(1 + W/2kT^2)e^{-W/kT}. \tag{10.9}$$

Similarly the probability that two adjoining wrong atoms become right in unit time is

$$f_{\beta\alpha}=f_{\alpha\beta}e^{V/kT}. \qquad (10.10)^{9}$$

We must next estimate the number of ways in which right A atoms can go wrong with adjacent B atoms. The number of A atoms upon α-sites is $r_\alpha F_A N$. Let each of these α-sites be surrounded by y adjacent β-sites. Each of these β-sites has the probability r_β of being occupied by a B atom. Thus on the average each of the $r_\alpha F_A N$ right A atoms has yr_β ways of going wrong; hence the total number of ways for A atoms to go wrong is

$$r_\alpha F_A N y r_\beta = N F_A y r_\alpha r_\beta. \qquad (10.11)$$

Similarly the number of ways in which A atoms can return to α-sites is

$$N F_A y w_\alpha w_\beta. \qquad (10.12)$$

Combining these with the probability that each of these interchanges takes place in unit time we obtain

$$n_w = N F_A y r_\alpha r_\beta f_{\alpha\beta}, \qquad (10.13)$$

$$n_r = N F_A y w_\alpha w_\beta f_{\beta\alpha}. \qquad (10.14)$$

We see easily that the condition for equilibrium, $n_r=n_w$, leads to the equation:

$$\frac{r_\alpha r_\beta}{w_\alpha w_\beta}=\frac{f_{\beta\alpha}}{f_{\alpha\beta}}=\exp\frac{V}{kT}, \qquad (10.15)$$

which is the equilibrium condition 1.7 of Section 1.

All the quantities occurring in n_w and n_r are either constants or known functions of r_α. Hence the derivative C, Eq. (10.5), can be evaluated and τ calculated from Eq. (10.7). We have

$$n_w-n_r=N F_A y r_\alpha r_\beta f_{\alpha\beta} \times[1-(w_\alpha w_\beta/r_\alpha r_\beta)\exp(V/kT)]. \qquad (10.16)$$

From (1.7), (1.8) and (1.37) we find that $r_\alpha r_\beta/w_\alpha w_\beta=\exp X_2(S)$; and from (1.12) and (1.36) that $V/kT=X_1(S)$. Differentiating (10.16) with respect to S and noting that the equilibrium value, S_e, satisfies $X_1(S_e)=X_2(S_e)$, we find

$$[(d/dS)(n_w-n_r)]_e=F_B[(d/dr_\alpha)(n_w-n_r)]_e$$
$$=F_BC=NF_Ayr_\alpha r_\beta f_{\alpha\beta}[X_2'(S_e)-X_1'(S_e)]$$
$$=NF_Ayf_{\alpha\beta}\left(\frac{1+S_e}{1-S_e}\right)\left(1-\frac{X_1'}{X_2'}\right).$$

Insertion of the value of C in Eq. (10.5) leads to

$$\tau^{-1}=\left(1-\frac{X_1'}{X_2'}\right)\frac{(1+S_e)y}{(1-S_e)F_B} \times 16\nu\varphi\omega^2(1+W/2kT)^2\exp(-W/kT). \qquad (10.17)$$

The term in $(1-X_1'/X_2')$ arises from the dependence of V upon S and hence upon r_α. If V did not depend on r_α then the term would be unity; however, its dependence is such as to increase the time of relaxation. This can be seen by thinking of a deviation towards greater disorder; with it comes a decrease in order and consequently a decrease in ordering force. Thus the rate of recovery is not as rapid as if the ordering force had remained constant. Near the critical temperature $X_1(S)$ and $X_2(S)$ cross at a slight angle and hence the ratio of slopes is nearly unity. Under these circumstances Bragg and Williams think that the length of the relaxation time may cause a lag in response of the structure to a change in temperature near the critical temperature. They site cases where such a lag has been observed.[10]

The dominant term in Eq. (10.17) is the exponential, and the variation of the other parts can be neglected except possibly for the case where $(1-X_1'/X_2')$ nearly vanishes. Thus we may write generally

$$\tau=Ae^{W/kT}. \qquad (10.18)$$

Taking

$\nu=10^{13}$ sec.$^{-1}$, corresponding to a characteristic temperature of 500°K
$\omega^2\varphi=5\times10^{-5}$
$y=4$,
$(W/kT)^2=600$,

they estimate that

$$A=10^{-12}\text{ sec.}$$

They have also estimated the value of A for a ring transition in which three atoms take part, and this leads to estimates of the same order of magnitude.

The order of magnitude chosen for W is reasonable. It should lie somewhere between values obtained from the energy required to melt the alloy and the energy necessary to separate it into free atoms. The latter is given by the binding

[9] Bragg and Williams establish this relationship by reasoning similar to that used in the mass action law.

[10] 34C, p. 725.

energy of the alloy and is about 80 kilogram calories per gram atom for alloys of the Cu-Au system; it gives a value of W/k of 40,000°K. From the energy required to melt the alloy we should obtain about 5000°K. Temperatures of interest for order-disorder phenomena in the Cu-Au system are about 600°K; hence W/kT should lie between 8 and 70; so that the value 24, assumed by Bragg and Williams, is of a reasonable order of magnitude.

The results of experimental investigations upon this field are given in reference 36I and described in Part II, Section 18.

11. The theory of temperature hysteresis

Borelius[34A, 37B] has developed a theory of temperature hysteresis based on the re-entrant portions of the energy *versus* entropy curves. In order to visualize his theory, suppose that the

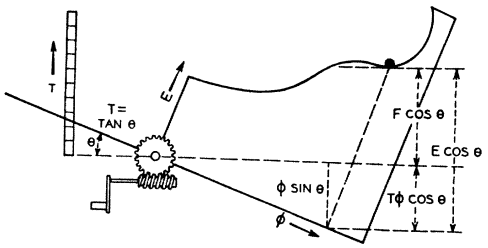

FIG. 31. Illustrating the origin of temperature hysteresis.

scales of the energy *versus* entropy plot are so chosen that a line at 45° corresponds to unit temperature. Then a line making angle θ with the entropy axis gives a temperature line with slope $T=\tan\theta$. Now instead of drawing a line with slope T, rotate the plot through angle θ as indicated in Fig. 31. It is seen that for any fixed temperature, height is proportional to free energy. Hence if a ball is allowed to roll on a track representing the curve, its lowest possible position specifies the stable state. In the figure the ball indicates a state with rather high entropy and consequently a high degree of disorder. This is not the stable state for there are lower points on the curve. However, the system cannot reach these without going through intermediate states of higher free energy; since this is impossible according to thermodynamics and highly improbable according to statistical mechanics, it stays where it is, in what is termed a "metastable state." Cooling the system decreases the bump in the free energy curve and finally it disappears entirely at a temperature, say T_1, for which the ball on the track would just roll down to the left. If the system is now heated, the bump reappears and at a temperature, say T_2, the minima to both sides are equally deep. According to the equilibrium theory of thermodynamics, this should be the transition temperature; however, the system is now caught to the left of the bump and cannot make the transition from its metastable state until a temperature T_3, again corresponding to the rolling of the ball, is attained. In Fig. 32, the solid line indicates the equilibrium behavior, and the dotted lines and arrows the hysteresis loop predicted on this theory.

By using various values for the coefficients in his energy as a function of order expression (8.1), Borelius is able to alter his energy *versus* entropy curve in such a way as to fit various observed cases which showed hysteresis.

Bragg and Williams[35E, 37U] point out that it is not necessary for the whole sample to travel over the bump in free energy, which would indeed be so improbable as to prevent a transition; instead it would suffice for a nucleus of the stable state to form—after which the change from one phase to the other would proceed like a recrystallization. The extra free energy needed to form such a nucleus would not be excessive and the probability of its occurrence would be appreciable. Bragg and Williams state that they have estimated the probability that a nucleus forms per unit time and that it is of such an order of magnitude that no appreciable hysteresis would be expected.

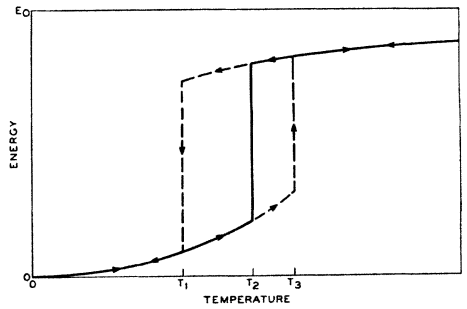

FIG. 32. Hysteresis loop for temperature hysteresis.

The experimental evidence on these points, which at present is none too conclusive, is presented in Part II, Section 18.

D. Adaptation of the idealized theory to actuality

So far in our theory, the atoms have been rather vague entities. They have been assumed to be distinguishable so that we could designate them by letters A and B and all their physical properties were exemplified by one or more of the three quantities z, v, and V_0. Now alloys are far too complicated to be adequately described by such a simple system; and as we shall see in Part II, they frequently depart from theoretical predictions made on this basis. In order to draw the theory nearer to reality, more of the characteristic properties of the metals forming the alloy must be included. In the following sections we describe some preliminary steps made in this direction.

12. The origin of the ordering energy

The theory of the origin of the ordering energy is not at present very advanced. Hume-Rothery[35N, 36L] has presented a valuable qualitative picture based on the ideas of strain in the lattice due to the presence of the two species of atoms. He notes, as we did early in this part, that superstructures are characterized in general by a tendency for like atoms to keep apart. This can be understood by supposing that one type of atom distorts the lattice of the other type and that the energy of distortion is least when the strain is distributed as evenly as possible. This leads to an effective short range repulsive force between like atoms and brings about the general kind of arrangement met with in superlattices. Hume-Rothery relates the strain in the lattice to the difference in size of the two atoms. If this difference is very small, the strain will be small and the ordering force so slight that superstructures do not form. On the other hand, if the difference is too great, the energy of mixing the metals will be positive and they will be relatively insoluble in each other (case of "unfavorable size factor"); under these conditions the solid solutions will be dilute and no superlattice will form. Only when the difference in size of the atoms lies in a certain restricted range will both the ordering energy and the solubility be favorable to the formation of a superlattice. Hume-Rothery's qualitative picture has so far been supported by experimental findings. However, the possibility of making quantitative predictions on its basis seems remote, and we expect that accurate theories will be founded on the quantum-mechanical electronic theory of metals.

Mott[37L] has made a quantum-mechanical calculation of the energy of the superlattice in β-brass. A detailed discussion of Mott's work, which would involve the modern electronic theory of metals, is beyond the scope of this review. He finds that the principle terms in the energy arise from the exchange repulsion between the ions and from electrostatic effects due to the fact that Cu and Zn ions do not possess equal charges in the alloy. His estimate of the energies per gram atom are:

Electrostatic	620 calories
Energy due to exchange repulsion	300 calories
Total energy (calculated)	920 calories

while he estimates that experiment gives

Total energy (observed) less than	990 calories.

His work also enables him to discuss the validity of the nearest neighbor assumption and he concludes that it is a good approximation to consider energies between nearest neighbors only but that the value of the interaction energy is not independent of the state of order but decreases with decreasing order. This will lead to increased abruptness in the rapid approach to disorder with rising temperature and may account for the fact that the peak, $5.1R$ in the anomalous specific heat for β-brass, shown in Figs. 4 and 35, is considerably higher than the values, $1.78R$ and $2.21R$, predicted by the nearest neighbor theory for the body-centered lattice, Table I. It is also evident from Mott's work that the energy of interaction between nearest neighbors will depend upon the composition. A further study of this question would be of considerable interest in explaining and analyzing curves of critical temperature *versus* composition such as Fig. 39, in Part II, Section 15.

An improvement of agreement between theory and experiment has been effected by Chang.[37Y] He achieves this by the introduction of interactions between next nearest neighbors into Bethe's theory. This procedure leads to a theory

which has two adjustable parameters that can be varied independently in order to alter the predictions of the theory. With the theories of the origin of the ordering energy in their present state, we regard results obtained by the introduction of further parameters more as an indication of possible types of behavior than as an explanation of experimental findings.

13. The effect of lattice vibrations

In the introduction to Part I, we stated that independence of the lattice vibrations and state of order would be assumed. This assumption is dictated by simplicity and a lack of knowledge as to what connection is to be expected. Some experimental evidence, cited in Part II, Section 20, shows that elastic properties, and consequently lattice vibration frequencies, are affected by the state of order. In this section we shall see how various kinds of dependence of Debye temperature on state of order may alter the symmetry about 50 atomic percent and may create or suppress latent heats.

Entropy of lattice vibrations

If the lattice vibrations depend upon the state of order, then their free energy must be added to the configurational free energy and the total free energy minimized to find the equilibrium state. In the free energy for the lattice vibrations, however, there is only one term which can depend on the state of order; it is the part of the entropy associated with the Debye temperature. This term may easily be found from the expression for the free energy of a harmonic oscillator.[11] Letting θ be the Debye temperature, whose value for the state of perfect order is θ_1, and chosing the zero of entropy as the state of perfect order, we find

$$\Phi_L(\theta) = 3R \ln (\theta_1/\theta). \qquad (13.1)$$

This expression is so important in the following remarks that we shall derive it by a simple physical argument. We are interested in temperatures well above the Debye temperature so that we may consider the energy of each of the $3N$ modes of vibration to be kT, independent of the value of θ. Hence the energy term in the free energy does not depend on order and can be disregarded. Now the spacing of the energy levels of the normal modes is proportional to θ—we assume that all frequencies vary in the same proportion as θ varies due to changing order. Hence if 1 and 2 are two states of the system and θ_1/θ_2 is greater than unity, then the energy levels are more closely spaced for 2, and there will be more ways of distributing the energy among the vibrational modes. In fact there will be θ_1/θ_2 more ways for each mode and consequently

$$(\theta_1/\theta_2)^{3N} \qquad (13.2)$$

more ways in all. Hence the difference in entropy between 1 and 2 is

$$\Phi_2 - \Phi_1 = k \ln (\theta_1/\theta_2)^{3N} = 3R \ln \theta_1/\theta_2. \qquad (13.3)$$

This is equivalent to the expression already given.

Energy versus total entropy curves

The relationship between configurational energy and entropy, henceforth denoted by $\Phi_c(E)$, was discussed in Sections 3 and 4. Due to the assumed relationship between the Debye temperature and state of order (we are here supposing that the effect due to thermal expansion can be separated off), we can consider $\Phi_L(\theta)$ as a function of the configurational energy and plot it on the same set of axes. Curves 1 to 6 in Fig. 33 indicate schematically some possible types of behavior. Curves AB and AB_3 correspond to the configurational curves for those compositions. They are drawn, as is described in Section 3, in accord with the ideas underlying Bethe's and

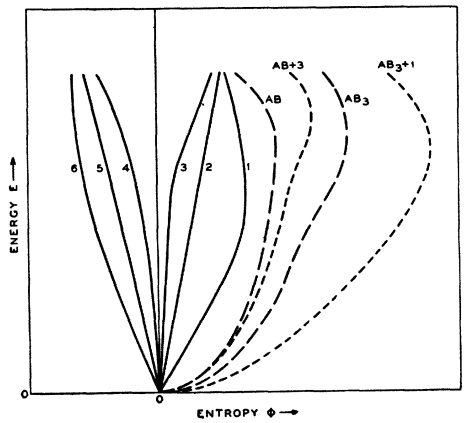

FIG. 33. Possible behaviors for entropy of lattice vibrations and the effect upon AB and AB_3 cases.

[11] See for example Mott and Jones, 36M, p. 2.

Kirkwood's theories so that the maximum entropy occurs with the energy, E_0, corresponding to the purely random state, with short range order $\sigma=0$. Energies above E_0 correspond to negative values of σ; they have less entropy than the random state and represent arrangements having like atoms clustered together.

The entire order dependent part of the entropy for a given configurational energy is found by adding the configurational entropy, $\Phi_c(E)$ and the entropy of lattice vibrations, $\Phi_L(E)$. Denoting this total entropy by $\Phi_T(E)$, we have

$$\Phi_T(E)=\Phi_L(E)+\Phi_c(E). \tag{13.4}$$

Φ_T is then a definite function of the energy E, and the new energy-entropy curve completely specified.

The simplest dependence of Φ_L upon E is a straight line as indicated by 2 and 5. In this case the influence of lattice vibrations is just to change the temperatures at which various stages of disorder are reached. Curve 2 which has increasing entropy with increasing disorder favors the destruction of the superlattice and lowers the temperatures. We find in accordance with Eq. (3.7) that the temperature corresponding to a given value of the configurational energy is determined from

$$\frac{1}{T}=\frac{d\Phi_T}{dE}=\frac{d\Phi_C}{dE}+\frac{d\Phi_L}{dE}=\frac{1}{T_0}+\frac{1}{T_L}, \tag{13.5}$$

where T_0 is the temperature obtained by neglecting the lattice vibrations and T_L is slope of the E *vs.* Φ_L line. We see that T is less than T_0 when T_L is positive so that the effect of the lattice vibrations is to shift the order-disorder transformation to lower temperatures. $T=\infty$ corresponds to

$$T_0=-T_L. \tag{13.6}$$

Thus for this case the high temperature state is not random but corresponds to a negative value of T_0, implying that it is past the maximum entropy state on the configurational curve and corresponds to negative short range order.

A negative slope for the straight line tends to make states of high order more stable and thus shifts the transformation to higher temperatures. $T=\infty$ corresponds to a positive finite value of T_0 in this case so that the random state is never reached and the alloy preserves a certain amount of its order to very high temperatures.

The effect of curvature in the Φ_L line is very interesting. As we have discussed above, latent heat is due to an inward curvature in the energy-entropy curve, as is indicated to a very exaggerated extent on the AB_3 curve. Calculations in the Bragg-Williams approximation show that this curvature is very slight indeed, consequently Φ_L curves like 1 or 4 when combined with AB_3 may entirely remove the reentrant portion and suppress the latent heat. The curve AB_3+1 on Fig. 33 illustrates this. On the other hand Φ_L curves like 3 and 6 will increase the reentrant portion and increase the latent heat. Thus a curve of type AB, which has no latent heat by itself, may acquire one when combined with a Φ_L curve like 3 or 6, which will give rise to a reentrant portion for Φ_T. Other possible behaviors will occur to the reader; however, it does not seem worthwhile at present to elaborate these speculations.

Some preliminary calculations by the writers[38c] indicate that certain features of the Cu-Au system may be explained by arguments along the following lines. The Φ_L curve for Cu_3Au is weakly of type 4. This will tend to raise the critical temperature, decrease the latent heat and prevent complete disordering at high temperature. On the other hand for $CuAu_3$, θ is nearly independent of order. Hence the critical temperature for $CuAu_3$ will be lower than for Cu_3Au, perhaps so much lower that the ordering process is frozen out to a considerable extent above the critical temperature thus accounting for the absence of a strong superstructure in $CuAu_3$.

Part II. Experimental Studies of Superstructures

The theories discussed in the foregoing pages have dealt principally with two attributes of the order-disorder transformation: the state of order itself, and quantities of the nature of energy. We shall now discuss measurements of the energy of transformation as well as determinations of specific heats at various temperatures, and compare with them the theoretical predictions.

We shall follow this discussion with a description of the results of x-ray analysis of the nature of the ordered structures and compare these experimental results with the demands of theory, recalling that the nearest neighbor conception demands that an ordered structure be so arranged that any given atom will be surrounded by the largest possible number of unlike neighbors.

The theories also predict, in some simple cases, how the "Curie point of order"—the temperature where long distance order begins on cooling—should vary with composition. Again we shall compare these predictions with the experimental results. Finally we shall discuss the effect of order on various mechanical, magnetic and electrical properties of alloys.

Section 14. Energy content measurements

Accurate measurements of the specific heats of order-disorder transformations yield direct data which can be compared with the theoretical predictions given above. The method of mixtures, commonly employed to determine the specific heats of solid bodies at high temperatures, fails to yield sufficiently accurate data to compare with theory, especially in the interesting region near the Curie point of order. A modification of the Nernst vacuum calorimeter has been devised by Sykes[35R, 36N] and his collaborators, and a somewhat similar modification independently by Moser,[36F] in order to obtain accurate specific heats at various temperatures. Sykes' modification consists essentially in using a specimen in the form of a closed hollow cylinder placed inside and thermally insulated from a second closed cylinder of copper. The outer cylinder is heated by the usual resistance wound furnace while the inner one, the specimen, is heated independently by a small auxiliary heating coil. By suitable adjustments of the heating currents, the two cylinders can be held at about the same temperature, and the radiation losses consequently minimized. From the knowledge of the energy input to the coil inside the specimen and the resulting rate of temperature rise of the latter, and with aid of certain corrections (for radiation losses and the like) the true specific heat values at various temperatures are obtained.

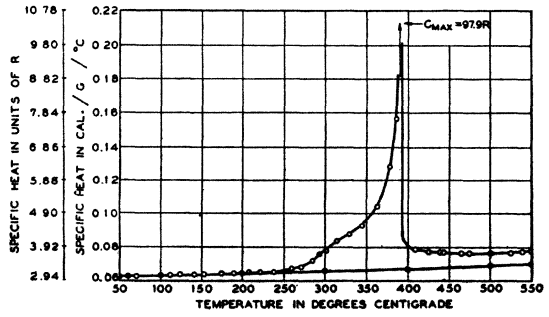

FIG. 34. Specific heat-*vs.*-temperature for a Cu_3Au alloy is shown by the curve (0). The curve (●) is calculated from the specific heats of Cu and Au assuming a pure mixture.

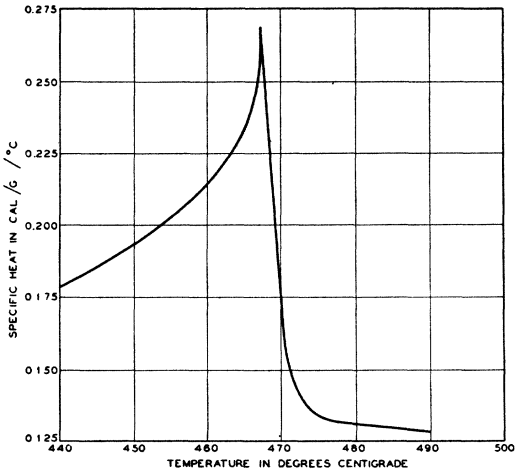

FIG. 35. Specific heat-*vs.*-temperature for a β-brass containing 50.4 atomic percent Zn.

Figure 34 gives the "anomalous" specific heat-*vs.*-temperature curve[36H] (curve with open circles) for a Cu_3Au alloy which had been previously ordered by slow cooling at the rate of 30°/hour from 450°C. The curve marked by solid circles was obtained by taking the experimentally determined specific heat values of Cu and Au and assuming the law of mixtures (Kopp-Neumann law) to be valid for the alloy. The observed specific heats did not depart appreciably from the thus-computed values below 225°C; at this temperature we infer that the divergence away from perfect order commences. The specific heat curve had a maximum at *ca.* 391°C, the Curie point of order. Above this it does not drop directly to the Kopp-Neumann line but approaches it towards higher temperatures. Thus there is an anomalous specific heat above as well as below the Curie point.

Figure 35 is a similar curve for β-brass, taken

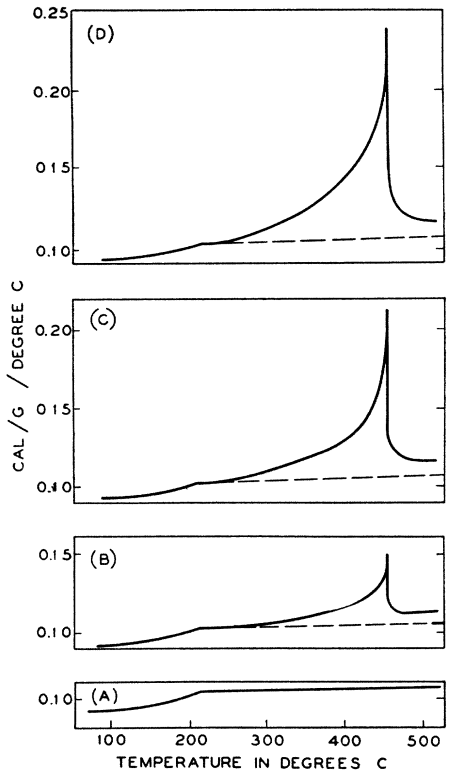

FIG. 36. Specific heat-*vs.*-temperature for a series of Cu-Zn alloys. *A* is for a pure α-brass containing 36.80 atomic percent Zn. *B*, *C*, *D*, refer to alloys in the $\alpha+\beta$ field containing 41.09, 43.44 and 45.64 atomic percent Zn, respectively.

from the work of Sykes and Wilkinson,[37P] showing in considerable detail the behavior near the Curie point of order. Fig. 4 of the introduction was obtained by Moser,[36F] also for β-brass; it covers a larger temperature range than Fig. 35. On the latter figure we note that the drop of specific heat beyond the peak is spread over a range of about 10°C. We return to this point below when comparing values on these curves with theory.

In Fig. 36 we give specific heat curves[37P] for several other compositions of Cu-Zn alloys. These have less Zn than the β-brass of Fig. 4, and lie in the $\alpha+\beta$ field so that the alloy does not consist of a single phase of β, as it did in Fig. 4, but of a mixture of the β-phase and the α-phase. The lowest curve is for the pure α-phase; it shows a kink in the specific heat curve at *ca.* 200°C, which is not understood. The second curve corresponds to a mixture of α and β consisting chiefly of α. The higher curves correspond to more Zn and hence a larger proportion of β. The peak in the curves is due to the β-phase and increases in height with increasing quantity of β; however, since the β-phase does not alter its composition appreciably the Curie point of order does not change.

The energy of transformation of an alloy can be obtained by integration of the specific heat curve, or it can be determined directly by simply measuring the energy necessary to transform the partially ordered specimen from a temperature T to a temperature immediately above the Curie point of order. Fig. 37 depicts such an experimentally determined curve[36H] for a Cu_3Au alloy along with the theoretical curves discussed above, as predicted by the Bragg-Williams and the Bethe-Peierls theories. In Fig. 38, we give the energy of transformation-*vs.*-composition for a series of Cu-Zn alloys, as determined by Sykes and Wilkinson.[37P] The increase in the energy of transformation with increasing zinc content in the two-phase $\alpha+\beta$ field is again due to the increasing amount of the β-phase. The curve shows, however, for the first time how the energy of transformation varies as a function of composition for pure β-phase alloys not possessing the composition, CuZn, necessary to give the ideal superlattice. We note that the energy necessary to transform the alloy from a highly ordered state at 240°C to the disordered condition at 500°C increases as the zinc content approaches 50 percent, i.e., CuZn. Easthope's theoretical results, shown in Fig. 25, predict that the energy of transformation at the copper-rich side of the β-phase field, *ca.* 45 atomic percent Zn, should be

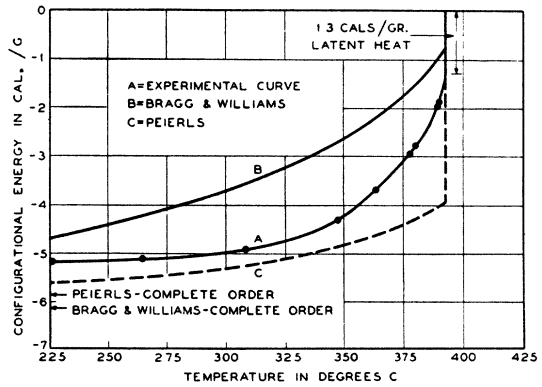

FIG. 37. Energy of transformation-*vs.*-temperature for Cu_3Au.

0.78 times that of a CuZn alloy. The experimental results of Sykes and Wilkinson yield 0.75, in quite good agreement.

On comparing the theoretical predictions with the experimental specific heat curves, we note a general qualitative agreement with the results, shown in Fig. 13, of Bethe and Kirkwood for alloys of 50–50 atomic compositions, e.g., β-brass, in particular regarding the high specific heat *above the Curie point* of long distance order. The Bragg-Williams theory, as given above, requires the configurational specific heat to vanish for temperatures above that point. The same general behavior is to be seen in Fig. 34 for a Cu_3Au alloy.

The agreement between theory and experiment for the specific heats *immediately below* T_c is not very satisfactory. Sykes and Jones[36H] report the configurational specific heat at this point for well ordered Cu_3Au, free from out-of-step domains, to be $62.0R$ whereas the Bragg-Williams theory gives (Table I) the value of $2.4R$. The experimentally determined value for β-brass is $5.1R$, whereas the theory of Bragg and Williams gives $1.5R$, Bethe's first approximation $1.78R$, and Kirkwood the somewhat higher value of $2.21R$. We note that alloys become disordered more rapidly immediately below T_c than the theories predict.

The numerical aspect of this disagreement between theory and experiment must not be taken too seriously, however, for the specific heat, being a derivative, will be drastically affected by small errors in the theory. We notice that for the simple cubic lattice, the Bethe and Kirkwood theories diverge by a factor of two. An explanation due to Mott has already been given (Section 12); he predicts on the basis of the electronic theory of metals that the effective ordering force will decrease more rapidly than any of the other three theories predicts. This process will result in a more abrupt disappearance of order with a consequently higher peak in the specific heat.

The rapid downward slope, or fall in the specific heat-*vs.*-temperature curve of β-brass for the temperature region immediately above T_c is thought to be due to the breaking up of coherent long distance order into small partially ordered domains. This explanation is analogous to that given by Mott and Potter[37M] to explain the similar

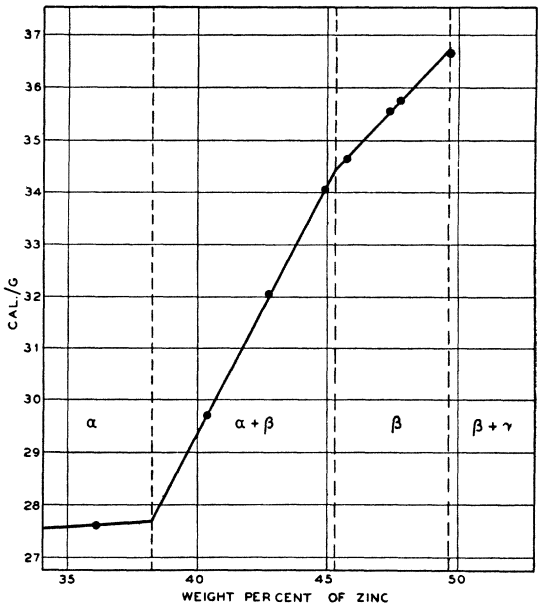

FIG. 38. Energy consumed in transforming a series of Cu-Zn alloys from 240°C to 500°C.

behavior in the specific heat curve of pure Ni above the magnetic Curie point. Sykes[38A] states that such behavior is generally observed in order-disorder transformations.

The curves of energy of transformation-*vs.*-temperature lend themselves better to a comparison between theoretical and experimental values in the vicinity of the Curie point. Fig. 37 shows the theoretically and experimentally determined values for such a transformation in Cu_3Au. Again the alloy disorders more rapidly at temperatures near the Curie point of order than either the Bragg-Williams or the Bethe-Peierls theories predict, whereas the agreement is much better at lower temperatures. The relationship between the critical temperature and the energy required to transform an alloy from some lower temperature to just above that critical temperature is nearly that given by the theories. The experimental value for $RT_c/E(T_c+)$ is 2.60, compared to 2.19 for Bragg-Williams and 2.38 for Peierls, as given in Table I.

As was discussed in Part I, Sections 1, 2, 4 and 7, a latent heat was predicted from the work of Bragg-Williams, Bethe, Peierls and Shockley for all atomic percentages save 50–50. Sykes and his collaborators have reported the presence of latent heats for Cu_3Au[36H] and $MgCd$[37U] alloys whereas

the transformations in β-brass[37P] and Cu_3Pd[37U] display no indication of a latent heat. Of these four cases of experimental evidence, the Cu_3Au and CuZn alloys agree with the theoretical predictions, whereas Cu_3Pd and MgCd do not.

One way of explaining these discrepancies has been suggested in Section 13; it was there shown that the manner of the dependence of the Debye temperature upon the state of order has an influence upon the presence or absence of latent heats. Although the correct explanation may be entirely different, measurements of Debye temperatures for these alloys would be of considerable interest.

The entropy changes associated with the destruction of the superlattice have been calculated by the various theorists, and their results are given in Table I. These quantities are only the configurational entropies, effects due to lattice vibrations, electronic specific heats, etc., being disregarded. For Cu_3Au Sykes and Jones[36H] estimate a change in entropy from perfect order to the state just above T_c amounting to $0.40R$ per gram atom. Table I gives the corresponding quantity $\phi(T_c+)$ as $0.562R$ by the Bragg-Williams theory and about $0.46R$ by Peierls' theory. Peierls' value is lower than Bragg and Williams' by virtue of the local order still present above T_c; according to Bragg-Williams theory the state just above T_c is entirely random. The fact that the experimental value is smaller than Peierls' value may indicate that the short range order is even greater than predicted by Peierls. In Fig. 37 there is another disagreement with Peierls: the experimental latent heat is smaller than he predicts. As pointed out above, the latent heat may be very sensitive to the behavior of the Debye temperature, and in Section 13 we showed how the entropy and latent heat would both be reduced by such effects. The corresponding entropy change for β-brass has been estimated by Sykes and Wilkinson by extrapolation for the 50–50 composition, CuZn, as $0.51R$. As in the preceding case, it turns out to be less than the predictions of $0.69R$ by the Bragg-Williams theory and $0.65R$ by the theories (including short range order) of Bethe and Kirkwood.

The agreement between theory and experiment for the β-brass transformation, although not exact, was sufficiently impressive to make the presence of a superstructure acceptable to most investigators; quite recently this conclusion has been definitely confirmed by the x-ray evidence of Jones and Sykes.[37I]

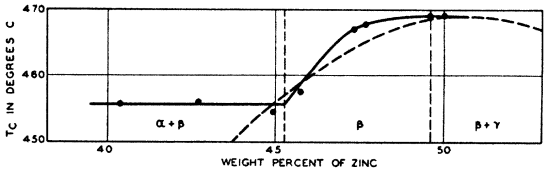

FIG. 39. Critical temperature of order-*vs.*-composition. Dashed curve represents this relationship as given in the theory of Easthope.

Section 15. Curie point of long distance order as a function of composition

Early investigators noted that what we today call the Curie point of long distance order depends on the composition of the alloy. Even small deviations in composition from the simple atomic ratio necessary to form an ideal superlattice entail a change in the Curie temperature. For the Cu_3Au region the available data[27A, 31A] indicate that an excess of either metal tends to lower this critical temperature of order, T_c. The theories based on the nearest neighbor assumption do not predict a maximum in the critical temperature at this composition; and for the reasons stated in Part I, Section 7 we believe this disagreement is due not to the mathematical approximations but rather to certain physical properties, neglected in the theory, which are characteristic of the Cu-Au system. This view is supported to some extent by evidence from other systems, for instance Cu-Pd in which ordered structures form at compositions just to one side of CuPd but apparently not at all at that composition itself.[32L]

The full line in Fig. 39 is the curve of critical temperature of order *vs.* composition for the β-brass phase as reported by Sykes and Wilkinson [37P] We note a falling off in T_c with decreasing zinc content as we proceed away from the composition CuZn. The dashed curve, depicting the behavior of T_c as a function of composition for a body-centered alloy as predicted by the theory of Easthope presented in Part I, Section 6, shows rather good agreement between theory and experiment.

Section 16. Ordered structures

Before discussing the ordered structures which have now been shown to exist in alloys, we shall review briefly the principal predictions of ordered structures made by theory. Although this introduction will serve as a basis for comparison between theory and experiment, its primary purpose is to describe in detail several important superstructures.

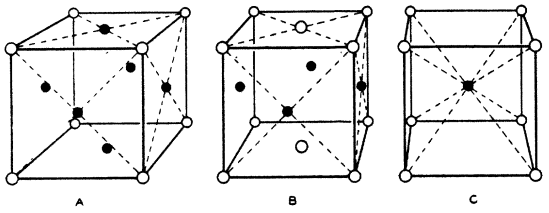

FIG. 40. Ordered structures (*A*) Cu_3Au, (*B*) CuAu: open circles, Au atoms; solid circles, Cu atoms; (*C*) CuZn: solid circles, Cu atoms; open circles, Zn atoms.

In the Part I, Section 5 we showed how in three cases the nearest neighbor assumption leads to definite ordered structures. In brief outline this comes about as follows: according to the nearest neighbor assumption the atoms tend to form unlike pairs, the energy of the crystal being in fact $(-v)$ times the number of unlike pairs, so that the lowest energy state corresponds to a maximum number of unlike pairs. For *composition AB in the body-centered lattice* this condition of maximum number of unlike pairs or minimum energy leads to the CsCl structure. In this structure every atom has only unlike nearest neighbors and the structure, shown in Fig. 40(C), is clearly uniquely determined. For *composition AB in the face-centered lattice*, the theory leads uniquely to the arrangement of Fig. 40(B). Here each atom has eight unlike and four like neighbors; it is impossible to get all neighbors unlike without changing lattice type. Any arrangement in which atoms have fewer than eight unlike neighbors would have higher energy according to theory, and therefore could not be the stable low temperature state. The third superstructure occurs *for composition* AB_3 and the equivalent A_3B in the face-centered lattice. In Fig. 40(A) we see it; each atom of the less abundant species is completely surrounded by unlike neighbors—obviously a condition of minimum energy. For the body-centered lattice of composition AB_3 or A_3B there is no prediction of a definite superlattice and it is possible to arrange the atoms in many ways all having the minimum energy. In the following discussion we shall see cases where the above predictions are fulfilled and others where they are not. These latter cases exhibit the failure of the simple theory.

The alloys of the Cu-Au system form an isomorphous series of solid solutions and crystallize upon a face-centered lattice. According to our theory there should be superstructures at Cu_3Au, CuAu, and $CuAu_3$. The first two compositions conform to prediction, as has been shown by the x-ray investigations of Johansson and Linde;[27A] but only inconclusive evidence of a superstructure has been obtained for the third.[36E] The Cu_3Au structure is, seemingly, just as predicted by theory. It has cubic symmetry and may be described by saying, as was done in Part I, Section 7, that three of the four simple cubic partial lattices, into which the face-centered lattice can be resolved, are of pure Cu and the fourth is pure Au. Resolving in the same way for the CuAu structure, we say that two of the partial lattices are Cu and two are Au; and the arrangement of atoms, as shown in Fig. 40(B), has tetragonal symmetry, the fourfold axis being perpendicular to the alternating planes of Au and of Cu atoms. The actual lattice has this tetragonal symmetry, and exhibits a slight distortion of the lattice sites from the cubic arrangement of the orderless alloy: in the ordered alloy, the axial ratio a/c is 1.080.[36E] Ordered structures like this have been found by Johansson and Linde for alloys having compositions from 47 to 53 atomic percent Au, which were annealed in

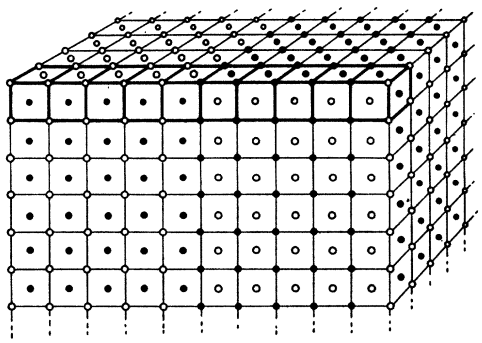

FIG. 41. Orthorhombic CuAu. Heavy lines outline unit cell. Open circles, Au atoms; solid circles , Cu atoms.

the temperature range 400°C to 200°C. In all of these, except of course the one which is exactly 50–50, there are extra atoms of Cu or Au above those needed to form the superstructure. These

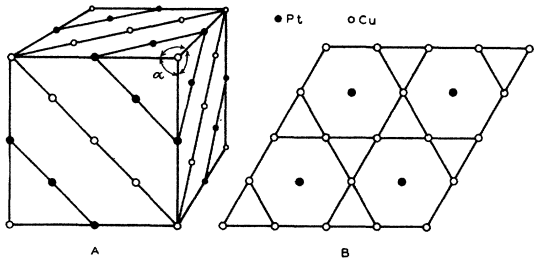

FIG. 42. (*A*) Trigonal CuPt. Alternate (111) planes are occupied by Cu and Pt atoms. (*B*) Illustrates the distribution of excess Pt among the Cu (111) planes of the CuPt structure for the Cu_3Pt_5 alloy.

apparently take up random positions in the lattice. This and cognate questions will be discussed in connection with the dependence of resistance upon composition.

Another superstructure, entirely different from any predicted above, has also been reported for the Cu-Au system by Johansson and Linde.[36E] It occurs for the just-mentioned tetragonal-lattice alloys, 47 to 53 atomic percent Au, when they are rapidly cooled after annealing between 410°C and 420°C, and also for alloys having between 36 and 47 or between 53 and 65 atomic percent Au which are annealed in the temperature range 400°C to 200°C. This decidedly complicated structure possesses orthorhombic symmetry; in Fig. 41 a unit cell is outlined by the broad black lines. We note that this orthorhombic structure can be thought of as formed from the tetragonal lattice of Fig. 40(B) by step shifts which occur at every fifth atom along the [010] direction, with the indicated structures extending indefinitely in the [001] and [100] directions. An alloy containing 50 atomic percent Au possessing the orthorhombic structure goes slowly over into the tetragonal lattice when annealed at temperatures between 200–380°C. This structure, insofar as it is like the tetragonal form, agrees with the nearest neighbor assumpiton, but the change-step boundaries introduce extra pairs of like nearest neighboring atoms.

Two other systems which, like Cu-Au, form an isomorphous series of solid solutions in their high temperature disordered states are Cu-Pd and Cu-Pt. The ordered alloy Cu_3Pt, like Cu_3Au, conforms to theory and has the cubic structure of Fig. 40(A). Ordered Cu_3Pd was formerly thought to possess precisely the same structure, but recent observations[37E] indicate that a slight distortion of axial ratio invests it with tetragonal symmetry, the arrangement of atoms being otherwise apparently the same as for Cu_3Au. For other compositions, even more difference from Cu-Au is observed. As for ordered CuPt, although it has a structure of alternate planes of Cu and of Pt atoms, they are not (100) planes but (111) planes. This structure was first ascertained by Johansson and Linde[27A] and has trigonal symmetry as is shown in Fig. 42(A). For it each atom has only 6 unlike neighbors, instead of 8 as for the CuAu structure, and the nearest-neighbor assumption is seen to fail. Linde[37K] has recently extended the studies to include other compositions in the CuPt region. He finds that alloys containing more Pt than 50 atomic percent tend to take the excess Pt atoms in preferred positions, i.e., the additional Pt atoms go into the (111) planes formerly wholly occupied by Cu atoms and furthermore are distributed in such a way as to be surrounded by Cu atoms in the manner shown in Fig. 42(B). This structure would be expected to exist for a composition of Cu_3Pt_5. As to CuPt alloys containing excess Cu atoms (i.e., 51–60 atomic percent Cu) there is evidence that they exhibit a random distribution of the Cu atoms among the Pt planes of the CuPt structure. This is in agreement with our inferences from data (presented below) of electrical resistivity as a function of composition (Fig. 49), it being found that ordered alloys with excess Pt atoms possess a resistivity much lower than the same alloys when rapidly cooled, whereas the resistivities of the annealed alloys with excess Cu atoms (51 to 60 atomic percent Cu) tend to approach those of the rapidly cooled alloys. For Cu-Pd alloys with between 37 and 48 atomic percent Pd, there is a more drastic change:[25A, 27A] the disordered face-centered cubic alloys alter their lattice type upon cooling and become ordered body-centered alloys, the structure being of the β-brass type described immediately below.

Among the most interesting of the ordered structures developed from the random body-

centered cubic lattice is that of β-brass.[37I] When ordered structures are produced in this system by suitable heat treatment, they conform closely to the predicted structure for the body-centered *AB* lattice, the CsCl structure of Fig. 40(C). The nature of this transformation was formerly the subject of many long controversies. Hume-Rothery has emphasized the analogy between the β-phases of various alloy systems. On the basis of such analogies one would thus expect to find ordered transformations in β-AgMg, β-AgZn, β-AgCd and β-AuZn. Superstructure lines have already been observed[35Y] for the β-AgZn phase which shows it to be similar to the ordered β-brass.

Other interesting ordered structures resulting from the transformation of a random body-centered cubic phase are those of Fe_3Al and FeAl. The ordered regions in the Fe-Al system have been subjected to a very careful x-ray study by Bradley and Jay.[32A] They studied alloys containing up to 50 atomic percent Al in both the ordered and random states.

In Fig. 43(A) we show the Fe_3Al lattice with notations permitting us to describe briefly the distributions of the atoms among the designated lattice sites as we pass to alloys containing greater percentages of Al. In Fig. 43(B) we show a plot, after Bradley and Jay, of the percentage of indicated positions occupied by Al atoms as a function of composition for both annealed and quenched alloys. The full-drawn line up to 18 atomic percent Al, marked *abcd*, indicates an equal distribution of the Al atoms among the *abcd* positions for both rapidly cooled and annealed alloys. At 18 atomic percent Al Bradley and Jay observed a diffuseness in the x-ray diffraction lines of the lattice which they attributed to the onset of order in the annealed alloys. They observed no superstructure lines in the annealed alloys until a composition of 24 atomic percent Al was reached, at which point they estimated that about 62 percent of the *b* positions were occupied by Al atoms, the remaining Al atoms occupying the *acd* positions. At 25 atomic percent Al, slow cooling produces the Fe_3Al ordered structure where about 92 percent of the *b* positions are occupied by Al atoms. On traversing the Fe_3Al lattice along the cube diagonal one meets Al atoms at alternate small cube centers. Bragg[33A] has pointed out that the Al atoms tend to keep as far apart as possible. In the Fe_3Al structure we note that each Al atom tries to take a position in which not only its nearest neighbors but also its next nearest neighbors are unlike atoms. This tendency has also been discussed by Hume-Rothery and Powell.[35N] On passing to alloys containing greater percentages of Al, we note that in the annealed specimens the additional Al atoms distribute themselves among the *b* and *d* positions, the distribution becoming equal at about 40 atomic percent Al. At the composition FeAl both rapidly cooled and annealed alloys acquire an ordered structure of the β-brass type with the cube centers occupied by Al atoms and the corners by the Fe atoms. Here again the Al atom surrounds itself with the maximum number of unlike neighbors.

A structure similar to Fe_3Al has been observed[25B] in the Fe-Si system at the composition Fe_3Si.

Among other ordered structures of interest are the close-packed hexagonal structures of

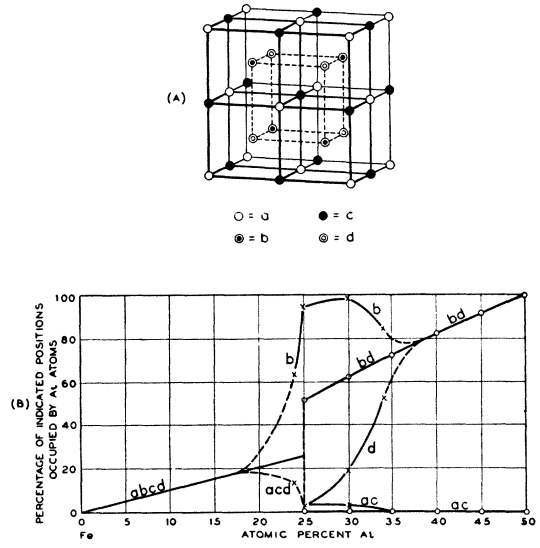

FIG. 43. (*A*) Enlarged cell with positions indicated in the manner necessary to describe the distribution of Al atoms in ordered Fe-Al alloys. (*B*) Distribution of Al atoms among the four indicated positions *a*, *b*, *c*, *d*. Full line up to 18 atomic percent Al depicts distribution for both rapidly and slowly cooled alloys. From 18 to 38 atomic percent Al, lines marked (○) refer to rapidly cooled alloys, and lines marked (×) refer to annealed alloys. The line from 38 to 50 atomic percent Al refers to both rapidly and slowly cooled alloys.

Mg_3Cd,[30B] with the following distribution of atoms

$$\mathrm{Mg}\begin{cases}000,\ \frac{1}{6}\ \frac{1}{3}\ \frac{1}{2}\\ \frac{1}{2}00,\ \frac{2}{3}\ \frac{1}{3}\ \frac{1}{2}\\ 0\frac{1}{2}0,\ \frac{2}{3}\ \frac{5}{6}\ \frac{1}{2}\end{cases}\qquad \mathrm{Cd}\left\{\frac{1}{2}\ \frac{1}{2}0,\ \frac{1}{6}\ \frac{5}{6}\ \frac{1}{2}\right.$$

and the similar structures of $MgCd_3$[37W] and Ni_3Sn.[37O] Laves and Moeller[37J] have also observed hexagonal close-packed ordered structures in the quasi-binary system Mg-$AgCd_3$ in the composition region from 37 to 70 atomic percent Mg. A somewhat more complicated structure has been reported by Rahlfs[37N] for Ni_2MgSn and β-$(Cu_3Ni)_3Sn$. The unit cell is similar to that of β-brass but twice as large. Bradley and Lu[37C] have recently reported a superstructure for tetragonal Cr_2Al. This structure forms upon the body-centered cubic lattice; and, if we consider planes of the (100) type, which are formed alternately of cube corners and of cube centers, we find that every third plane contains Al atoms and the remaining planes Cr atoms.

The Heusler alloy, Cu_2MnAl, in the ferromagnetic condition is highly ordered,[34F] and according to Bradley and Rodgers[34B] the atoms have the following distribution in a body-centered cubic cell

$$\mathrm{Cu}\begin{cases}000,\ 0\frac{1}{2}\frac{1}{2},\ \frac{1}{2}0\frac{1}{2},\ \frac{1}{2}\frac{1}{2}0\\ \qquad\qquad \mathrm{Al}\left\{\frac{1}{4}\ \frac{1}{4}\ \frac{1}{4},\ \frac{1}{4}\ \frac{3}{4}\ \frac{3}{4},\ \frac{3}{4}\ \frac{1}{4}\ \frac{3}{4},\ \frac{3}{4}\ \frac{3}{4}\ \frac{1}{4}\right.\\ \frac{1}{2}\ \frac{1}{2}\ \frac{1}{2},\ \frac{1}{2}00,\ 0\frac{1}{2}0,\ 00\frac{1}{2}\\ \qquad\qquad \mathrm{Mn}\left\{\frac{3}{4}\ \frac{3}{4}\ \frac{3}{4},\ \frac{3}{4}\ \frac{1}{4}\ \frac{1}{4},\ \frac{1}{4}\ \frac{3}{4}\ \frac{1}{4},\ \frac{1}{4}\ \frac{1}{4}\ \frac{3}{4}\right.\end{cases}$$

Section 17. Phenomena which may indicate the degree of order

(a) The degree of long distance order in a highly ordered alloy, free from out-of-step domains, can be determined with a fair degree of accuracy by comparing the intensities of the x-ray superstructure lines with the lines of the normal lattice. An example has been given by Bradley and Jay[32A] in their thorough studies of the Fe-Al ordered alloys, from which they were able to deduce the percentage of lattice sites of each type occupied by Al atoms. We gave a graphical representation of their results in Fig. 43(B). Ageew and Shoyket[35A] have given corresponding curves for a CuAu alloy.

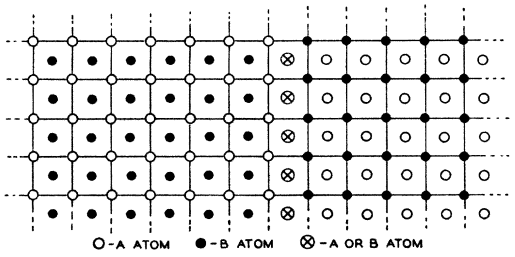

FIG. 44. Out-of-step domains.

When an alloy is only partially ordered and small out-of-step domains are present, many disturbing factors arise, rendering a quantitative determination of the degree of order difficult if not impossible. Borelius, Johansson and Linde[28A] discussed this difficulty as far back as 1928. In Fig. 44 we reproduce from their paper a drawing depicting such out-of-step domains. Such a situation might easily arise in an alloy such as β-brass. At the onset of order the α-sites might be occupied by copper atoms in one part of the crystal and by zinc atoms in another part. In the face-centered cubic lattice, exemplified by the Cu_3Au alloy, there are four partial lattices, any one of which can be the particular partial lattice onto which the Au atoms might order. Here the relatively great complexity makes it a good deal harder to reason from the x-ray pattern to the degree of order than in the simpler case of β-brass. These so-called out-of-step domains form at random throughout the body of the alloy, and increase in their internal degree of order as well as in size. When two nuclei which are out-of-step meet under certain conditions, they coalesce into one coherent ordered scheme. This is thought to take place in a manner analogous to the grain growth in metals commonly called grain-boundary migration.[36I]

(b) The presence of small ordered nuclei results in a diffuseness in the superstructure lines, which makes it extremely difficult to obtain the ratio of the intensity of the superstructure lines to the lines of the normal lattice. Thus such measurements, for alloys not possessing a coherent scheme of long distance order, are of little value in ascertaining the degree of order. Sykes and Jones have used the diffuseness in the superstructure lines to determine the size of these nuclei, utilizing the Scherrer equation which

correlates the size of the particles with the width of the lines of its x-ray diffraction-pattern.

(c) Another method proposed for estimating the degree of order is based on the fact—discovered by Johansson and Linde[27A]—that the lattice of a CuAu alloy changes from cubic to tetragonal when ordering occurs. Immediately below the Curie temperature of order, the axial ratio—the measure of the "tetragonality"—is $a : c = 1.067$, and it continues to increase with decreasing temperature until, when the alloy is in a highly ordered state, it reaches *ca.* 1.080. Borelius and his collaborators have utilized the values of the axial ratio as a quantitative measure of the degree of order of the alloy, and feel that it is the most reliable measure of the degree of order available from x-ray data. This feeling rests on the assumption that it is the ordering which causes the deformation of the cubic structure, resulting in either the tetragonal or orthorhombic lattice. The fact that the tetragonality increases with increasing degree of order must be taken as support of Borelius' assumption, but otherwise there is very little evidence to substantiate it. X-ray diffraction patterns of alloys quenched from temperatures immediately below the Curie temperature of order often show the presence of both the random cubic and partially-ordered tetragonal CuAu.[30E, 32H]

(d) Still another method proposed for estimating the degree of order consists in measuring the electrical resistivity which, as we have shown in the introduction, is drastically affected by ordering. In the use of such measurements one must take into consideration the contribution of normal thermal agitation to the electrical resistance. The same objections, however, can be raised to this method of measurement as were raised above to the use of the intensity and width of the superstructure lines, for electrical resistivity also is influenced by the size and irregularity of the partially ordered nuclei. Sykes and Jones, however, have shown that ordered domains must attain a size comparable to the mean free path of the conduction electrons before this influence commences. The existence of anti-phase or out-of-step domains of larger sizes would tend to contribute some degree of disorderliness and consequently give rise to a higher resistance than one would obtain from a crystal possessing a uniform coherent scheme of long distance order throughout. Like intensity measurements of the x-ray superstructure lines, however, electrical resistivity measurements yield a fair measure of the degree of long distance order for a uniformly ordered alloy free of small anti-phase nuclei.

The presence of order in alloys is indicated in other ways than by x-ray and electrical resistivity measurements.

(e) Among physical properties affected by order is the magnetic susceptibility; this is found in the Cu-Au alloys, which we discuss in some detail below. Very little information has been obtained to date, however, permitting a correlation between the magnetic properties of alloys and the prevailing state of order.

(f) The ordering phenomenon in alloys, whether of the long or short distance type, is also almost always accompanied by a diminution in volume. Since the volume change can be measured with a relatively high degree of precision, accurate measurements of this kind will also probably prove valuable as a measure of the degree of order.

(g) The knowledge of the energy necessary to transform a partially ordered alloy in equilibrium at a temperature T to the random state immediately above T_c, along with the knowledge of the energy necessary to transform a highly ordered alloy into the random state, might also be of some value in ascertaining the degree of order.

Section 18. Behavior of alloys not in thermal equilibrium

Relaxation time

The equilibrium state of order in an alloy comes into existence by atomic interchanges of the type responsible for diffusion. A theory of the process based on this conception was presented in Part I, Section 10. It was there shown that the deviation of the system from the state of equilibrium diminishes exponentially with a certain characteristic "time of relaxation," τ. This time is dependent on the temperature and has the form

$$\tau = Ae^{W/kT}. \qquad (18.1)$$

Here W represents the potential barrier which

TABLE II.

TEMPERATURE, °C	τ, IN HOURS
361	8.7
350	14.4
321	64.0
300	212.0

TABLE III.

TEMPERATURE, °C	τ, IN HOURS
340	5.0
330	6.9
320	8.3
300	12.9
280	19.0

must be surmounted for interchange to take place.

Each state of order is the equilibrium state of order for a certain temperature θ, which we shall use in our argument to stand for the state. If the actual temperature T is greater (less) than θ, the degree of order is too great (too small) for the condition prevailing, and tends toward the state corresponding to T. In terms of θ and T the "relaxation equation" is

$$d\theta/dt=(T-\theta)/\tau. \qquad (18.2)$$

Sykes and Evans[36I] measured resistivity in order to ascertain the rate of approach of a Cu_3Au wire to equilibrium at a number of different temperatures. In Table II we give a few of their values of τ for relaxation at several different temperatures.

A graphical plot of $\log \tau - vs.\ (1/T)$ gave a straight line relationship from which one obtained a value of $A=10^{-8.5}$ sec. and $W/K=19{,}100°K$ for the constants of Eq. (18.1). These values are of the order predicted in Part I, Section 10 by the Bragg-Williams theory.

Sykes and Evans have also made measurements at constant rates of cooling. In order to find the relaxation time from these, it is necessary to investigate solutions of the equation

$$(d\theta/dt)=(T-\theta)/Ae^{W/kT}, \qquad (18.3)$$

taking into account the dependence of temperature T upon time t and to use these solutions to work backwards from the experimental results to find τ. The results of such a process are given in Table III.

A graphical plot of these data also gave a straight line relationship between $\log \tau$ and $1/T$, but with quite different values of W/k and A : 8250°K and $10^{+0.45}$ sec. A comparison of the value of τ and the derived constants as determined by the two methods show a disagreement too large to be accounted for by experimental error. Thus for 300°C, τ as determined for relaxation at constant temperature was found to be 212 hours whereas the value of τ as determined from cooling at a constant rate is 12.9 hours. This disconcerting fact can be rationalized by saying that the alloy possesses two kinds of relaxation times, which are separately obtainable by different experimental processes. There is nothing in the theory of relaxation time presented above which could account for this. In that theory, however, one coherent scheme of long distance order was assumed.

Irreversible cycles

The theories of Bethe and Peierls, based on the nearest neighbor assumption, lead one to expect the formation of local domains of order at temperatures much above the Curie point of long distance order. The quenching of alloys from temperatures above T_c would then leave these local domains of order in the quenched specimens at room temperature. The higher the temperature of quench, the less should be the amount of local order found in the specimens.

Sykes and Jones[36H] made specific heat measurements on a Cu_3Au alloy quenched in water from 450°C, which appeared, from electrical resistivity measurements to be in a perfectly random state. The resistivity of the quenched alloy, measured at room temperature, fell on the extrapolation to room temperature of the linear portion of the resistivity-*vs.*-temperature curve for temperatures above the Curie point of order (see Fig. 5). X-ray diffraction patterns displayed no superlattice lines. The specific heat measurements disclosed, however, that considerable local ordering had taken place. In Fig. 45 we reproduce such a specific heat-*vs.*-temperature curve, displaying the onset of the release of configurational energy at temperatures as low as 60°C, much below the point (230°C) where it had previously been supposed that atomic interchange ceases. The amount of energy released between 60°C

and 230°C was greater the higher the temperature of quench. Back-reflection x-ray diffraction patterns of specimens which had been heated at 130°C for two hours, releasing a considerable portion of the configurational energy, still failed to show any superlattice lines. Wires of the same alloy on being subjected to a comparable thermal treatment had resistivities characteristic of a disordered alloy. Sykes and Jones conclude, from studies of the width of the first superstructure lines to become detectable, that the ordered domains must have linear dimensions of at least $5.5 \cdot 10^{-7}$ cm or 14–20 atomic distances.

These interesting experiments show that neither the absence of x-ray superstructure lines, nor an electrical resistivity such as has been deemed characteristic of random alloys, are to be considered as proof that such an alloy is completely disordered. Specific heat studies show that such an alloy may possess a rather large amount of local order, and that in some cases more than forty percent of the configurational energy is released before ordering is manifested in x-ray and resistivity measurements.

Sykes and Jones assume that the ordered nuclei grow during the initial dip in the curve of Fig. 45 and finally touch with the surface layer of each ordered domain remaining in a random condition. On assuming that the ordered domains are cubes with d atoms along an edge, "then to a first approximation the energy released will be the fraction $(1-6/d)$ of the total energy provided the energy of any atom is fixed only by the identity of its immediate neighbors." From such considerations Sykes and Jones find the size of the domains at the end of the second dip in the specific heat curve of Fig. 45 to be 12 atoms along an edge, a value to be compared with 14–20 estimated from the width of the superstructure lines. By similar means they estimate the size of the ordered domains at the end of the first dip to be 6–8 atoms along an edge.

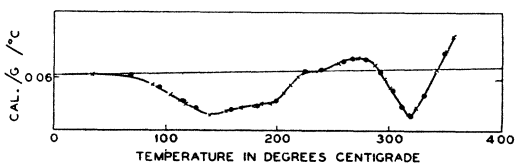

FIG. 45. Specific heat-*vs.*-temperature for a Cu_3Au alloy previously quenched in water from 550°C.

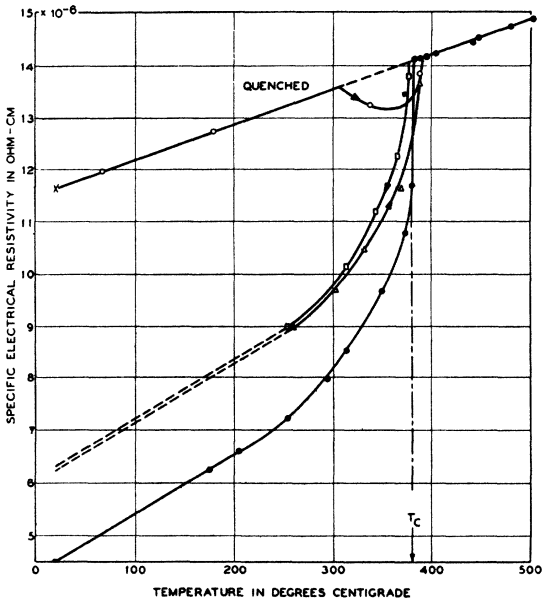

FIG. 46. Electrical resistivity-*vs.*-temperature for Cu, Au. The curve marked (●) is the equilibrium curve (Fig. 5). The curve with (○) markings represents the change in resistivity with temperature on reheating the previously quenched alloy at a rate of 2°C/min. The (□) markings represent the change in resistivity with temperature on cooling at a rate of 30°C/hour. The curve with (Δ) marking show the change in resistance with temperature on reheating the same alloy at the rate of 30°C/hour.

In Fig. 46 we show resistivity-*vs.*-temperature curves[36I, 36H] for a Cu_3Au alloy under various conditions of heating and cooling. The full dots refer to the equilibrium condition attained with extremely slow rates of cooling. The extrapolation of the straight line portion of the equilibrium curve to the resistivity axis, the point marked X, coincides with the resistivity value obtained by quenching the alloy in water from some temperature above T_c. On reheating this quenched alloy, the resistivity follows the curve marked with open circles. The resistivity decrease produced by ordering did not begin at 60°C, the temperature where heat began to be evolved in the specific heat-*vs.*-temperature curve of Fig. 45, but only at about 310°C, showing that the formation of the small nuclei which gave rise to the evolution of heat from 60°C to 230°C does not affect the electrical resistivity. In the curve marked with squares we depict the dependence of resistivity on temperature for a wire of the same alloy cooled at a rate of 30°C/hour; the alloy is far from being in equilibrium,

for the resistivity is considerably higher (e.g. at 250°C) than the equilibrium value. If the alloy had been uniformly ordered throughout, it should on reheating tend to relax toward the respective equilibrium values. In fact, however, when the alloy which was previously cooled at 30°C/hour is reheated at 40°C/hour, the curve (with triangular markings) falls slightly below that obtained on cooling and has an identical slope from 250°C to 330°C. Sykes and Evans[36I] explain this behavior by assuming that the alloy cooled at 30°C/hour was not uniformly ordered but consisted of small highly ordered domains which were internally in equilibrium at all temperatures throughout the cooling period and also in the heating cycle at temperatures up to 330°C.

The appearance of different Curie points of order on heating and on cooling, as derived from measurements of electrical resistivity, has led many investigators to insist on the existence of a real hysteresis. Recent work of Sykes and Evans[36I] on a Cu_3Au alloy has shown that, when sufficient time is allowed for equilibrium to be established, the difference between the Curie points on heating and on cooling is reduced to a few degrees. Results have been reported on Cu_3Au giving the two Curie temperatures as far as 20° apart, when the rates of heating and cooling were presumably too great to permit an approach to equilibrium. We are not prevented by the available data from having faith that if the heating and the cooling could be carried on slowly enough, the two Curie temperatures would coincide. Borelius,[37B] however, believes that a real hysteretic effect exists in CuAu and CuPd alloys; indeed for the latter he reports a difference of about 100°C.

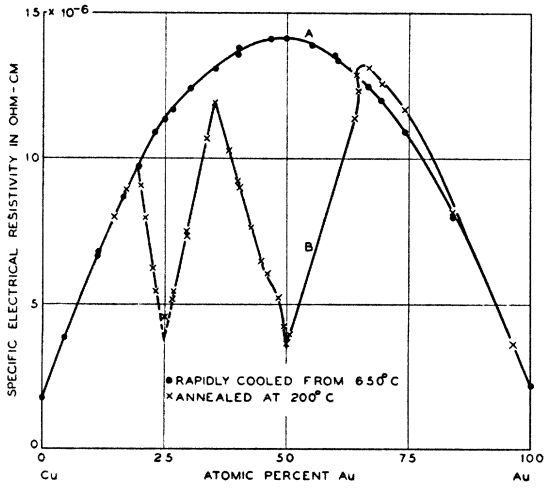

FIG. 47. Electrical resistivity-*vs.*-composition for the Cu-Au system. (*A*) for rapidly cooled alloys, (*B*) for alloys annealed at 200°C.

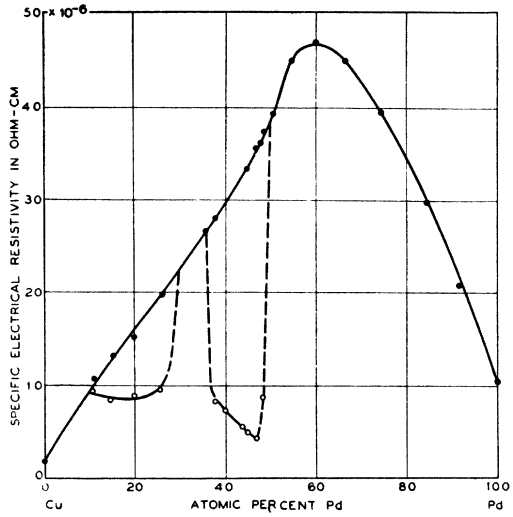

FIG. 48. Electrical resistivity-*vs.*-composition for the Cu-Pd system. (●) rapidly cooled alloys, (0) annealed alloys.

Section 19. Influence of order and composition on the electrical resistivity

In Fig. 5 of the introduction we showed the effect of uniform long distance order on the resistivity of a Cu_3Au alloy. At room temperature the resistivity R_r of the rapidly cooled random alloy, free from large volumes of long distance order, was found to be $11.4 \cdot 10^{-6}$ ohm-cm, whereas an alloy cooled sufficiently slowly to possess a uniform scheme of long distance order of high degree, has a resistivity R_0 of $4.3 \cdot 10^{-6}$ ohm-cm. In Fig. 47 we show R_0 and R_r plotted against composition for the system of Cu-Au alloys.[36E] The smooth parabolic curve *A* represents electrical resistivity values, measured at room temperature, as a function of composition, for a series of alloys quenched from 650°C. Such alloys should, according to the discussion above, be free from any domains possessing coherent schemes of order with dimensions greater than $5.5 \cdot 10^{-7}$ cm along one edge.

These alloys may contain many small areas possessing a high degree of local or short distance order, but as we have shown above these do not affect such properties as electrical resistivity. Curve B in Fig. 47 depicts the electrical resistivity values measured at room temperature as a function of composition for the same alloys after being subjected to prolonged annealing at 200°C. Such a prolonged annealing treatment at temperatures below T_c but sufficiently high to permit atomic interchange should produce coherent schemes of long distance order throughout the composition regions which give rise to ordered structures. The figure shows that in some regions, those near the pure Cu and pure Au, R_0 and R_r coincide: i.e. in these composition regions there is insufficient long distance order to affect the electrical resistivity. In the composition region from about 18 to 65 atomic

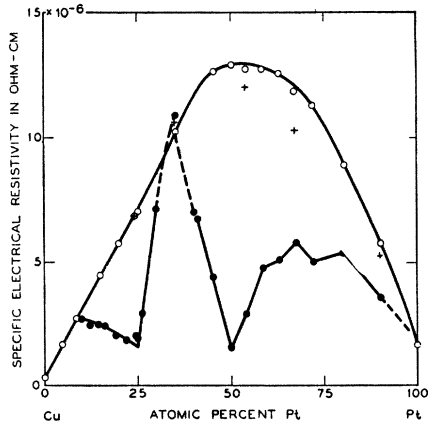

FIG. 49. Electrical resistivity-*vs.*-composition for the Cu-Pt system. (○) rapidly cooled and cold worked, (●) annealed at 300°C, (+) rapidly cooled from 900°C.

percent Au the annealed alloys possess lower, and at the critical compositions Cu_3Au and CuAu much lower, resistivities than the quenched random ones. The values at 25 atomic percent Au coincide with those of Fig. 5 for quenched and ordered Cu_3Au, respectively. The minima in the curve for the annealed alloys occur at 25 and 50 atomic percent Au. Annealing of the alloys in the region from 65 to 85 atomic percent Au provoked a small increase in the electrical resistance over that of the same alloys when quenched from 650°C. This increase might be due to a segregation. Johansson and Linde[36E] report, however, the presence of very weak superstructure lines in the region $CuAu_3$.

Figure 48 gives a graphical representation of similar measurements on a series of Cu-Pd alloys.[27A, 32L] Their behavior is similar to that of the Cu-Au alloys discussed above, except for the striking difference in the symmetry around the Cu_3Pd and CuPd compositions: prolonged annealing failed to provoke an ordered structure in the 50 atomic percent Pd alloy. The ordered alloy at compositions near. Cu_3Pd possesses a structure similar to the Cu_3Au, but according to recent results[37E] the lattice suffers a slight distortion producing tetragonal symmetry. The ordered alloys from 37 to 48 atomic percent Pd are body-centered cubic structures of the CsCl type.[27A, 35L]

In some alloys the atoms in excess of those necessary to form an ideal ordered structure distribute themselves in an orderly manner in the lattice. Such an arrangement might be expected to affect the electrical resistivity of the annealed alloys, and Fig. 49 shows such an effect in the Cu-Pt alloys. In the above discussion of Section 16 the structure of the CuPt ordered alloy, it was mentioned that in ordered alloys containing greater than 50 atomic percent Pt the excess Pt atoms took definite positions in the (111) Cu planes of the ordered CuPt, in such a manner that at the composition corresponding to Cu_3Pt_5 each excess Pt atom is surrounded by 6 Cu atoms (see Fig. 42(B)). On the other hand, the

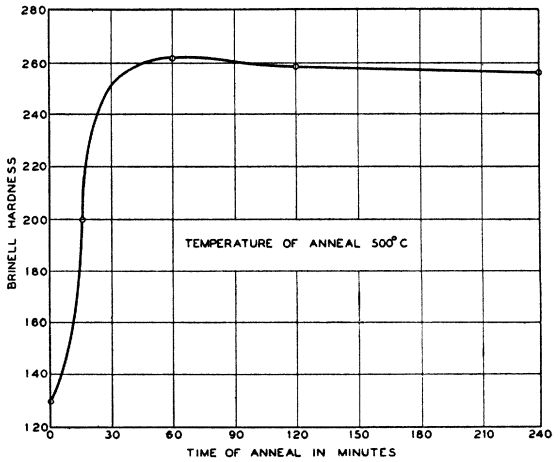

FIG. 50. Age-hardening curve for a CuPt alloy. The alloy was rapidly cooled before the annealing.

excess Cu atoms, in alloys containing more than 50 atomic percent Cu, apparently take a perfectly random distribution among the (111) Pt planes of the ordered CuPt structure. This conclusion is drawn from x-ray studies of the structure and is consistent with the nature of the electrical resistivity-*vs*.-composition curve for the annealed alloys. In the region from 50 atomic percent Pt to nearly pure Pt the annealed alloys possess a markedly lower electrical resistivity than the quenched or random alloys. The annealed alloys containing excess Cu atoms, however, show a marked increase in resistivity with increasing number of excess Cu atoms, and finally at about 37 atomic percent Pt the resistivity coincides with that of the quenched alloy.

From our discussion of Easthope's theory in Section 5 we recall that it predicts the existence of a superstructure in alloys containing as little as $1/z$th (z is the number of nearest neighbors of each atom) of the atoms of either kind. There do not appear to be any experimental cases to which this theory is strictly applicable. For the body-centered cubic lattice the limiting atomic percentage should be 12.5; the experimental value, 18 atomic percent Al in the Fe-Al system, shown in Fig. 43, is higher than Easthope's; furthermore it arises from next nearest neighbor interactions. Thus in this case, the nearest neighbor interactions are considerably less operative than the theory predicts. Easthope's theory was only intended to be applied to the body-centered cubic and simple cubic lattices. On applying it, however, to the face-centered cubic lattice where $z=12$, we note that superlattices begin at *ca.* 9, 11 and 19 atomic percent Pt, Pd and Au, respectively, in alloys of these metals with copper. These values are to be compared with 8.5 atomic percent according to the formula $1/z$. With the theory in its present state, especially with respect to the dependence of ordering energy upon order and composition, no significant conclusions can be drawn from a comparison of the predicted and observed values.

We shall point out in a later section how electrical resistivity measurements may be used as a criterion for establishing the presence of an ordered phase.

Section 20. Effect of order on mechanical properties

It was observed by Nowack[30G] that the annealing of a rapidly cooled CuPt alloy, containing 50 atomic percent Pt, provoked an increase in hardness, as measured with the Brinell hardness test, which was similar in many respects to the age-hardening behavior of precipitation-hardening alloys. In Fig. 50 we show a curve obtained by annealing a previously quenched CuPt alloy, which increases in hardness with increasing time of anneal. The quenching retains at room temperature the random high temperature structure and the annealing treatment provokes an ordering of the alloy. Thus the highly ordered CuPt possesses a greater hardness and tensile strength than an alloy of the same composition in the random state. Similar behavior has been observed for CuAu, CuPd and to some extent for a Cu_3Au alloy.[35Y] Sachs and Weerts[31E] report that the shear stress at the elastic limit of a Cu_3Au alloy suffers a decrease on ordering of approximately the same percent as does the electrical resistivity.

Röhl,[33G] working in Grüneisen's laboratory, made measurements on the effect of order on Young's modulus, a much more fundamental property than hardness and tensile strength, in several alloys known to order on annealing. He found that Young's modulus increased on order-

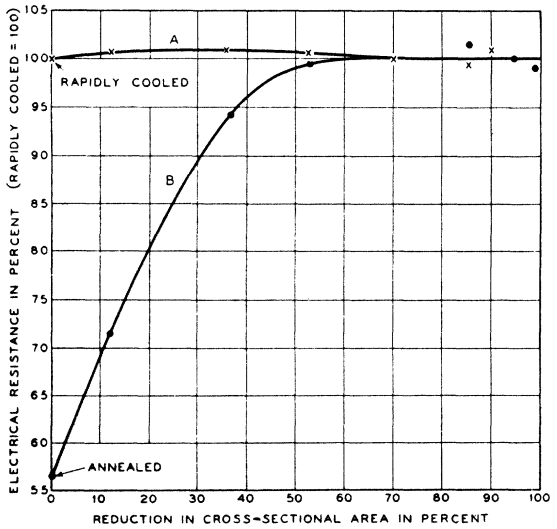

FIG. 51. Effect of plastic deformation on the electrical restistivity of a Cu_3Au alloy.

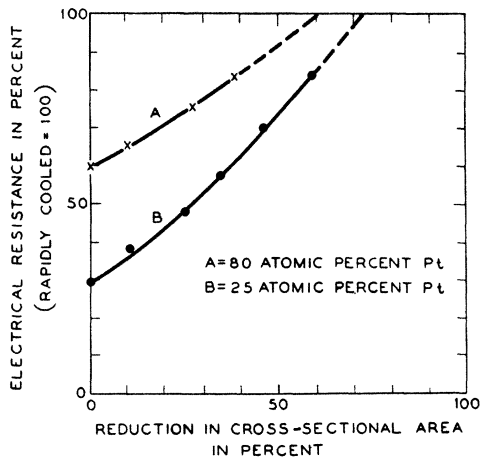

FIG. 52. Effect of plastic deformation on the electrical resistivity of previously annealed Cu-Pt alloys.

ing for Cu_3Pd and Cu_3Au phases whereas it decreased on ordering for the CuAu and CuPd alloys.

Section 21. Effect of plastic deformation on order

Dehlinger and Graf[30A] proved that plastic deformation of an ordered CuAu alloy destroyed the order, by finding that the superstructure lines were absent from the x-ray diffraction pattern given by the plastically deformed alloy. Schäfer[33H] observed a similar behavior on plastically deforming a FeAl ordered alloy. This behavior has been shown even more convincingly by Dahl[36A] for a Cu_3Au alloy, and has been used by him, as well as more recently by Linde,[37K] to show the presence of an ordered phase where the existence of such a structure escapes detection by other physical tests.

Severe plastic deformation of most pure metals and random solid solutions produces only small changes in electrical resistivity. The change is about 2 percent for most pure metals such as Ag, Cu, Al, Ni and for random solid solutions such as the iron-nickel alloy of 35 atomic percent Ni. Some exceptions have been reported: an 18 percent change in the case of the rather brittle metal tungsten, and a 50 percent change for molybdenum. However, such a brittle metal as tungsten cannot be considered to display the same response to mechanical deformation at room temperature as most of the more plastic metals and alloys. Fig. 51 depicts the effect of cold working or plastic deformation on the electrical resistivity of a Cu_3Au alloy.[36A] As a measure of the degree of cold work we plot the percentage reduction in cross-sectional area of the Cu_3Au wire on being drawn through the drawing dies in the cold working operation. Curve *A* of Fig. 51 represents the change in resistivity as a function of the degree of cold work for samples of the alloy which were quenched in water from an elevated temperature in order to retain the orderless state, before subjecting them to plastic deformation. We note that even after severe cold working the change in resistivity is less than two percent, as is to be expected from the cold working of a random solid solution. Curve *B* depicts the change in electrical resistivity as a function of the degree of plastic deformation for samples of the same alloy which, previous to the cold working operation, were annealed at a low temperature to develop a highly ordered condition. The two curves illustrate in a striking way the effect of plastic deformation on long distance order in an alloy as manifested by its effect on electrical resistivity. To judge from the resistivity, the coherent ordered structure was completely destroyed after 60 percent reduction in cross-sectional area. X-ray diffraction patterns taken at various stages in the cold working process displayed decreasing intensity of the superstructure lines with increasing degree of cold work, and their ultimate disappearance at about 60 percent

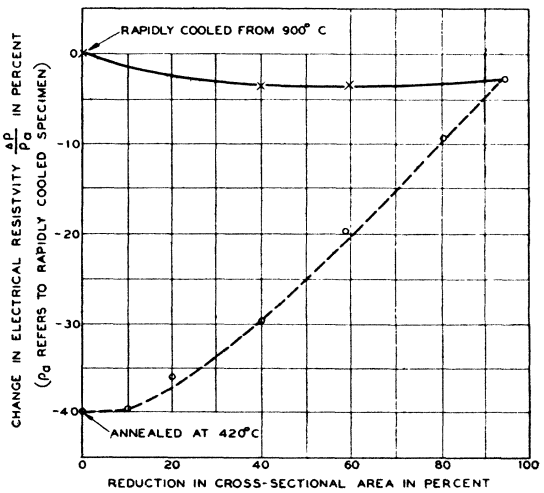

FIG. 53. Effect of plastic deformation on the electrical resistivity of Ni_3Mn.

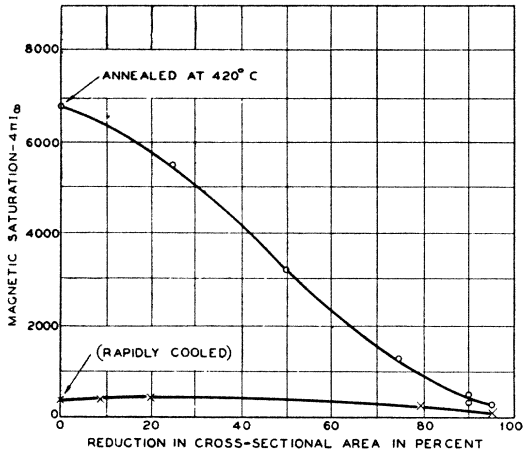

FIG. 54. Effect of plastic deformation on magnetic saturation ($4\pi I_\infty$) of Ni_3Mn.

reduction in cross-sectional area. Such a substantial increase in resistance with severe cold work has been observed in all cases studied where a superstructure was originally present.

In Fig. 52 we give results recently published by Linde,[37K] showing how such studies can be used for ascertaining the presence of ordered structures in the Cu-Pt system. Curve *A* of that figure refers to the change in resistivity effected by cold working of an annealed Cu-Pt alloy containing 80 atomic percent Pt. Fig. 49 shows that there is also a marked difference between the electrical resistivities of the alloy of this composition in the quenched and annealed conditions. Curve *B* of Fig. 52 depicts similar measurements made on an annealed alloy containing 25 atomic percent Pt, known from x-ray studies to possess a superstructure similar to that of Cu_3Au.

At this point we wish to explain the significance of the points marked by circles and crosses for the random alloys of Fig. 49. Linde[37K] found that cold working applied to some of the quenched alloys, containing greater than 50 atomic percent Pt, produced an increase in resistivity. Whenever in Fig. 49 a cross and an open circle appear at the same abscissa, they give the resistivity of the same alloy before and after cold working respectively. Thus in alloys of these compositions, even such drastic cooling as is achieved by quenching in water from 900°C is not sufficient to prevent some degree of ordering. The small degree of order which forms in spite of the drastic cooling seems then to be destroyed by cold working, so that presumably only cold worked specimens are representative of the random alloys.

In the Fe-Ni system the effect of cold working on the resistivity has been investigated by Dahl[36A] with a view to drawing inferences as to presence of a superstructure. He found that Ni and Fe-Ni alloys containing less than 35 atomic percent Ni suffer only slight changes in resistivity on cold working, whether the specimens had been annealed or rapidly cooled; but that all alloys containing between 40 and 90 atomic percent Ni suffer a change in resistivity greater than would be expected were the alloys already in the orderless state before being subjected to the cold working treatment, the maximum occurring at about 75 atomic percent Ni. At any composition the change ΔR on cold working is greater for alloys which had been previously annealed for prolonged periods of time, a treatment which would be favorable to the formation of a superstructure, than for alloys which had been slowly cooled in a furnace from 900°C. Alloys quenched from 900°C also display a similar change, ΔR being greater than would be expected for the plastic deformation of disordered alloys. These data, along with the general behavior of the electrical resistivity of Fe-Ni alloys of this composition-range for the rapidly cooled and annealed states without cold work, are indicative of a superstructure in the Ni_3Fe region. The nearness to equality of the scattering powers of Fe and Ni atoms for x-rays, makes it almost if not quite impossible to detect any superstructure by x-ray analysis.

Dahl[36A] has extended this type of study to

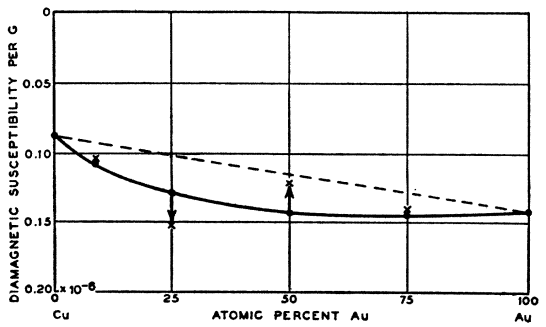

FIG. 55. Diamagnetic susceptibility-*vs.*-composition for the Cu-Au system, (●) rapidly cooled alloys (×) annealed alloys.

another interesting system, the Ni-Mn alloys, where the presence of a superlattice would again escape detection by virtue of the nearly identical scattering powers for x-rays of the constituent atoms. Here, for alloys initially subjected to various heat treatments, he follows the effects of cold work not only on the electrical resistivity but also on the magnetic properties. Fig. 53 depicts the change ΔR in resistivity on cold working for annealed and rapidly cooled wires of a Ni-Mn alloy containing 25 atomic percent Mn. It is small for rapidly cooled wire, whereas the annealed wire (like ordered Cu_3Au) exhibits a large value. In Fig. 54 we give Dahl's magnetic measurements carried out on the same alloy similarly treated. The Ni_3Mn alloy is non-ferromagnetic when it has been rapidly cooled, and this remains the case even after severe cold working; but if it has been annealed, it exhibits strong ferromagnetic properties which are progressively destroyed with increasing degree of cold work. We shall return to the discussion of the effect of cold work on superstructures later in reviewing the various criteria for establishing the presence of an ordered phase.

Section 22. Effect of order on magnetic properties

Paramagnetic and diamagnetic alloys

The influence of order on the magnetic properties of alloys was first reported by Vogt and Seemann[29B] for the alloys Cu_3Au and CuAu. The full line of Fig. 55 depicts the diamagnetic susceptibility of a series of orderless Cu-Au alloys. Ordering the Cu_3Au alloy *increased* its diamagnetic susceptibility by some 18 percent whereas ordering CuAu provoked a *decrease* of about the same amount. Since measurements were made only on two states assumed to be those of perfect order and perfect randomness, they do not indicate how the magnetic susceptibility depends on the degree of long distance order; nor is it known whether the presence of short distance or local order affects the magnetic susceptibility. These magnetic measurements were made before the existence of local ordering had been established. The alloys to which the full curve refers were assumed to be in the disordered state because superstructure lines were not observed or resistivity values corresponded to those of a disordered alloy.

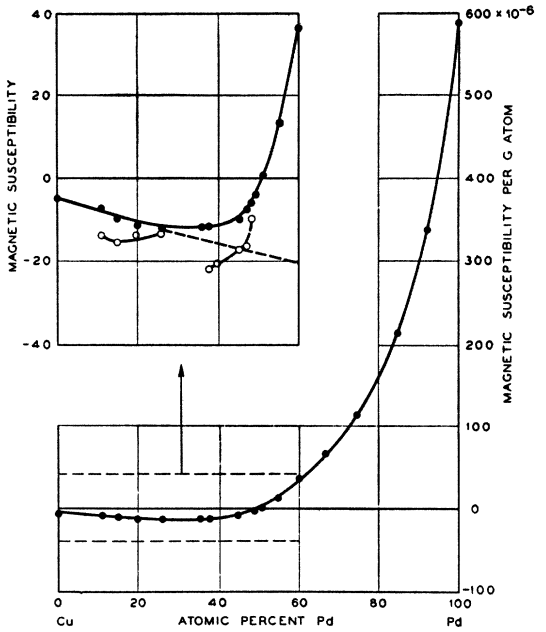

FIG. 56. Diamagnetic susceptibility-*vs.*-composition for the Cu-Pd system, (●) rapidly cooled alloys (○) annealed alloys.

On Fig. 56, we show how magnetic susceptibility depends on composition for a series of orderless Cu-Pd alloys.[32L] With addition of the strongly paramagnetic Pd to the weakly diamagnetic Cu the alloys become at first more strongly diamagnetic, until the concentration reaches about 25 atomic percent Pd, at which point the curve turns upwards and rises rapidly toward the high *paramagnetic* value of pure Pd. On ordering, alloys with compositions near Cu_3Pd and CuPd display an increase in diamagnetic susceptibility; the greatest change for the CuPd region occurs at about 37 atomic percent Pd, and progressively less change takes place in alloys with increasing Pd content. It is of some interest to point out that the minimum in the electrical resistivity curve for ordered alloys in the CuPd region occurs at 47 atomic percent Pd, whereas at this composition order produces the smallest change in the magnetic susceptibility. In the Cu_3Pd region, on the other hand, the maximum degree of order as determined by x-ray measurements occurs at about 17 atomic percent Pd, the same point where ordering provokes a maximum effect on both electrical resistivity and magnetic susceptibility.

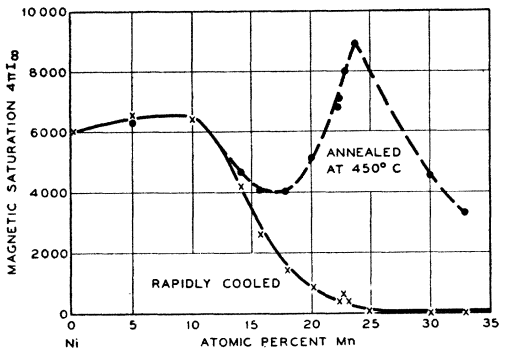

FIG. 57. Magnetic saturation ($4\pi I_{\infty}$)-*vs.*-composition for a series of Ni-Mn alloys.

Effect of order on ferromagnetic alloys

In Figs. 53 and 54, we presented evidence indicative of a superstructure in the alloy Ni_3Mn. The annealed alloy shows the phenomenon of saturation, with a magnetic moment even greater than that of pure Ni; whereas the same alloy in the rapidly cooled state is not even ferromagnetic. The saturation of annealed alloys is shown in Fig. 57.[31G] Here we see the magnetic intensity at saturation for a series of Ni-Mn alloys when rapidly cooled and when annealed at 450°C. Annealing substantially increases the magnetic intensity at saturation in alloys containing greater than 17 atomic percent Mn. In the composition region from 24 to 35 atomic percent Mn, annealing changes a nonferromagnetic alloy into a strongly ferromagnetic one. The presence of a superstructure has not yet been established by x-ray means. Nevertheless, the indirect evidence clearly indicates the presence of a superstructure in this alloy when annealed. This structure is clearly associated with the strongly ferromagnetic state.

Some interesting data have been reported by Jellinghaus[36D] on the relationship between order and ferromagnetic properties in a Fe-Pd alloy containing 50 atomic percent Pd. The alloy after rapid cooling had a coercive force of some 2 oersteds, which on annealing for 15 hours at 500°C increased to 260 oersteds and on further anneal finally reached a steady value of 150 oersteds. The annealing treatment provoked a change from the face-centered cubic structure of the rapidly cooled random alloy to an ordered tetragonal structure similar to that of CuAu. Other observers,[36K] however, report that they find a superstructure only in the $FePd_3$ region. Jellinghaus[36D] also reports the presence of an ordered structure in an alloy containing 50 atomic percent Fe, 45 atomic percent Pt and 5 atomic percent Rh, of the CuAu tetragonal type. With this ordered structure is associated a coercive force of 1400 oersteds and a remanence of 3700 gauss.

The alloys of chromium and platinum containing from 20 to 50 atomic percent Cr have been observed[35G] to be ferromagnetic, with the maximum in the curve of saturation-magnetization-*vs.*-composition occurring at about 30 atomic percent Cr. The saturation intensity is influenced by the heat treatment, the annealed alloys exhibiting higher values than the rapidly cooled ones. X-ray examination showed no evidence of superstructure lines for alloys containing less than 40 atomic percent Cr; beyond 40 atomic percent there were such lines, increasing in strength with increasing proportion of Cr. In this system the ferromagnetism is clearly *not* associated with a high degree of coherent long distance order, since the alloy containing 30 atomic percent Cr, where superlattice lines are not detectable, displays the highest ferromagnetic saturation.

The famous Heusler alloys have been shown by recent investigation to have an ordered structure associated with the ferromagnetic state. Bradley and Rodgers,[34B] Heusler[34F] and others have shown that an alloy of the composition Cu_2AlMn

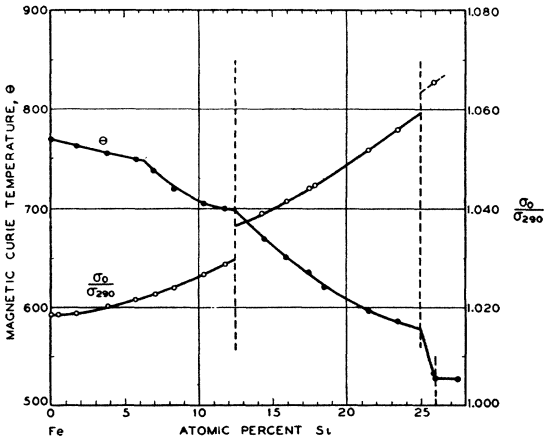

FIG. 58. Magnetic Curie temperature θ, in degrees centigrade, and the ratio of magnetic saturation at 0°K to that at 290°K, plotted against composition for a series of Fe-Si alloys.

is ferromagnetic when rapidly cooled from about 600°C after annealing and is highly ordered. We have already given the structure of this ordered phase as determined by Bradley and Rodgers.

Fallot[36B] has used magnetic measurements to detect and study ordered structures in the alloy systems Fe-Si, Fe-Al, Fe-Cr, Fe-V, Fe-Au and Fe-Sn. In Fig. 58 we reproduce Fallot's measurements of σ_0/σ_{290}, the ratio of magnetic saturation at 0°K to that at 290°K, on alloys of the Fe-Si system containing up to about 30 atomic percent Si. For annealed alloys the curve displays pronounced discontinuities at 12.5 and 25 atomic percent Si. The latter composition corresponds to the well-known Fe_3Si ordered phase. The plot of the ferromagnetic Curie point *vs.* composition, shown in the same figure, likewise displays a break at 25 atomic percent Si. Fallot also regards the change in the direction of the Curie point-*vs.*-composition curve at 12.5 atomic percent Si as of some significance. In general he considers the occurrence of singular points, such as appear at 12.5 and 25 atomic percent Si in the curves both of σ_0/σ_{290} and of the magnetic Curie point as functions of composition, as indicating the presence of ordered structures. Independent x-ray evidence[25B] has established the presence of an ordered structure at 25 atomic percent Si, but we know of no conclusive x-ray evidence indicating a superlattice at 12.5 atomic percent Si. Fallot finds a similar break at 25 atomic percent Al in the two comparable plots for the Fe-Al alloys, well known to form ordered structures. We feel that similar evidence might be used to supplement other data, but such evidence as is presented by Fallot must be considered, at least for the present, to be insufficient when taken alone to establish the existence of a superlattice.

Some of the permanent magnet alloys have been shown[35H, 35F, 35U, 37Q] to display a superstructure when in the magnetically hard state. An example is the so-called Mishima alloy,[33K] containing Fe, Ni and Al. Burgers and Snoek[35F] have shown, however, that the coercive force is not proportional to the intensity of the superstructure lines. We do not consider it established that the presence of a superstructure is responsible for the magnetic properties, although the increase in magnetic hardness provoked by annealing is accompanied by a superlattice.

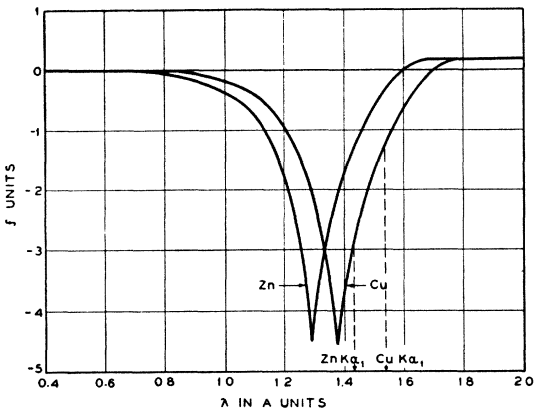

FIG. 59. Dispersion of atomic structure factor for Zn and Cu.

Section 23. Criteria for establishing the presence of ordered structures

As we have already intimated, in alloy systems where the component atoms have almost identical scattering powers for x-rays the presence of an ordered structure would, under the usual x-ray investigations, escape detection because of the faintness of superstructure lines. These lines arise, as we described in the introduction, by virtue of the fact that although the x-rays scattered from the α-sites are 180° out of phase with the rays scattered from the β-sites, the difference in scattering powers of the two atoms prevents cancellation of the rays. If the component atoms possess not very different scattering powers for x-rays, the lines may be too faint to be discerned; whereas when the difference in scattering power is sufficiently great they are rather intense, as for the ordered Cu_3Au alloy of Fig. 2.

It is however a fact, and an important one, that even though elements adjacent to each other in the periodic table have scattering-powers nearly the same for most wave-lengths, yet there are small intervals of wave-length for which there is a marked difference; and judicious selection of the x-ray wave-length to be used has in some cases made it possible to detect superstructure lines when the Cu or Fe $K\alpha$ radiations, which are ordinarily used in such investigations, failed to show the presence of the superlattice. Fig. 59 depicts the atomic scattering curves for Zn and Cu as derived from experimental data of Bradley and Hope[32B] for Fe, taken from Jones and

Sykes,[37I] along with the additional knowledge of the critical absorption wave-lengths for Cu and Zn. Jones and Sykes, on the basis of the data in Fig. 59, selected Zn $K\alpha$ radiation as being of a wave-length such that it would be scattered by Cu and Zn atoms with sufficient difference in intensity. By using the radiation of a Zn anticathode filtered through copper, these investigators were able for the first time to obtain superlattice lines from ordered β-brass. Bradley and Rodgers[34B] had previously used the same policy of selecting a suitable x-ray wave-length for the study of the Heusler alloys in order to assign definite locations to the Cu and Mn atoms. An exact knowledge of the atomic form factor curves should be of great assistance in the selection of a suitable anti-cathode material for studies of systems where the component atoms have similar scattering powers.

Many indirect means are also extremely useful in establishing the presence of an ordered structure. In alloy systems consisting of isomorphous series of solid solutions, annealing after quenching decreases the resistivity of compositions which form ordered structures, as illustrated by Figs. 47, 48, 49 and as observed in the Ni-Mn and the Fe-Ni alloys also. One must consider this as indicative of the formation of a superstructure in the composition regions where such an effect is observed. Two such regions are found in the Ni-Mn system, one about the Ni_3Mn and another about the NiMn compositions. In the Fe-Ni system the effect is observed in alloys containing 35 to 90 atomic percent Ni.

Changes in the electrical resistivity of a homogeneous solid solution on cooling, similar to the change shown for Cu_3Au in Fig. 5, can also be used to indicate the onset of an ordering process. Since similar changes in electrical resistivity are also provoked by ferromagnetic changes, however, one must exercise great caution in the use of such data.

The drastic changes in the electrical resistivity of ordered alloys provoked by plastic deformation can also be used in many cases to indicate the presence of an ordered structure. The fact that appreciable changes in resistivity also occur in molybdenum and tungsten on cold working forces one to proceed cautiously in interpreting data of this sort, but we feel that changes of the magnitudes shown above for Cu_3Au and Cu-Pt alloys can be taken to indicate strongly that a superlattice is being destroyed by plastic deformation. It was such data that led Dahl,[36A] as was discussed by one of us,[37T] to consider the possibility of an ordered region around Ni_3Fe. The behavior of the electrical resistivity and magnetic properties on cold working a previously annealed Ni_3Mn alloy permits a similar interpretation.

The nature of the $\beta-\beta'$ transformation in the Cu-Zn system was first suggested by Tammann and Heusler[26A] from rather crude specific heat data. The accurate specific heat work of Sykes and his collaborators,[35R, 36H, 37P] along with the resistivity-*vs.*-temperature characteristics, agree so well with the Bragg-Williams theory that it has been customary in recent years to think of this transformation as of the order-disorder type. Only recently has this viewpoint been confirmed by the x-ray studies of Jones and Sykes[37I] mentioned above. We consider similar specific heat measurements to be of real value in establishing the nature of many transformations.

Magnetic measurements such as those reported by Fallot[36B] may also be mentioned as having some possible value when further confirmatory evidence is accumulated. The break in the σ_0/σ_{290} curve of Fig. 58 at 12.5 atomic percent Si is certainly similar in nature to the break at 25 atomic percent Si where x-ray evidence has established that a superstructure exists. We feel, however, that much further confirmation must be obtained before real significance can be attached to such breaks.

Acknowledgments

We are indebted to a number of people who have aided us in completing this article. In particular thanks are due to many of our colleagues for helpful discussion. We are also indebted for discussions or communications of a technical nature to Drs. J. G. Kirkwood, F. Seitz, and C. Sykes. Especial thanks are extended to our colleague K. K. Darrow for effort expended upon a manuscript which was in a disordered condition. It gives pleasure to the three of us to have shown that the transition from disorder towards

order is possible not only in lattices but also in the literature of lattices, although between the two cases there exists the important and lamentable difference that the transformation of disorder into order liberates energy in the metallurgical but absorbs it in the literary case.

Appendix 1. Simplification of the Nearest Neighbor Energy Expression and Energies of Formation of Alloys

Relationships between the Q's

Consider a lattice containing N atomic sites each surrounded by z nearest neighbors; the total number of pairs will then be

$$Q=\tfrac{1}{2}zN. \tag{A1.1}$$

Let Q be made up of Q_{AA}, Q_{BB}, and Q_{AB} pairs of the different types. Next imagine that a model of the alloy, consisting of wooden balls and wooden rods representing the atoms and the lines between pairs, is pulled apart into pairs, each pair carrying with it $1/z$th of a ball at either end. Each AA pair then has the fraction $(2/z)$ of an A ball, etc. If the total numbers of A and B balls in the model are F_AN and F_BN then we must have

$$F_AN=(2/z)Q_{AA}+(1/z)Q_{AB}, \tag{A1.2}$$

$$F_BN=(2/z)Q_{BB}+(1/z)Q_{AB}. \tag{A1.3}$$

We can solve these for the like neighbor pairs:

$$Q_{AA}=F_AQ-\tfrac{1}{2}Q_{AB}, \tag{A1.4}$$

$$Q_{BB}=F_BQ-\tfrac{1}{2}Q_{AB}. \tag{A1.5}$$

Let us next consider the energy of the alloy as compared to the energy of two pure crystals of A and B from which it could be made. The energy of a crystal of pure A with F_AN atoms will be v_{AA} times the number of pairs, which is $(z/2)$ $F_AN=F_AQ$. Hence the energy in question is

$$E=v_{AA}Q_{AA}+v_{BB}Q_{BB}+v_{AB}Q_{AB} -F_Av_{AA}Q-F_Bv_{BB}Q, \tag{A1.6}$$

which reduces to

$$E=[v_{AB}-\tfrac{1}{2}(v_{AA}+v_{BB})]Q_{AB}. \tag{A1.7}$$

It is best to define a new quantity

$$v=\tfrac{1}{2}(v_{AA}+v_{BB})-v_{AB}. \tag{A1.8}$$

In terms of v the energy is

$$E=-vQ_{AB}. \tag{A1.9}$$

The meaning of V is indicated in the diagram below:

$A\ A$ $A-B\ A-B$ $A\ A$		$A\ A$ $A-A\ B-B$ $A\ A$
lesser energy	difference $2v$	greater energy

We see that v must be positive or else there will be tendency at low temperature for the alloy to separate into two components of pure A and B, contrary to the assumption that we are dealing with an alloy which forms a superlattice at low temperatures.

Energy *versus* composition

Random state.—For the random state the probability that any site is occupied by an A atom is F_A and that it is occupied by a B atom is F_B. Hence the probability that any two adjacent sites are occupied by an AB pair is $2F_AF_B$, the factor of two corresponding to the two possibilities AB and BA. Hence the fraction of AB pairs is $2F_AF_B$ and the energy is

$$\begin{aligned}E(\text{random})&=-2vQF_AF_B\\&=-NvzF_AF_B.\end{aligned} \tag{A1.10}$$

Best ordered state.—Due to the symmetry about 50 atomic percent we need consider only $F_A\leq F_B$. The lowest possible energy corresponds to a maximum value for Q_{AB}, and by Eq. (A1.4) to a minimum of Q_{AA}. The least possible value of Q_{AA} is zero, and this can be attained for the body-centered lattice: consider the perfectly ordered AB case; in it there are no AA pairs and Q_{AA} is zero. If we replace A atoms by B atoms without rearrangement, thus never producing AA pairs, then all values of F_A less than one-half can be attained with $Q_{AA}=0$. Hence, from (A1.4) and (A1.9), we have

$$E=-vQ_{AB}=-2vQF_A=-NvzF_A. \tag{A1.11}$$

This equation applies for $F_A\leq\frac{1}{2}$ for the simple cubic and body-centered cubic lattices. For the face-centered lattice, the situation is complicated because for $F_A>\frac{1}{4}$ it is impossible to avoid AA pairs. This leads to the kink at 25 atomic percent A in Fig. 23. A detailed establishment of the curve is given in reference 38C.

Appendix 2. Bethe's First Approximation

The consistency condition

We suppose that the interior consists of one α-site and the boundary of z β-sites and that no two β-sites are nearest neighbors. Let the ordering energy of the exterior be u so that the relative probability of an A atom in the boundary compared to a B atom is given by the Boltzmann factor

$$\exp(-u/kT)=\epsilon. \tag{A2.1}$$

Let us arbitrarily choose $v_{AA}=v_{BB}=v$ and $v_{AB}=0$; this is legitimate according to Eqs. (A1.8) and (A1.9) for the reasons given in Section 2; i.e., it gives v for the value of $\frac{1}{2}(v_{AA}+v_{BB})-v_{AB}$. Hence the Boltzmann factor weighting unfavorably the occurrence of a wrong (that is, an AA or a BB) pair compared to right (i.e. an AB) pair is

$$\exp(-v/kT)=x=\exp(-4E_0/RTz). \tag{A2.2}$$

Assume that the central atom is A, a right atom. Then the relative probability, r_n, of finding n wrong A atoms in the boundary is the *a priori* probability of n wrong atoms

times the Boltzmann factor. The first is given by binomial coefficient $\binom{z}{n}$, the number of ways of arranging n wrong A atoms in z sites. The second is $\epsilon^n x^n$. Hence

$$r_n=\binom{z}{n}\epsilon^n x^n. \tag{A2.3}$$

Assume that the central atom is B, a wrong atom. Then, by similar reasoning the relative probability of finding n wrong A atoms in the boundary is

$$w_n=\binom{z}{n}\epsilon^n x^{z-n}, \tag{A2.4}$$

because in this case each of the $z-n$ right B atoms in the boundary gives interaction v with the wrong interior B atom.

Accordingly, the total relative probability for the interior atom being right is

$$r_i=\sum_{n=0}^{z} r_n=(1+\epsilon x)^z \tag{A2.5}$$

and for being wrong

$$w_i=\sum_{n=0}^{z} w_i=(\epsilon+x)^z. \tag{A2.6}$$

Hence the normalized probability of the center atom (which is on an α-site) being right is

$$r_\alpha=r_i/(r_i+w_i). \tag{A2.7}$$

We next calculate the relative probability of an atom in the boundary being wrong. This is equal to the average number (that is, the statistical mechanical average) of wrong atoms in the boundary divided by z. The relative probability of finding n wrong atoms in the boundary is r_n+w_n. Multiplying this by n, averaging, and normalizing gives

$$n_{Av}=zw_\beta=\left(\sum_{n=0}^{z} n(r_n+w_n)\right)\Big/\left(\sum_{n=0}^{z}(r_n+w_n)\right)$$
$$=z\left[\frac{\epsilon x r_i}{(1+\epsilon x)}+\frac{\epsilon w_i}{(\epsilon+x)}\right]\Big/(r_i+w_i). \tag{A2.8}$$

From this we can find $r_\beta=1-w_\beta$, the probability of finding a B atom on a β-site. By the symmetry described in the text, we must have $r_\alpha=r_\beta$; this consistency equation can now be used for determining u, or rather the equivalent quantity ϵ.

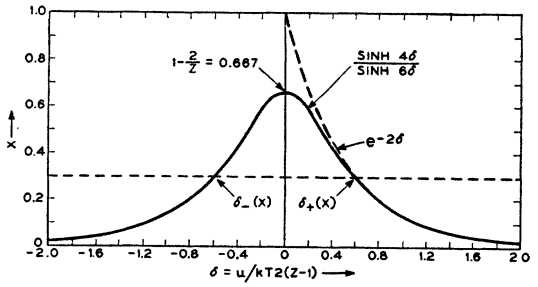

FIG. A1. Relationship between δ and X for Bethe's first approximation.

Instead of using $r_\alpha=r_\beta$, we use $w_\alpha=w_\beta$ and multiply through by (r_i+w_i). This gives

$$w_i=\epsilon x r_i/(1+\epsilon x)+\epsilon w_i/(\epsilon+x). \tag{A2.9}$$

Dividing by r_i and collecting terms with w_i/r_i,

$$\frac{w_i}{r_i}\left(1-\frac{\epsilon}{\epsilon+x}\right)=\frac{w_i}{r_i}\frac{x}{(\epsilon+x)}=\frac{\epsilon x}{(1+\epsilon x)}. \tag{A2.10}$$

Substituting the values for w_i and r_i we readily find

$$\left(\frac{\epsilon+x}{1+\epsilon x}\right)^{z-1}=\epsilon=e^{-2\delta(z-1)}. \tag{A2.11}$$

Where the new variable $\delta=(u/kT)/2(z-1)$ has been introduced for convenience in solving Eq. (A2.11) for x. We find

$$x=\frac{\sinh(z-2)\delta}{\sinh z\delta}. \tag{A2.12}$$

Figure A1 shows a plot of the right side of this equation for $z=6$, the simple cubic lattice. For δ greater than about 0.5, the right side of Eq. (A2.12) differs negligibly from the function $\exp(-2\delta)$, shown dashed. Hence for low temperatures, that is, small x and large δ, we find $\ln x=-v/kT\cong-2\delta=-u/kT(z-1)$ or $u=(z-1)v$. This is just the ordering energy which should be exerted at low temperatures upon an atom in the boundary due to its $(z-1)$ right neighbors in the exterior. It is seen that values of x greater than x_c,

$$x_c=1-2/z, \tag{A2.13}$$

do not occur on the curve. For values of x less than x_c there are two values of δ which have opposite signs. This corresponds to reversing the sign of u and is in accordance with the fact that α- and β-sites are equivalent. When x and ϵ are expressed in terms of δ, the quantities $r_\alpha=r_\beta=r$ and $w_\alpha=w_\beta=w$ can be evaluated and $S=2(r_\alpha-\frac{1}{2})$ becomes:

$$S=\tanh z\delta. \tag{A2.14}$$

Negative values of S, like negative values of δ correspond to interchange of α- and β-sites. For x greater than x_c, there is no solution of this type and we must set $\epsilon=1$ which leads to $r_\alpha=r_\beta=w_\alpha=w_\beta=\frac{1}{2}$. The critical temperature is readily found:

$$v/kT_c=-\ln x_c=-\ln(1-2/z) \tag{A2.15}$$

and

$$RT_c/E_0=-4\div z\ln(1-2/z). \tag{A2.16}$$

Evaluation of σ

We next consider the order of neighbors. There are z pairs in the interior and the boundary. For a right center atom the number of AB pairs is $(z-n)$ and for a wrong center atom it is n. On the average, therefore the fraction of pairs which are AB (that is, q by definition (2.9)) is

$$q=\frac{1}{z}\frac{\Sigma(z-n)r_n+\Sigma n w_n}{r_i+w_i}. \tag{A2.17}$$

Hence according to (2.11), the value of σ, or rather $E/E_0=(1-\sigma)$, is found after some algebraic manipulations to be

$$(1-\sigma)=\frac{4}{z}\frac{\Sigma n r_n}{r_i+w_i}=\frac{4\epsilon x}{1+\epsilon x}\frac{1}{1+\epsilon^{z/(z-1)}}$$
$$=\frac{2\sinh(z-2)\delta}{\sinh(2z-2)\delta\cosh z\delta}. \tag{A2.18}$$

Calculations of quantities at T_c

By expansion in series near the critical temperature, Bethe finds the specific heat per gram atom just below T_c:

$$C/R=\frac{dE}{RdT}=\frac{z}{4}(\ln x)^2\frac{d(1-\sigma)}{dx}$$
$$=\frac{z-2}{4}\left(\frac{z}{z-1}\right)^2(\tfrac{3}{2}z-1)\left(\log\frac{z-2}{z}\right)^2. \quad \text{(A2.19)}$$

Above the critical temperature, $\epsilon=1$ and

$$1-\sigma=2x/(1+x). \quad \text{(A2.20)}$$

The specific heat just above T_c is less by a factor

$$(3z-2) \quad \text{(A2.21)}$$

than that just below T_c.

The fraction of E_0 required to reach T_c is $(1-\sigma_c)$ and in terms of x_c and z it is

$$E(T_c\pm)/E_0=(1-\sigma_c)=\frac{2x_c}{1+x_c}=\frac{z-2}{z-1}. \quad \text{(A2.22)}$$

The entropy at T_c can be found from the entropy change between T_c and $T=\infty$. The writers have evaluated this from the simple expression for $(1-\sigma)$ in terms of x as follows:

$$S(\infty)-S(T_c)=\int_{T_c}^{\infty}\frac{dE}{T}=\frac{E}{T}\Big]_{T_c}^{\infty}-\int_{T_c}^{\infty}Ed\left(\frac{1}{T}\right)$$
$$=-\frac{E_c}{T_c}-\int_{x_c}^{1}E_0(1-\sigma)\left(-\frac{Rz}{4E_0}\right)\frac{dx}{x} \quad \text{(A2.23)}$$
$$=(z/2)\left[-\ln(1-1/z)+\frac{z-2}{2z-2}\ln(1-2/z)\right]R.$$

This expression was used in obtaining the entropy values of Table I.

z approaches ∞

In the Bragg-Williams theory the ordering energy is dependent upon the order on all the sites in the lattice. Physically this is equivalent to assuming that every β-site is a nearest neighbor of every α-site and *vice versa*. Thus if the Bethe method is correct, it should converge upon the Bragg-Williams theory as z approaches ∞. Bethe shows in his work that this is indeed the case.

Appendix 3. Expression for the Free Energy in Terms of the Semi-Invariants of Thiele

We shall here derive the relationship established by Kirkwood[38B] between the free energy and the semi-invariants. Let the energy of each of the W allowed arrangements of the atoms be E_i, $i=1, 2, \cdots W$. Then by the partition function method, the free energy is determined from

$$\exp(-F/kT)=\sum_i\exp(-E_i/kT). \quad \text{(A3.1)}$$

The value of F defined by this equation can be shown for our case of large numbers of atoms to differ negligibly from the value of F given by the most probable value of E_i in the sum.

Consider the equation

$$\sum_i e^{xE_i}=e^{\lambda_0+x\lambda_1+(x^2\lambda_2)/2!+\cdots} \quad \text{(A3.2)}$$

where for brevity we let

$$x=-1/kT. \quad \text{(A3.3)}$$

If this equation is regarded as an identity in x, it serves to determine the "semi-invariants" λ_i in terms of the E_i. The relationship is established by expanding the exponentials of the left side obtaining

$$\sum_{i=1}^{W}1+x\sum_{i=1}^{W}E_i+\frac{x^2}{2!}\sum_{i=1}^{W}E_i^2+\cdots=e^{\lambda_0+x\lambda_1+(x^2/2!)\lambda_2+\cdots}. \quad \text{(A3.4)}$$

The sums of the various powers of E_i are denoted by

$$\Sigma_0=\sum_{i=1}^{W}1=W \quad \text{(A3.5)}$$

$$\Sigma_n=\sum_{i=1}^{W}E_i^n$$

Letting $$C(x)=\Sigma_0+x\Sigma_1+(x^2/2!)\Sigma_2+\cdots \quad \text{(A3.6)}$$

and $$D(x)=\lambda_0+x\lambda_1+(x^2/2!)\lambda_2+\cdots, \quad \text{(A3.7)}$$

we can write

$$C(x)=e^{D(x)}$$

and $$\frac{dC(x)}{dx}=e^{D(x)}\frac{dD(x)}{dx}=C(x)\frac{dD(x)}{dx}. \quad \text{(A3.8)}$$

The left and right terms of the last equation are expressed as series in x. Equating coefficients we find

$$\begin{aligned}&\Sigma_1=\Sigma_0\lambda_1,\\&\Sigma_2=\Sigma_0\lambda_2+\Sigma_1\lambda_1,\\&\Sigma_n=\sum_{m=1}^{n}\binom{n-1}{m-1}\Sigma_{n-m}\lambda_m.\end{aligned} \quad \text{(A3.9)}$$

The value of λ_0 is easily found by setting $x=0$: $\lambda_0=\ln\Sigma_0=\ln W$. Denoting average values over the allowed arrangements by

$$\langle E^n\rangle_{Av}=\Sigma_n/\Sigma_0 \quad \text{(A3.10)}$$

and mean deviations from the average by

$$\Delta_n=\langle(E-E_{Av})^n\rangle_{Av}=\frac{1}{\Sigma_0}\sum_{m=0}^{n}\binom{n}{m}\Sigma_m(-E_{Av})^{n-m}, \quad \text{(A3.11)}$$

we find for the first few λ's:

$$\begin{aligned}&\lambda_0=\ln\Sigma_0=\ln W,\\&\lambda_1=\Sigma_1/\Sigma_0=E_{Av},\\&\lambda_2=\langle E^2\rangle_{Av}-E_{Av}^2=\Delta_2,\\&\lambda_3=\langle E^3\rangle_{Av}-\langle 3E^2\rangle_{Av}E_{Av}+2E_{Av}^3=\Delta_3,\\&\lambda_4=\Delta_4-3\Delta_2^2.\end{aligned} \quad \text{(A3.12)}$$

Replacing x by $-1/kT$ we find

$$-\frac{F}{kT}=D(-1/kT)=\lambda_0-\frac{\lambda_1}{kT}+\frac{\lambda_2}{2!(kT)^2}+\cdots \quad \text{(A3.13)}$$

and multiplying through by $-kT$ and writing $k\ln W=\Phi$, we have

$$F=-T\Phi+E_{Av}-\frac{\Delta_2}{2!kT}+\frac{\Delta_3}{3!(kT)^2}-\frac{\Delta_4-3\Delta_2^2}{4!(kT)^3}+\cdots, \quad \text{(A3.14)}$$

which is Eq. (4.3) of the text.

Appendix 4. Application of Kirkwood's Method

Calculation of the second moment

In calculating the moments needed in Kirkwood's method, it is convenient to introduce some new variables associated with the pairs of nearest neighboring sites. There are $zN/2=Q$ of these pairs and for each of them we shall introduce a variable p_i, $i=1, 2, \cdots Q$ defined by the conditions

$p_i=1$ (if the ith pair of sites are occupied by A atoms),
$p_i=0$ (otherwise).

For any arrangement of the atoms, the total number of AA pairs is

$$Q_{AA}=\sum_{i=1}^{Q} p_i. \tag{A4.1}$$

We wish to calculate the value of $\Delta_2=\langle(E-E_{Av})^2\rangle_{Av}$ averaged over all arrangements of the atoms with order S. In terms of Appendix 1 we readily find

$$\Delta_2=4v^2\langle(Q_{AA}{}^2-\langle Q_{AA}\rangle_{Av}{}^2)\rangle_{Av}\equiv 4v^2\Delta. \tag{A4.2}$$

Since we are dealing here with a lattice such as the simple cubic or body-centered, we may divide the sites into an α-sublattice and a β-sublattice, such that each p_i corresponds to a pair of nearest neighboring sites one in each sublattice—never both in one sublattice. We further restrict ourselves to the composition AB, and may write:

$$r_\alpha=r_\beta=r=(1+S)/2, \quad w_\alpha=w_\beta=w=(1-S)/2. \tag{A4.3}$$

Now consider the pair associated with p_i. Its α-atom is A in a fraction r_α of the arrangements and its β-atom is A in a fraction w_β of the arrangements. Since the arrangements on the α- and β-lattice are independent (we emphasize here that this is an *a priori* average and that a correlation between the lattices owing to the Boltzmann factor is not implied), an AA pair will be obtained in the fraction $r_\alpha w_\beta=rw$ of the arrangements. Hence p_i is unity in a fraction rw of the arrangements and zero in the remaining fraction $(1-rw)$. The average of p_i is therefore

$$\langle p_i\rangle_{Av}=(rw)\cdot 1+(1-rw)\cdot 0=rw=(1-S^2)/4. \tag{A4.4}$$

By expanding the terms in Eq. (A4.2) we find

$$\begin{aligned}\Delta&=\sum_{i=1}^{Q}\sum_{j=1}^{Q}(\langle p_ip_j\rangle_{Av}-\langle p_i\rangle_{Av}\langle p_j\rangle_{Av}\\&=\sum_{i=1}^{Q}\sum_{j=1}^{Q}(\langle p_ip_j\rangle_{Av}-r^2w^2).\end{aligned} \tag{A4.5}$$

In the sum of the $\langle p_ip_j\rangle_{Av}$ terms, there are four distinct cases:

(1) $i=j$, that is the two sites of p_i are the same as the two sites of p_j.
(2) p_i and p_j have a common α-site.
(3) p_i and p_j have a common β-site.
(4) p_i and p_j have no common sites.

There are Q terms of type (1) in Δ; for each of them $p_i{}^2=1$ in a fraction rw of the arrangements, hence $\langle p_i{}^2\rangle_{Av}=rw$ and their contribution to Δ is

$$\Delta(1)=Q(rw-r^2w^2). \tag{A4.6}$$

For type (2) there are $(N/2)$ α-sites, for each of these there are $z(z-1)$ ways of choosing adjoining β-sites, hence the number of terms from them is $(z-1)Q$. The fraction of the arrangements which leads to $p_ip_j=1$ is $r_\alpha w_\beta w_\beta=rw^2$ (neglecting terms of the order of $1/N$), hence the contribution to Δ is

$$\Delta(2)=(z-1)Q(rw^2-r^2w^2). \tag{A4.7}$$

A similar treatment for type (3) gives

$$\Delta(3)=(z-1)Q(r^2w-r^2w^2). \tag{A4.8}$$

All the remaining Q^2 terms of Δ are of type (**4**); however in spite of their greater number, they are individually enough smaller that their contribution is of the same order as for (1), (2) and (3). The value of p_ip_j is unity only for arrangements having A atoms on both α-sites and on both β-sites. On the $N/2$ α-sites there are $rN/2$ A atoms. Two of these will occur on the designated α-sites in a fraction

$$\frac{\frac{1}{2}rN(\frac{1}{2}rN-1)}{\frac{1}{2}N(\frac{1}{2}N-1)}. \tag{A4.9}$$

of the arrangements. Combining this with a similar term for the β-sites gives

$$\begin{aligned}\langle p_ip_j\rangle_{Av}-r^2w^2&=\frac{r^2w^2(1-2/rN)(1-2/wN)}{(1-2/N)^2}-r^2w^2\\&=r^2w^2\left(\frac{4rw-2}{Nrw}\right)+0\left(\frac{1}{N^2}\right).\end{aligned} \tag{A4.10}$$

Multiplying by Q^2, thus neglecting terms of order less than N in the final result, we get

$$\Delta(4)=zQ(2r^2w^2-rw). \tag{A4.11}$$

Hence the value of Δ is

$$\begin{aligned}\Delta&=\Delta(1)+\Delta(2)+\Delta(3)+\Delta(4)\\&=Qr^2w^2=Q(1-S^2)^2/16.\end{aligned} \tag{A4.12}$$

Calculation of free energy and allied quantities

When this result is put in the definition of Δ_2

$$\Delta_2=\tfrac{1}{4}v^2Q(1-S^2)^2=\tfrac{1}{8}Nzv^2(1-S^2)^2 \tag{A4.13}$$

and combined with the value of $E_{Av}(S)$ calculated in Section 3

$$E_{Av}(S)=E_0(1-S^2)=\tfrac{1}{4}Nzv(1-S^2) \tag{A4.14}$$

we obtain

$$\begin{aligned}F&=-T\Phi(S)+E_{Av}-\Delta_2/2kT+\cdots\\&=E_0(1-S^2)-TR[\ln 2-\tfrac{1}{2}(1+S)\ln(1+S)\\&\quad-\tfrac{1}{2}(1-S)\ln(1-S)]-\frac{E_0{}^2(1-S^2)^2}{zRT}+\cdots.\end{aligned} \tag{A4.15}$$

Kirkwood uses the variable α,

$$\alpha=\frac{zv}{2kT}=\frac{2E_0}{RT}. \tag{A4.16}$$

In terms of α

$$\begin{aligned}-F/NkT&=[\ln 2-\tfrac{1}{2}(1+S)\ln(1+S)\\&\quad-\tfrac{1}{2}(1-S)\ln(1-S)]-\alpha(1-S^2)/2\\&\quad+\alpha^2(1-S^2)^2/4z+\cdots.\end{aligned} \tag{A4.17}$$

The condition that F be a minimum for a given tempera-

ture is $(\partial F/\partial S)_\alpha=0$, which leads to

$$S=\tanh \gamma S, \tag{A4.18}$$

$$\gamma=\alpha-\alpha^2(1-S^2)/z. \tag{A4.19}$$

The solution of these equations leads to a nonzero value of S only for α greater than a certain critical value α_c corresponding to $S=0$ and $\gamma=1$ in Eq. (A4.19):

$$\alpha_c=\tfrac{1}{2}z[1-(1-4z)^{\frac{1}{2}}]. \tag{A4.20}$$

Values of the critical temperature

$$T_c=zv/2k\alpha_c \tag{A4.21}$$

computed from this are given in Table I. Kirkwood also gives equations for energy, entropy, and specific heat, corresponding to the equilibrium state obtained by minimizing the free energy:

$$E/NkT=(\alpha(1-S^2)-\alpha^2(1-S^2)^2/z)/2$$
$$\Phi/Nk=\ln 2-\tfrac{1}{2}[(1+S)\ln(1+S)+(1-S)\ln(1-S)]-\alpha^2(1-S^2)^2/4z. \tag{A4.22}$$

$$C/Nk=\alpha^2\left(\frac{S^2[1-2\alpha(1-S^2)/z]^2}{\cosh^2\gamma S-\gamma-2\alpha^2S^2/z}+\frac{(1-S^2)^2}{2z}\right). \tag{A4.23}$$

The specific heat has a discontinuity at $\alpha=\alpha_c$. The larger and smaller values being, respectively,

$$\frac{C}{Nk}=\alpha^2\left(\frac{(1-2\alpha/z)^2}{\frac{2}{3}-2\alpha^2/z}+\frac{1}{2z}\right) \tag{A4.24}$$

and

$$C/Nk=\alpha^2/2z. \tag{A4.25}$$

Limiting form as T approaches infinity

As T approaches ∞, Kirkwood's series converge rapidly and his approximate results become accurate. The limiting form for the energy is

$$E/E_0=1-2E_0/RT. \tag{A4.26}$$

The reader can easily verify that the theory of Bethe also gives this expression.

Appendix 5. Calculation of the Energy *Versus* Entropy Curve from the Free Energy

In obtaining the relationship between energy and entropy from the expansion of the free energy given in the Appendix 3, it proves convenient to shift the zero of the energy scale to E_{Av}. We let the new energy variable be U

$$U=E-E_{Av} \tag{A5.1}$$

and the new free energy be

$$F'=F-E_{Av}. \tag{A5.2}$$

Let the entropy be expressed as a power series in U:

$$\Phi(U)=\Phi_0+\Phi_1U+\frac{\Phi_2U^2}{2!}+\frac{\Phi_3U^3}{3!}+\cdots. \tag{A5.3}$$

In order to have a similar expansion for F' in $1/T$ we write

$$1/T=G, \tag{A5.4}$$

$$\Psi(G)=\frac{F-E_{Av}}{T}=\Psi_0+\Psi_1G+\frac{\Psi_2G^2}{2!}+\frac{\Psi_3G^3}{3!}+\cdots. \tag{A5.5}$$

The coefficients in this series are simply related to the λ's:

$$\begin{aligned}&\Psi_0=-k\lambda_0=-k\ln W,\\&\Psi_1=\lambda_1-E_{Av}=0,\\&\Psi_2=-\lambda_2/k=-\Delta_2/k,\\&\Psi_3=+\lambda_3/k^2=+\Delta_3/k^2,\\&\Psi_4=-\lambda_4/k^3=(-\Delta_4+3\Delta_2^2)/k^3.\end{aligned} \tag{A5.6}$$

Although Ψ_1 vanishes, Ψ_2 does not. The vanishing of Ψ_2 would imply no spread of energy and hence the trivial case of a system with constant energy.

One equation relating the various quantities in the above expressions is the definition of free energy

$$F'=U-T\Phi. \tag{A5.7}$$

From it we find

$$\Psi(G)+\Phi(U)=UG. \tag{A5.8}$$

Another relation is given by the equation relating temperature and the slope of the energy *vs.* entropy curve. This gives

$$T=dU/d\Phi, \quad \text{or} \quad G=d\Phi(U)/dU. \tag{A5.9}$$

A third relation follows from the thermodynamical equation

$$-T^2(d/dT)(F'/T)=U \quad \text{or} \quad U=d\Psi(G)/dG. \tag{A5.10}$$

We see that these three equations are symmetrical with $\Psi(G)$ and G corresponding to $\Phi(U)$ and U.

In order to solve these equations we substitute Eq. (A5.10) in Eq. (A5.8) thus obtaining

$$\Phi\left(\frac{d\Psi(G)}{dG}\right)=G\frac{d\Psi(G)}{dG}-\Psi(G). \tag{A5.11}$$

Both sides of this equation are in terms of series in G, and since it must be an identity in G we can equate coefficients of like powers. Since Ψ_1 is zero $d\Psi(G)/dG$ has no constant term, hence we obtain

$$\begin{aligned}&\Phi_0=-\Psi_0,\\&\Phi_1\Psi_2=0, \quad \text{or} \quad \Phi_1=0,\\&\frac{\Phi_2}{2!}\Psi_2^2=\tfrac{1}{2}\Psi_2.\\&\cdots\cdots\end{aligned} \tag{A5.12}$$

These equations can be solved for the Φ_i in terms of the Ψ_i and give for the first few terms

$$\begin{aligned}&\Phi_0=-\Psi_0=k\ln W,\\&\Phi_1=\Psi_1=0,\\&\Phi_2=1/\Psi_2, && \Psi_2=1/\Phi_2,\\&\Phi_3=-\Psi_3/\Psi_2^3, && \Psi_3=-\Phi_3/\Phi_2^3,\\&\Phi_4=\frac{3\Psi_3^2-\Psi_2\Psi_4}{\Psi_2^5}, && \Psi_4=\frac{3\Phi_3^2-\Phi_2\Phi_4}{\Phi_2^5}.\end{aligned} \tag{A5.13}$$

Inserting the values of the Ψ's in terms of the Δ_n's and replacing U by $E-E_{Av}$ and $k\ln W$ by $\Phi(S)$, we obtain the expansion of (4.4) given in the text.

Bibliography

1916

16A. N. Kurnakow, S. Zemczuzny and M. Zasedatelev, "The Transformations in Alloys of Gold with Copper," J. Inst. Metals **15**, 305 (1916).

1919

19A. G. Tammann, "Die chemischen und galvanischen Eigenschaften von Mischkristallreihen und ihre Atomverteilung," Zeits. f. anorg. allgem. Chemie **107**, 1 (1919).

1921

21A. C. Tammann, *Lehrbuch der Metallographie* (L. Voss, Leipzig, 1921), p. 325.

1922

22A. A. Fisher, *The Mathematical Theory of Probabilities*, second edition, Vol. 1 (Macmillan Co., N. Y., 1922), p. 191.

1923

23A. E. C. Bain, "Cored Crystals and Metallic Compounds," Chem. & Met. Eng. **28**, 65 (1923).

1924

24A. G. Borelius, "Die Tammannschen Resistenzgrenzen und die Atomverteilung der metallischen Mischkristalle," Ann. d. Physik **74**, 216 (1924).

24B. S. Holgersson and E. Sedström, "Experimentelle Untersuchungen über die Gitterstruktur einiger Metallegierungen," Ann. d. Physik **75**, 143 (1924).

24C. E. Sedström, "Zur Kenntnis der Gold-Kupfer-Legierungen," Ann. d. Physik **75**, 549 (1924).

1925

25A. C. H. Johansson and J. O. Linde, "Röntgenographische Bestimmung der Atomanordnung in den Mischkristallreihen Au-Cu und Pd-Cu," Ann. d. Physik **78**, 439 (1925).

25B. G. Phragmén, "Ueber den Aufbau der Eisen-Silizium Legierungen," Stahl u. Eisen, **45**, 299 (1925).

1926

26A. G. Tammann and O. Heusler, "Über Umwandlungen, die in homogener anisotroper Phase ohne Umkristallisation verlaufen," Zeits. f. anorg. allgem. Chemie **158**, 349 (1926).

1927

27A. C. H. Johansson and J. O. Linde, "Gitterstruktur und elektrisches Leitvermögen der Mischkristallreihen Au-Cu, Pd-Cu und Pt-Cu," Ann. d. Physik **82**, 449 (1927).

1928

28A. G. Borelius, C. H. Johansson and J. O. Linde, "Die Gitterstrukturumwandlungen in metallischen Mischkristallen," Ann. d. Physik **86**, 291 (1928).

28B. W. Gorsky, "Röntgenographische Untersuchung von Umwandlungen in der Legierung CuAu," Zeits. f. Physik **50**, 64 (1928).

28C. M. LeBlanc, K. Richter and E. Schiebold, "Eine Prüfung der Tammannschen Theorie der Resistenzgrenzen am System Gold-Kupfer. Aufstellung neuer Gesichtspunkte," Ann. d. Physik **86**, 929 (1928).

28D. A. E. van Arkel and J. Basart, "Atomabstände in Mischkristallen von Gold and Kupfer," Zeits. f. Krist. **68**, 475 (1928).

1929

29A. H. H. Potter, "The X-Ray Structure and Magnetic Properties of Single Crystals of Heusler Alloy," Proc. Phys. Soc. London **41**, 135 (1929).

29B. H. J. Seemann and E. Vogt, "Überstruktur und magnetische Suszeptibilität im System Kupfer-Gold," Ann. d. Physik **2**, 976 (1929).

1930

30A. U. Dehlinger and L. Graf, "Über Umwandlungen von festen Metallphasen. I. Die tetragonale Gold-Kupferlegierung AuCu," Zeits. f. Physik **64**, 359 (1930).

30B. U. Dehlinger, "Röntgenographische Untersuchungen am System Cd-Mg," Zeits. f. anorg. allgem. Chemie **194**, 223 (1930).

30C. C. H. Johansson and J. O. Linde, "Kristallstruktur, elektrischer Widerstand, Thermokräfte, Wärmeleitfähigkeit, magnetische Suszeptibilität Härte und Vergütungserscheinungen des Systems AuPt in Verbindung mit dem Zustandsdiagram," Ann. d. Physik **5**, 762 (1930).

30D. C. H. Johansson and J. O. Linde, "Kristallstruktur, elektrische Leitfähigkeit, Thermokräfte und Vergütungserscheinungen des Systems AgPt in Verbindung mit dem Zustandsdiagram," Ann. d. Physik **6**, 458 (1930).

30E. K. Ohshima and G. Sachs, "Röntgenuntersuchungen an der Legierung AuCu," Zeits. f. Physik **63**, 210 (1930).

30F. H. J. Seemann, "Die elektrische Leitfähigkeit der Cu_3Au-Legierungen mit und ohne Überstruktur in tiefer Temperatur," Zeits. f. Physik **62**, 824 (1930).

30G. L. Nowack, "Vergütbare Edelmetall-Legierungen," Zeits. f. Metallkunde **22**, 94 (1930).

1931

31A. G. Grube, G. Schönmann, F. Vaupel and W. Weber, "Das Zustandsdiagramm der Kupfer-Goldlegierungen," Zeits. f. anorg. allgem. Chemie **201**, 41 (1931).

31B. J. L. Haughton and R. J. M. Payne, "Transformations in the Gold-Copper Alloys," J. Inst. Metals **46**, 457 (1931).

31C. N. S. Kurnakow and N. W. Ageew, "Physico-Chemical Study of the Gold-Copper Solid Solutions," J. Inst. Metals **46**, 481 (1931).

31D. H. Röhl, "Änderung des Elastizitätsmoduls von AuCu-Legierungen bei Überstrukturbildung," Zeits. f. Physik **69**, 309 (1931).

31E. G. Sachs and J. Weerts, "Atomordnung und Eigenschaften (Untersuchungen an der Legierung $AuCu_3$)," Zeits. f. Physik **67**, 507–515 (1931).

31F. C. Wagner and W. Schottky, "Theorie der geordneten Mischphasen," Zeits. f. physik. Chemie **11B**, 163 (1931).

31G. S. Kaya and A. Kussmann, "Ferromagnetismus und Phasengestaltung im Zweistoffsystem Nickel-Mangan," Zeits. f. Physik **72**, 293 (1931).

1932

32A. A. J. Bradley and A. H. Jay, "The Formation of Superlattices in Alloys of Iron and Aluminium," Proc. Roy. Soc. **136A**, 210 (1932).

32B. A. J. Bradley and R. A. H. Hope, "The Atomic Scattering Power of Iron for Various X-Ray Wave-Lengths," Proc. Roy. Soc. **136A**, 272 (1932).

32C. U. Dehlinger, "Über Umwandlungen von festen Metallphasen. III. Kinetik auf atomistischer Grundlage," Zeits. f. Physik **74**, 267 (1932).

32D. L. Graf, "Die Umwandlungen im System Gold-Kupfer und ihre grundsätzliche Bedeutung für die Umwandlungen fester Metallphasen," Zeits. f. Metallkunde **24**, 248 (1932).

32E. L. Graf, "Korrosionsgefüge, Korrosionsmechanismus und die Tammann'schen Resistenzgrenzen Röntgenographische Untersuchung an Gold-Kupfer-Einkristallen," Metallwirtschaft **11**, 77 (1932).

32F. L. Graf, "Korrosionsgefüge, Korrosionsmechanismus und die Tammann'schen Resistenzgrenzen Röntgenographische Untersuchung an Gold-Kupfer-Einkristallen," Metallwirtschaft **11**, 91 (1932).

32G. M. LeBlanc and G. Wehner, "Untersuchungen über die Umwandlungen in fester Phase beim System Kupfer-Gold," Ann. d. Physik **14**, 481 (1932).

32H. G. Sachs, "Allgemeine Gesetzmässigkeiten der Gefüge- und Eigenschaftsänderungen bei Umwandlungsvorgängen," Zeits. f. Metallkunde **24**, 241 (1932).

32I. H. J. Seemann, "Atomordnung und magnetisches verhalten in den Systemen Kupfer-Gold, Kupfer-Palladium und Kupfer-Platin," Zeits. f. Metallkunde **24**, 299 (1932).

32J. E. M. Wise, W. S. Crowell and J. T. Eash, "The Roll of the Platinum Metals in Dental Alloys," Trans. A.I.M.E. **99**, 363 (1932) (Inst. of Metals Div.).

32K. J. H. Van Vleck, *The Theory of Electric and Magnetic Susceptibilities*. (The Clarendon Press, Oxford, 1932) p. 327.

32L. B. Svensson, "Magnetische Suszeptibilität und elektrischer Widerstand der Mischkristalreihen Pd-Ag und Pd-Cu," Ann. d. Physik **14**, 699 (1932).

1933

33A. W. L. Bragg, "Structure of Alloys," Nature **131**, 749 (1933).

33B. U. Dehlinger, "Über Umwandlungen von festen Metallphasen. V. Berechnung kinetischer Kurven im System Au-Cu," Zeits. f. Physik **83**, 832 (1933).

33C. L. Graf, "Zur Frage des Korrosionsschutzes und der Korrosionsbeständigkeit binärer Mischkristalle," Metallwirtschaft **12**, 602 (1933).

33D. L. Graf, "Zur Frage des Korrosionsschutzes und der Korrosionsbeständigkeit binärer Mischkristalle," Metallwirtschaft **12**, 585 (1933).

33E. E. R. Jette and E. S. Greiner, "An X-Ray Study of Iron-silicon Alloys Containing 0 to 15 Percent Silicon," A.I.M.E. **105**, 259 (1933) (Iron & Steel Div.).

33F. V. Pospišil, "Untersuchung des Systems Au-Cu durch Messung des Widerstandes in tiefen Temperaturen," Ann. d. Physik **18**, 497 (1933).

33G. H. Röhl, "Die elastischen Eigenschaften der Mischkristallreihen Au-Cu und Au-Pd und der Legierungen Cu_3Pt, Cu_3Pd und CuPd," Ann. d. Physik **18**, 155 (1933).

33H. K. Schäfer, "Einfluss einer Verformung (Pulverisierung) auf die Überstruktulinien und die Gitterkonstante einer FeAl-Legierung," Naturwiss. **21**, 207 (1933).

33I. H. J. Seemann, "Die elektrische Leitfähigkeit der Cu_3Pd- und Cu_3Pt-Legierungen mit ungeordneter und geordneter Atomverteilung in tiefer Temperatur," Zeits. f. Physik **84**, 557 (1933).

33J. N. S. Kurnakow and W. A. Nemilow, "Über Legierungen des Platins mit Kupfer," Zeits. f. anorg. allgem. Chemie **210**, 1 (1933).

33K. T. Mishima, "Nickel-Aluminium-Stahl für Dauermagnete," Stahl u. Eisen **53**, 79 (1933).

1934

34A. G. Borelius, "Zur Theorie der Umwandlungen von metallischen Mischphasen," Ann. d. Physik **20**, 57 (1934).

34B. A. J. Bradley and J. W. Rodgers, "The Crystal Structure of the Heusler Alloys," Proc. Roy. Soc. **144A**, 340 (1934).

34C. W. L. Bragg and E. J. Williams, "The Effect of Thermal Agitation on Atomic Arrangement in Alloys," Proc. Roy. Soc. London **145A**, 699 (1934).

34D. W. S. Gorsky, "On the Transitions in the CuAu Alloy. II. On the Migration of Atoms in the Lattice of CuAu," Physik. Zeits. Sowjetunion **6**, 69 (1934).

34E. W. S. Gorsky, "On the Transitions in the CuAu Alloy. III. On the Influence of Strain on the Equilibrium in the Ordered Lattice of CuAu," Physik. Zeits. Sowjetunion **6**, 77 (1934).

34F. O. Heusler, "Kristallstruktur und Ferromagnetismus der Mangan-Aluminium-Kupferlegierungen," Ann. d. Physik **19**, 155 (1934).

34G. H. J. Seemann, "Die elektrische Leitfähigkeit der CuPd-Legierungen mit ungeordneter und geordneter Atomverteilung in tiefer Temperatur. (Mit einem Nachtrag betr. Cu_3Pt)," Zeits. f. Physik **88**, 14 (1934).

34H C. Sykes and H. Evans, "Some Peculiarities in the Physical Properties of Iron-Aluminium Alloys," Proc. Roy. Soc. **145**, 529 (1934).

34I. R. Taylor, "Transformations in the Copper-Palladium Alloys," J. Inst. Metals **54**, 255 (934).

34J. L. Vegard and A. Kloster, "Gold-Kupferlegierungen, insbesondere bei hohen Temperaturen," Zeits. f. Krist. **89**, 560 (1934).
34K. W. Broniewski and K. Wesolowski, "Sur les propriétés mecaniques des alliages Or-cuivre," Comptes rendus **198**, 569 (1934).
34L. W. Broniewski and K. Wesolowski, "Sur la structure des alliages Or-cuivre," Comptes rendus **198**, 370 (1934).

1935

35A. N. W. Ageew and D. N. Shoyket, "Untersuchungen über molekulare feste Lösungen im System Kupfer-Gold," Ann. d. Physik **23**, 90 (1935).
35B. H. A. Bethe, "Statistical Theory of Superlattices," Proc. Roy. Soc. **150A**, 552 (1935).
35C. G. Borelius, "Zur Theorie der Umwandlungen von metallischen Mischphasen. III. Zustandsdiagramme teilweise geordneter Mischphasen," Ann. d. Physik **24**, 489 (1935).
35D. W. L. Bragg, "Atomic Arrangement in Metals and Alloys," J. Inst. Metals **56**, 275 (1935).
35E. W. L. Bragg and E. J. Williams, "The Effect of Thermal Agitation on Atomic Arrangement in Alloys. II," Proc. Roy. Soc. London **151A**, 540 (1935).
35F. W. G. Burgers and J. L. Snoek, "Lattice Distortion and Coercive Force in Single Crystals of Nickel-Iron-Aluminium," Physica **2**, 1064 (1935).
35G. E. Friederich and A. Kussmann, "Über den Ferromagnetismus der Platin-Chrom-Legierungen," Physik. Zeits. **36**, 185 (1935).
35H. R. Glocker, H. Pfister and P. Wiest, "Röntgenuntersuchungen an α-Eisenmagnetlegierungen," Arch. f. Eisenhüttenwesen **8**, 561 (1935).
35I. W. S. Gorsky, "Die elastische Nachwirkung in geordneter CuAu-Legierung. (Elastische Nachwirkung erster Art)," Physik. Zeits. Sowjetunion **8**, 562 (1935).
35J. W. S. Gorsky, "Theorie der elastischen Nachwikrung in ungeordneten Mischkristallen (Elastische Nachwirkung zweiter Art)," Physik. Zeits. Sowjetunion **8**, 457 (1935).
35K. W. S. Gorsky, "Theorie der Ordnungsprozesse und der Diffusion in Mischkristallen von CuAu. (Die Ordnungsumwandlungen in Legierungen. IV Mitteilung)," Physik. Zeits. Sowjetunion **8**, 443 (1935).
35L. L. Graf, "Kinetik und Mechanismus der allotropen Umwandlung im System Palladium-Kupfer," Physik. Zeits. **36**, 489 (1935).
35M. L. Graf and A. Kussmann, "Zustandsdiagramm und magnetische Eigenschaften von Platin-Eisen-Legierungen," Physik. Zeits. **36**, 544 (1935).
35N. W. Hume-Rothery and H. M. Powell, "On the Theory of Super-Lattice Structures in Alloys," Zeits. f. Krist. **91**, 23 (1935).
35O. H. J. Seemann, "Über ein Kriterium für das Auftreten geordneter Atomverteilungen in metallischen Mischkristallreihen," Zeits. f. Physik **95**, 796 (1935).
35P. H. J. Seemann, "Weitere Untersuchungen über die elektrische Leitfähigkeit metallischer Mischphasen in tiefer Temperatur (CuPt-Legierungen)," Zeits. f. Physik **95**, 97 (1935).
35Q. R. Smoluchouski, "Über die Feinstruktur der Röntgenabsorptionskanten von Legierungen. II CuBe, NiO und $AuCu_3$ (statistische und geordnete Phasen)," Zeits. f. Physik **95**, 588 (1935).
35R. C. Sykes, "Methods for Investigating Thermal Changes Occurring During Transformations in a Solid Solution," Proc. Roy. Soc. **148A**, 422 (1935).
35S. S. Valentiner and G. Becker, "Über das System Nickel-Mangan," Zeits. f. Physik **93**, 795 (1935).
35T. S. Valentiner and G. Becker, "Über Heuslersche Legierungen," Zeits. f. Physik **93**, 629 (1935).
35U. L. Werestschiagin and G. Kurdjumow, "Röntgenographische Untersuchung der Wärmebehandlung von magnetischen Legierungen Fe-Ni-Al," Techn. Phys. U.S.S.R. **2**, 431 (1935).
35V. E. J. Williams, "The Effect of Thermal Agitation on Atomic Arrangement in Alloys. III," Proc. Roy. Soc. **152A**, 231 (1935).
35W. M. LeBlanc and G. Wehner, "Über die Gold-Kupfer-Legierungen," Ann. d. Physik **23**, 570 (1935).
35X. A. Schulze, "Über eine besondere Erscheinung bei Umwandlungen, die sich über ein Temperaturgebeit erstrecken," Zeits. f. Metallkunde **27**, 251 (1935).
35Y. G. Sachs, *Praktische Metallkunde* (Dritter Teil) (Julius Springer, Berlin, 1935) p. 68.

1936

36A. O. Dahl, "Kaltverformung und Erholung bei Legierungen mit geordneter Atomverteilung," Zeits. f. Metallkunde **28**, 133 (1936).
36B. M. Fallot, "Ferromagnétisme des Alliages de Fer. Ann. de physique **6**, 305 (1936).
36C. E. R. Jette and F. Foote, "X-ray Study of Iron-Nickel Alloys," Trans. A.I.M.E. **120**, 259 (1936) (Iron & Steel Div.).
36D. W. Jellinghaus, "Neue Legierungen mit hoher Koerzitivkraft," Zeits. f. tech. Physik **17**, 33 (1936).
36E. C. H. Johansson and J. O. Linde, "Röntgenographische und elektrische Untersuchungen des CuAu-Systems," Ann. d. Physik **25**, 1 (1936).
36F. H. Moser, "Messung der wahren spezifischen Wärme von Silber, Nickel, β-Messing, Quarzkristall und Quarzglas zwischen +50 und 700°C nach einer verfeinerten Methode," Physik. Zeits. **37**, 737 (1936).
36G. R. Peierls, "Statistical Theory of Superlattices with Unequal Concentrations of the Components," Proc. Roy. Soc. **154A**, 207 (1936).
36H. C. Sykes and F. W. Jones, "The Atomic Rearrangement Process in the Copper-Gold Alloy Cu_3Au," Proc. Roy. Soc. London **157A**, 213 (1936).
36I. C. Sykes and H. Evans, "The Transformation in the Copper-Gold Alloy Cu_3Au," J. Inst. Metals **58**, 255 (1936).
36J. R. H. Fowler, *Statistical Mechanics*, second edition, (Cambridge University Press, 1936).

36K. M. Hansen, *Der Aufbau der Zweistofflegierungen*, (Julius Springer, Berlin, 1936).

36L. W. Hume-Rothery, *The Structure of Metals and Alloys*, (The Institute of Metals, London, 1936) p. 83.

36M. N. F. Mott and H. Jones, *The Theory of the Properties of Metals and Alloys*, (The Clarendon Press, Oxford, 1936).

36N. C. Sykes and F. W. Jones, "Methods for the Examination of Thermal Effects due to Order-Disorder Transformations," J. Inst. Metals **59**, 257 (1936).

1937

37A. R. Becker, "Die geordnete Verteilung in metallischen Mischkristallen," Metallwirtschaft **16**, 573 (1937).

37B. G. Borelius, "Resistance of Alloys with Disordered and Ordered Arrangement of Atoms," Proc. Phys. Soc. **49**, 77 (1937) (Extra part).

37C. A. J. Bradley and S. S. Lu, "The Crystal Structures of Cr_2Al and Cr_5Al_8," Zeits. f. Krist. **96**, 20 (1937).

37D. A. J. Bradley, A. H. Jay and A. Taylor, "The Lattice Spacing of Iron-Nickel Alloys," Phil. Mag. **23**, 545 (1937).

37E. W. L. Bragg, C. Sykes and A. J. Bradley, "A Study of the Order-Disorder Transformation," Proc. Phys. Soc. **49**, 96 (1937) (Extra part).

37F. U. Dehlinger, "Zur Verformungsempfindlichkeit der metallischen Überstrukturen," Zeits. f. Physik **105**, 588 (1937).

37G. E. E. Easthope, "The Dependence on Composition of the Critical Ordering Temperature in Alloys," Proc. Camb. Phil. Soc. **33**, 502 (1937).

37H. H. Jones and N. F. Mott, "The Electronic Specific Heat and X-Ray Absorption of Metals, and Some Other Properties Related to Electron Bands," Proc. Roy. Soc. **162A**, 49 (1937).

37I. F. W. Jones and C. Sykes, "The Superlattice in β-Brass," Proc. Roy. Soc. **161**, 440 (1937).

37J. F. Laves and K. Moeller, "Über die Mischkristallreihe Mg-$AgCd_3$ im ternären System Magnesium-Silber-Kadmium," Zeits. f. Metallkunde **29**, 185 (1937).

37K. J. O. Linde, "Röntgenographische und elektrische Untersuchungen des CuPt-Systems," Ann. d. Physik **30**, 151 (1937).

37L. N. F. Mott, "The Energy of the Superlattice in β-Brass," Proc. Phys. Soc. **49**, 258 (1937).

37M. N. F. Mott and H. H. Potter, "Sharpness of the Magnetic Curie Point," Nature **139**, 411 (1937).

37N. P. Rahlfs, "Über einige neue ternäre Verbindungen mit einer Überstruktur des β-Messings," Metallwirtschaft **16**, 640 (1937).

37O. P. Rahlfs, "Die Kristallstruktur des Ni_3Sn. (Mg_3Cd-Typ = Überstruktur der hexagonal dichtesten Kugelpackung)," Metallwirtschaft **16**, 343 (1937).

37P. C. Sykes and H. Wilkinson, "The Transformation in the β-Brasses," J. Inst. Metals **61** (1937) (Advanced copy).

37Q. A. J. Bradley and A. Taylor, "An X-Ray Investigation of the Cause of High Coercivity in Iron-Nickel-Aluminium Alloys," Nature **140**, 1012 (1937).

37R. J. H. Van Vleck, "The Influence of Dipole-Dipole Coupling on the Specific Heat and Susceptibility of a Panamagnetic Salt," J. Chem. Phys. **5**, 320 (1937).

37S. J. H. Van Vleck, "On the Role of Dipole-Dipole Coupling in Dielectric Media," J. Chem. Phys. **5**, 556 (1937).

37T. F. C. Nix, "Superstructures in Alloy Systems," J. App. Phys. **8**, 783 (1937).

37U. N. F. Mott, "Discussion of Papers by Borelius, Bragg and Desch," Proc. Phys. Soc. **49**, 108 (1937) (Extra part).

37V. T. S. Chang, "Specific Heats of Solids due to Molecular Rotation," Proc. Camb. Phil. Soc. **33**, 524 (1937).

37W. K. Riederer, "Das System Magnesium-Kadmium," Zeits. f. Metallkunde **29**, 423 (1937).

37X. E. S. Greiner and E. R. Jette, "X-Ray Study on the Constitution of Iron-silicon Alloys Containing from 14 to 33.4 Per Cent Silicon," Trans. A.I.M.E. **125**, 473 (1937) (Iron & Steel Div.).

37Y. T. S. Chang, "An Extension of Bethe's Theory of Order-Disorder Transitions in Metallic Alloys," Proc. Roy. Soc. London **161A**, 546 (1937).

37Z. R. Becker, "Über den Aufbau binärer Legierungen," Zeits. f. Metallkunde **29**, 245 (1937).

37ZZ. J. C. Slater, "Thermodynamical Considerations of Order and Disorder." Abstract of Symposium on Structure of Metallic Phases. Cornell University (1937).

1938

38A. Personal communication.

38B. J. G. Kirkwood, "Order and Disorder in Binary Solid Solutions," J. Chem. Phys. **6**, 70 (1938).

38C. W. Shockley, "Theory of Order for the Copper-Gold Alloy System," J. Chem. Phys. **6**, 130 (1938).

38D. Personal communication from H. A. Bethe.

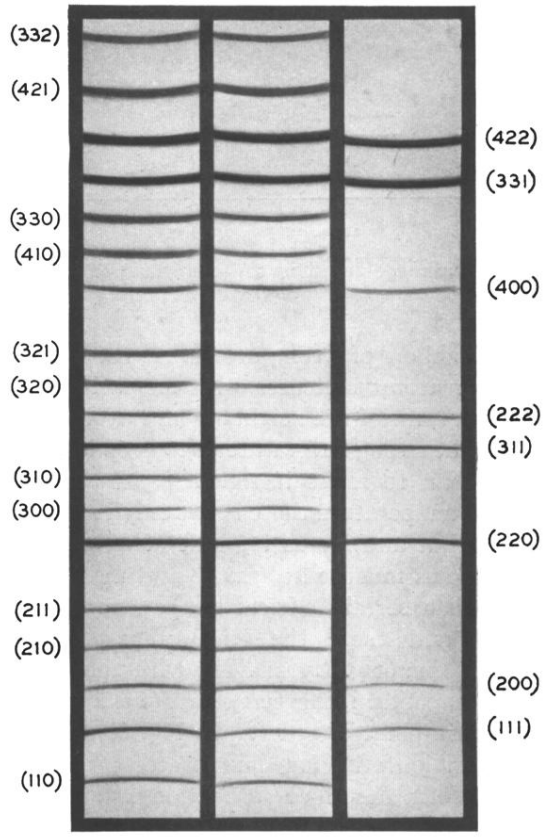

FIG. 2. X-ray diffraction pattern showing superstructure lines (retouched).